

The role of hydrogen peroxide  
in the lifespan of *Caenorhabditis elegans*

I n a u g u r a l d i s s e r t a t i o n

zur

Erlangung des akademischen Grades

doctor rerum naturalium (Dr. rer. nat.)

an der Mathematisch-Naturwissenschaftlichen Fakultät

der Ernst-Moritz-Arndt-Universität Greifswald

vorgelegt von

Daniela Knoefler

geboren am 20. Januar 1981

in Potsdam/ Babelsberg

Ann Arbor, 22. Juni 2012

Dekan:	Prof. Dr. Klaus Fesser .....
1. Gutachter:	Prof. Dr. Hans-Joachim Schüller .....
2. Gutachter:	PD Dr. Tobias P. Dick .....
Tag der Promotion:	10. Oktober 2012 .....

Für Jutta Knöfler



---

## Table of Contents

<b>List of Figures</b>	<b>10</b>
<b>List of Tables</b>	<b>12</b>
<b>1 Summary</b>	<b>13</b>
1.1 Zusammenfassung . . . . .	14
<b>2 Introduction</b>	<b>17</b>
2.1 Why we age – The inception of the Free Radical Theory of Aging . . . . .	17
2.2 Sources of Reactive Oxygen Species . . . . .	19
2.2.1 ROS generation in the mitochondrial electron transport chain . . . . .	19
2.2.2 Oxidant generation by NADPH oxidases and dual oxidases . . . . .	20
2.2.3 Oxidants as by-products of biochemical reactions . . . . .	22
2.3 Antioxidants - Maintaining the balance . . . . .	23
2.3.1 Detoxification systems and ROS scavengers . . . . .	23
2.3.2 Maintaining and restoring the redox homeostasis . . . . .	24
2.4 Levels of oxidants and antioxidants during the lifespan . . . . .	26
2.5 Manipulation of the antioxidant capacity and the effect on lifespan . . . . .	29
2.6 A model organism for aging studies: <i>Caenorhabditis elegans</i> . . . . .	31
2.7 Lifespan-extending interventions in <i>C. elegans</i> . . . . .	32
2.7.1 Manipulation of the Insulin/IGF-1 signaling pathway . . . . .	32
2.7.2 Caloric restriction . . . . .	34
2.7.3 Impairment of the Electron Transport Chain . . . . .	35
2.8 Theoretical background . . . . .	36
2.8.1 Measurement of intracellular reactive oxygen species . . . . .	37
2.8.1.1 Fluorescent dyes . . . . .	37
2.8.1.2 Genetically encoded fluorescent sensor proteins . . . . .	38
<b>3 Objective of the thesis</b>	<b>41</b>

<b>4 Results</b>	<b>43</b>
4.1 <i>C. elegans</i> encounter high levels of hydrogen peroxide during development . . . . .	43
4.1.1 Redox state of peroxiredoxin 2 as read-out for endogenous peroxide level .	43
4.1.1.1 Peroxide-induced peroxiredoxin 2 dimers increase upon peroxide treatment . . . . .	44
4.1.1.2 Peroxide-induced peroxiredoxin 2 dimers are increased during development . . . . .	44
4.1.1.3 Levels of overoxidized peroxiredoxin 2 are higher in early development . . . . .	45
4.1.2 Measurement of hydrogen peroxide release from live worms . . . . .	47
4.1.3 Determination of tissue-specific hydrogen peroxide level over the lifespan of <i>C. elegans</i> . . . . .	48
4.1.3.1 The H <sub>2</sub> O <sub>2</sub> sensor HyPer . . . . .	48
4.1.3.2 Determination of endogenous H <sub>2</sub> O <sub>2</sub> level in living wildtype worms	50
4.1.3.3 The H <sub>2</sub> O <sub>2</sub> detoxifying system seemed to be lowered during development . . . . .	55
4.2 Hydrogen peroxide as signaling molecule in <i>C. elegans</i> development and lifespan .	56
4.2.1 H <sub>2</sub> O <sub>2</sub> level in mutants of the Insulin/ IGF-1 signaling pathway . . . . .	56
4.2.2 Developmental cultivation temperature influences H <sub>2</sub> O <sub>2</sub> level and lifespan .	57
4.2.2.1 Elevated temperatures result in low HyPer ratios in early development . . . . .	60
4.2.2.2 Developmental growth temperature influences adult lifespan . . .	60
4.2.3 Glucose restriction and its effect on H <sub>2</sub> O <sub>2</sub> level and lifespan . . . . .	61
4.2.3.1 Glucose restriction during adulthood extends lifespan . . . . .	61
4.2.3.2 Developmental Glucose restriction seems to be harmful . . . . .	62
4.3 Manipulation of the oxidant homeostasis in <i>C. elegans</i> . . . . .	66
4.3.1 Manipulation of antioxidant capacity through catalase 2 deletion . . . . .	66
4.3.1.1 Lower HyPer ratios and shorter lifespans in catalase 2 deletion worms . . . . .	66
4.3.2 Induction of developmental oxidative stress . . . . .	68

---

4.3.2.1	Wildtype <i>C. elegans</i> can tolerate a short bolus of paraquat . . . . .	68
4.3.2.2	Paraquat treatment induces oxidative stress . . . . .	69
4.3.2.3	Paraquat treatment of L4 larvae shortens lifespan . . . . .	71
4.3.3	Induction of oxidative stress during adulthood . . . . .	73
4.4	Can developmental hydrogen peroxide level predict subsequent lifespan? . . . . .	73
<b>5</b>	<b>Discussion</b>	<b>79</b>
5.1	Peroxide generation during cuticle formation . . . . .	79
5.2	Oxidant generation in metabolic processes . . . . .	80
5.3	Peroxide as mediator in ROS signaling . . . . .	80
5.3.1	Apoptosis . . . . .	81
5.3.2	Proliferation . . . . .	81
5.4	Evidence for developmental ROS signaling . . . . .	82
5.4.1	Effect of cultivation temperature on endogenous peroxide level . . . . .	82
5.4.2	Fluctuations in peroxide as modulator of reproduction . . . . .	84
5.4.3	Manipulation of the redox homeostasis . . . . .	85
5.5	Can events early in life affect the lifespan of <i>C. elegans</i> ? . . . . .	85
5.5.1	Developmental glucose restriction . . . . .	86
5.5.2	Developmental oxidant exposure . . . . .	88
5.5.3	Could developmental variations in peroxide level affect lifespan? . . . . .	89
5.6	Conclusions . . . . .	90
<b>6</b>	<b>Materials &amp; Methods</b>	<b>93</b>
6.1	Cultivation of <i>C. elegans</i> . . . . .	93
6.2	Synchronization of a worm population . . . . .	94
6.2.1	Hypochlorite-NaOH Lysis . . . . .	94
6.2.2	Synchronization without hypochlorite treatment . . . . .	95
6.3	Assessment of physiological processes and lifespan . . . . .	95
6.4	Oxidative stress treatment . . . . .	96
6.4.1	Treatment of worms with the superoxide generator paraquat . . . . .	96
6.4.2	Treatment with sublethal concentrations of hydrogen peroxide . . . . .	96

---

6.5	Manipulation of <i>C. elegans</i> gene expression . . . . .	96
6.5.1	Generation of transgenic animals . . . . .	96
6.5.2	Generation of transgenic mutant animals . . . . .	97
6.5.2.1	Generating and maintaining a male <i>C. elegans</i> stock . . . . .	97
6.5.2.2	Crosses and selection of transgenic mutants . . . . .	98
6.5.2.3	Genotyping . . . . .	98
6.6	Imaging of HyPer fluorescence . . . . .	102
6.6.1	Confocal Microscopy . . . . .	102
6.6.2	Image quantification . . . . .	103
6.6.2.1	Tracing worm spine and body wall to define worm and back-ground region . . . . .	103
6.6.2.2	Defining the HyPer regions and obtaining the HyPer ratio . . . . .	104
6.6.2.3	Reference ratios for normalization . . . . .	104
6.6.3	Fluorescence microscopy . . . . .	104
6.6.4	Recovery of <i>C. elegans</i> after image acquisition . . . . .	105
6.7	Determination of hydrogen peroxide release . . . . .	105
6.7.1	Amplex <sup>®</sup> UltraRed assay . . . . .	106
6.7.2	Measurement of the protein concentration . . . . .	106
6.8	Determination of Peroxiredoxin 2 redox state . . . . .	107
6.8.1	Lysis of worms and protein precipitation . . . . .	107
6.8.2	Labeling of protein thiols . . . . .	109
6.8.3	Determination of the protein concentration . . . . .	109
6.8.4	SDS-PAGE and Western Blot . . . . .	109
6.8.5	Quantification and Analysis . . . . .	111
6.9	Isolation of RNA and proteins from <i>C. elegans</i> . . . . .	112
6.9.1	Sample preparation and lysis . . . . .	112
6.9.2	Preparation of RNA using the TRIzol <sup>®</sup> Reagent and the RNeasy Kit . . . . .	112
6.9.3	Isolation and precipitation of protein . . . . .	113
6.10	Analysis of protein expression level . . . . .	113
6.10.1	Statistical Analysis . . . . .	115



**7 References**

**117**

**8 List of Abbreviations**

**141**

## List of Figures

2.1	Redox Homeostasis . . . . .	19
2.2	Sources of ROS and their removal by antioxidants . . . . .	21
2.3	Lifespan-extending interventions in <i>C. elegans</i> . . . . .	33
2.4	Timing requirements for lifespan extension in <i>C. elegans</i> . . . . .	37
2.5	Fluorescence emission spectra of the HyPer sensor . . . . .	39
4.1	Redox cycle of 2-cysteine peroxiredoxins . . . . .	44
4.2	Redox status of <i>C. elegans</i> PRDX-2 as a read-out for H <sub>2</sub> O <sub>2</sub> levels . . . . .	45
4.3	Utilization of the PRDX-2 redox state as read-out for endogenous peroxide . . . . .	46
4.4	Overoxidized PRDX-2 as read-out for endogenous peroxide level . . . . .	46
4.5	Determination of H <sub>2</sub> O <sub>2</sub> release rates . . . . .	47
4.6	Fluorescence of <i>C. elegans</i> expressing <i>myo-2::GFP</i> and <i>unc-54::HyPer</i> . . . . .	48
4.7	Lifespans of transgenic and wildtype <i>C. elegans</i> . . . . .	49
4.8	The HyPer ratio is independent of HyPer protein expression . . . . .	50
4.9	HyPer fluorescence in the body wall muscle cells of wildtype <i>C. elegans</i> . . . . .	51
4.10	Hydrogen peroxide level in the body wall muscle cells of HyPer transgenic <i>C. elegans</i> . . . . .	52
4.11	HyPer ratios of unbleached developing and adult animals . . . . .	53
4.12	Hydrogen peroxide level in the head region of HyPer transgenic wildtype <i>C. elegans</i> . . . . .	54
4.13	Peroxiredoxin 2 protein level during development and adulthood . . . . .	55
4.14	Mutants of the IIS pathway differ in lifespan . . . . .	56
4.15	Mutants of the IIS pathway differ in endogenous peroxide level . . . . .	58
4.16	The lifespan of <i>C. elegans</i> depends on the cultivation temperature . . . . .	59
4.17	Peroxide level in development are influenced by the growth temperature . . . . .	61
4.18	Developmental growth temperature affects adult lifespan . . . . .	62
4.19	DOG exposure of adult wildtype worms transiently increases HyPer ratio and extends lifespan . . . . .	63
4.20	Developmental DOG exposure retards development of wildtype worms . . . . .	64
4.21	Developmental DOG exposure reduces HyPer ratios during development and shortens lifespan . . . . .	65

---

4.22	Catalase 2 deletion animals have lower HyPer ratios during adulthood . . . . .	66
4.23	Peroxiredoin 2 protein level of catalase 2 deletion animals . . . . .	67
4.24	Lifespan of catalase 2 deletion and wildtype animals . . . . .	68
4.25	Survival of paraquat-stressed wildtype <i>C. elegans</i> . . . . .	69
4.26	Motility upon paraquat exposure of wildtype animals . . . . .	70
4.27	HyPer ratio of paraquat-stressed animals . . . . .	71
4.28	Paraquat stress at L4 stage effects physiology and lifespan . . . . .	72
4.29	Paraquat-mediated effect on lifespan is temperature-dependent . . . . .	74
4.30	Lifespan of young adults upon exposure to paraquat . . . . .	75
4.31	Histogram of the HyPer ratios of a synchronized population . . . . .	76
4.32	Mortality and lifespan of <i>C. elegans</i> sub-populations which differ in their HyPer ratios	78
6.1	Schematic overview of the cross between wildtype and mutant animals . . . . .	98
6.2	Agarose gel electrophoresis after PCR-genotyping of <i>ctl-2</i> deletion worms . . . . .	101
6.3	Genotyping of <i>daf-2(e1370)</i> using DNA sequencing . . . . .	102
6.4	ImageJ display of “wormsuite” image analysis . . . . .	103
6.5	Quantification of the redox state of PRDX-2 . . . . .	108

**List of Tables**

2.1	Effects of deletion of antioxidant genes on stress resistance and lifespan . . . . .	30
2.2	Effects of overexpression of antioxidant genes on stress resistance and lifespan . . .	31
4.1	Larval development is influenced by the cultivation temperature . . . . .	59
6.1	Overview of mutant <i>C. elegans</i> strains used in this thesis . . . . .	97
6.2	PCR programs for the genotyping of mutant alleles and transgenes . . . . .	101

## 1 Summary

The leading hypothesis of why organisms age is the “Free Radical Theory of Aging”, which states that the accumulation of reactive oxygen species (ROS), such as superoxide ( $O_2^-$ ) and hydrogen peroxide ( $H_2O_2$ ), causes protein, lipid and DNA damage and leads to the observed age-related decline of cells and tissues. A major obstacle in analyzing the role of oxidative stress in aging organisms is the inability to precisely localize and quantify the oxidants, to identify proteins and pathways that might be affected, and ultimately, to correlate changes in oxidant levels with the lifespan of the organism. To directly monitor the onset and extent of oxidative stress during the lifespan of *Caenorhabditis elegans*, we utilized the fluorescent  $H_2O_2$  sensor protein HyPer, which enabled us to quantify endogenous peroxide levels in different tissues of living animals in real time. We made the surprising observation that wildtype *C. elegans* is exposed to very high peroxide levels during development. Peroxide levels drop rapidly as the animals mature, and low peroxide levels then prevail throughout the reproductive age, after which an age-accompanying increase of peroxide level is observed. These results were in excellent agreement with findings obtained by using the highly quantitative redox proteomic technique OxICAT, which monitors the oxidation status of redox-sensitive proteins as read-out for onset, localization, and protein targets of oxidative stress (Knoefler *et al.*, 2012a). By using OxICAT, we detected increased protein thiol oxidation during the development of *C. elegans* and in aging animals (Knoefler *et al.*, 2012a). Many processes in *C. elegans* might potentially contribute to the elevated peroxide levels observed during development, including cuticle formation, apoptosis, proliferation, gametogenesis, or ROS signaling. The finding that all investigated *C. elegans* mutants regardless of their lifespan are exposed to high developmental peroxide levels argues for ROS accumulation to be a universal and necessary event. Yet, recovery from the early oxidative boost might determine the subsequent adult lifespan, as we found that long-lived *daf-2* mutants transition faster to reducing conditions than short-lived *daf-16* mutants, which retain higher peroxide levels throughout their mature life. These results suggest that changes in the cellular oxidant homeostasis, encountered at a very early stage in life, might determine subsequent redox levels and potentially the lifespan of organisms. Manipulation of developmental oxidant levels using glucose restriction or a short bolus of superoxide caused a disruption in developmental growth, a delay in reproduction, and a shortened lifespan. These re-

sults suggest that developmental oxidant levels are fine-tuned and optimized. Future experiments are aimed to investigate the sources of developmental hydrogen peroxide, and to elucidate whether active down-regulation of antioxidant enzymes during the larval period might foster peroxide accumulation. Preliminary results indicate that this might indeed be the case for peroxiredoxin 2, whose expression was significantly lower during development than at later stages in life. Finally, we investigated whether the observed variances in the developmental peroxide levels of individual worms within a synchronized wildtype population might be responsible for the observed significant variances in lifespan, and hence could serve as a predictor for adult lifespan. Preliminary results revealed that neither too low nor too high peroxide levels during development are beneficial for the lifespan of wildtype worms, suggesting that ROS level during development might be optimized for maximized lifespan. Future experiments aim to reveal the processes that are affected by ROS and which might influence the individual's lifespan early in life.

## 1.1 Zusammenfassung

Die führende Hypothese, um zu erklären warum Organismen altern, ist die "Free Radical Theory of Aging". Sie postuliert, dass sich reaktive Sauerstoffspezies (Reactive Oxygen Species, ROS), wie beispielsweise Hydroperoxid-Anion ( $O_2^-$ ) und Wasserstoffperoxid ( $H_2O_2$ ), über die Zeit anhäufen und Schäden an Proteinen, Lipiden und DNA verursachen, die zu der beobachteten altersbedingten Degeneration von Zellen und Geweben führt. Die Analyse der Rolle von oxidativem Stress in alternden Organismen wird behindert durch 1) die Unfähigkeit, die Sauerstoffspezies genau zu lokalisieren und zu quantifizieren, 2) Proteine und Signalwege, die betroffen sein können, zu identifizieren und 3) Fluktuationen von oxidativem Stress mit der Lebensdauer von Organismen zu korrelieren. Um den Beginn und den Umfang des oxidativen Stresses über die Lebensspanne von *Caenorhabditis elegans* zu studieren, wurde das fluoreszierende Sensorprotein HyPer verwendet, welches endogene  $H_2O_2$ -Spiegel in spezifischen Geweben nachweist. Zu unserer Überraschung fanden wir, dass Wildtyp Nematoden schon während ihrer Entwicklung sehr hohen Peroxidspiegeln ausgesetzt sind, die sehr schnell sinken, sobald die Würmer ihr fruchtbares Alter erreichen. Eine erneute Erhöhung von Peroxidspiegeln wurde beobachtet, sobald die Tiere Alterungserscheinungen zeigten. Diese Ergebnisse passten hervorragend zu den Erkenntnissen, die wir mit Hilfe von OxICAT, einer quantitativen Redox-Proteomik-Technik, gewonnen haben. OxICAT bestimmt den Oxidationsstatus von

vielen redox-sensitiven Cysteinen, und erlaubt dadurch Rückschlüsse auf die Sauerstoffspezies, das betroffene Protein sowie den Zeitpunkt des Einsetzens der Oxidation (Knoefler *et al.*, 2012a). Wir fanden, dass *C. elegans* während der Entwicklung und im Alter eine erhöhte Oxidation der Protein-Thiol-Gruppen aufwies (Knoefler *et al.*, 2012a).

Viele physiologische Prozesse in *C. elegans*, wie zum Beispiel die Bildung der Kutikula, Apoptose, Gametogenese, Proliferation, oder ROS-regulierte Signalwege, tragen möglicherweise zur Erhöhung der Peroxidspiegel während der Entwicklung bei. Dass alle untersuchten *C. elegans*-Mutanten unabhängig von ihrer Lebensdauer hohe Peroxidspiegel während ihrer Entwicklung zeigten, spricht dafür, dass die Akkumulation von ROS universell und notwendig sein könnte. Die Fähigkeit zur Erholung von diesem frühen oxidativen Stress könnte dagegen noch auf die spätere Lebenserwartung von erwachsenen Nematoden Einfluss haben. Wir fanden beispielsweise, dass die langlebigen *daf-2*-Mutanten Peroxidspiegel schneller reduzieren als kurzlebige *daf-16*-Mutanten, welche höhere Peroxidspiegel in der (noch) verbleibenden Lebenszeit aufwiesen. Diese Ergebnisse deuten darauf hin, dass sich Änderungen in der zellulären Redox-Homöostase, welche sich in einem frühen Entwicklungsstadium abspielen, auf die Redox-Spiegel im Erwachsenenalter auswirken und damit womöglich die Lebensdauer der Organismen beeinflussen können. Die Manipulation von Peroxidspiegeln, beispielsweise durch Restriktion der Glukosezufuhr oder kurzzeitigem superoxidativen Stress, führte zu negativen Effekten in der Entwicklung, Fortpflanzung und Lebensdauer. Diese Ergebnisse deuten darauf hin, dass die Redox-Homöostase im Larvenstadium genau reguliert und optimiert ist. Zukünftige Experimente sollen den Ursprung der Wasserstoffperoxidbildung in der Entwicklung untersuchen und aufzeigen, ob beispielsweise die Aktivität und/ oder die Expression antioxidativer Enzyme im Larvenstadium verändert sein könnte. Vorläufige Ergebnisse deuten darauf hin, dass dies für die Peroxidase Peroxiredoxin 2 tatsächlich zutreffen könnte. Die Expression von Peroxiredoxin 2 ist während der Entwicklung wesentlich niedriger als in späteren Entwicklungsstufen.

Schließlich untersuchten wir, ob die beobachteten Fluktuationen in den Peroxidspiegeln individueller Würmer während des Larvenstadiums möglicherweise mit der Lebensdauer der Nematoden zusammenhängen könnte. Erste Ergebnisse weisen darauf hin, dass weder erniedrigte noch erhöhte Peroxidspiegel während der Entwicklung die Lebensdauer der Würmer positiv beeinflussen. Dies könnte bedeuten, dass eine optimierte Dosierung von Sauerstoffspezies im Larvenstadium zu

einer Maximierung der Lebenserwartung beiträgt. Zukünftige Experimente sollen zeigen, welche Prozesse von ROS beeinflusst werden, und ob die individuelle Lebensdauer eines Organismus möglicherweise schon sehr früh im Leben festgelegt wird.



---

## 2 Introduction <sup>1</sup>

### 2.1 Why we age – The inception of the Free Radical Theory of Aging

The question of why we age has given rise to many different theories over the last decades. One of the most popular and long-lasting hypothesis is the “Free Radical Theory of Aging”. Max Rubner was one of the first to suggest that aging might be connected to energy metabolism after he observed that organisms with different lifespans expend the same amount of energy over their lifespan (Rubner, 1908). The idea that organisms have a fixed amount of “vital substances”, which, when utilized faster, would shorten lifespan formed the basis of the “rate-of-living” theory proposed by Raymond Pearl in 1921 (Pearl, 1921).

Although this theory was never proven to be valid, it drew attention to the concept that oxygen metabolism and lifespan might be connected. When Denham Harman realized that ionizing radiation, which induces the formation of oxygen radicals, causes biological effects (e.g. mutations, cancer) that are very similar to the physiological changes that occur during aging, he postulated the “Free Radical Theory of Aging” (FRTA) (Harman, 1956). This hypothesis suggested that free radicals, which are generated by cells themselves, accumulate over time, leading to increased cell and tissue damage and eventually causing physiological decline and death. The suggestion that harmful reactive oxygen species (ROS) are endogenously produced was initially received with skepticism but gained acceptance with the discovery of superoxide dismutase (SOD), an enzyme whose sole function is the specific removal of superoxide from cells and organisms (McCord and Fridovich, 1969). The FRTA was later modified to the “Mitochondrial Free Radical Theory of Aging” to take into account the fact that mitochondria are the major source and also the major target of ROS. To acknowledge the involvement of other non-radical oxygen species, like hydrogen peroxide, Harman’s theory underwent a final re-definition and is now often referred to as the “Oxidative Stress Hypothesis of Aging” (Yu and Yang, 1996).

Since the inception of the “Free Radical Theory of Aging”, numerous studies have been conducted providing convincing evidence that cells constantly produce ROS, not only during mitochondrial respiration but also during host defense, cell signaling and many other physiological and

---

<sup>1</sup>The main part of the introduction is going to be published as the book chapter “Role of Oxidative Stress in Aging” in: “Oxidative Stress and Redox Regulation”(Editors: Ursula Jakob & Dana Reichmann), see Knoefler *et al.* (2012b)

pathological events (Trachootham *et al.*, 2008; Dröge, 2002). To counteract free oxygen radicals, aerobic organisms have evolved a number of highly efficient antioxidant defense systems, which include ROS detoxifying enzymes, small molecule ROS scavengers and oxidoreductases. These systems appear to work together to maintain a crucial balance of pro-oxidants and antioxidants within cells and sub-cellular compartments, a process commonly referred to as redox homeostasis (Finkel and Holbrook, 2000). Shifting the equilibrium towards more oxidizing conditions (i.e., oxidative stress) either by increasing the levels of pro-oxidants or by decreasing the cell's anti-oxidant capacity, leads to the toxic accumulation of ROS, which damages cellular macromolecules, including nucleic acids, lipids and proteins (Figure 2.1). Oxidative stress conditions have been associated with aging as well as many age-related conditions, including cancer, diabetes, atherosclerosis, cardiovascular diseases and a variety of neurodegenerative diseases (Barnham *et al.*, 2004; Ceriello and Motz, 2004; Victor *et al.*, 2009; Reuter *et al.*, 2010).

Yet, despite the wealth of studies that have been conducted to test the “Free Radical Theory of Aging”, the jury is still out on whether radical formation is the primary cause of aging or represents a secondary effect of aging and age-related diseases. This is in part due to the recent realization that ROS are not toxic per se. In fact, it is now clear that cells need to maintain certain levels of oxidants to be able to differentiate, develop and to overall function properly (Finkel and Holbrook, 2000). Many physiological processes, including cell signaling (Finkel, 2011b; D’Aur aux and Toledano, 2007; Ghezzi *et al.*, 2005), protein folding (Kakihana *et al.*, 2011; Margittai and B nhegyi, 2010), development (Hern ndez-Garc a *et al.*, 2010), and immune response require the presence of certain levels of oxidants (Finkel, 2011a). These oxidants are typically sensed by redox-regulated proteins, which use the redox status of one or more highly oxidation-sensitive cysteine thiols to directly or indirectly control their own cellular function and hence the function of the pathway that they are part of. Redox sensitive proteins are found to play roles in the majority of cellular functions, ranging from signal transduction (e.g., phosphatases and kinases), gene expression (e.g., p53) to metabolism (e.g., GapDH) and proteostasis (e.g., cdc-48), constantly fine-tuning these pathways according to the cellular redox status (Brandes *et al.*, 2009; Kumsta *et al.*, 2011). These findings imply that while shifting the redox balance towards pro-oxidants is clearly toxic to the cell, shifting the redox balance towards antioxidants might possibly not be beneficial either, as it will interfere with the physiological role that low ROS levels play in cells and organisms (Figure 2.1).

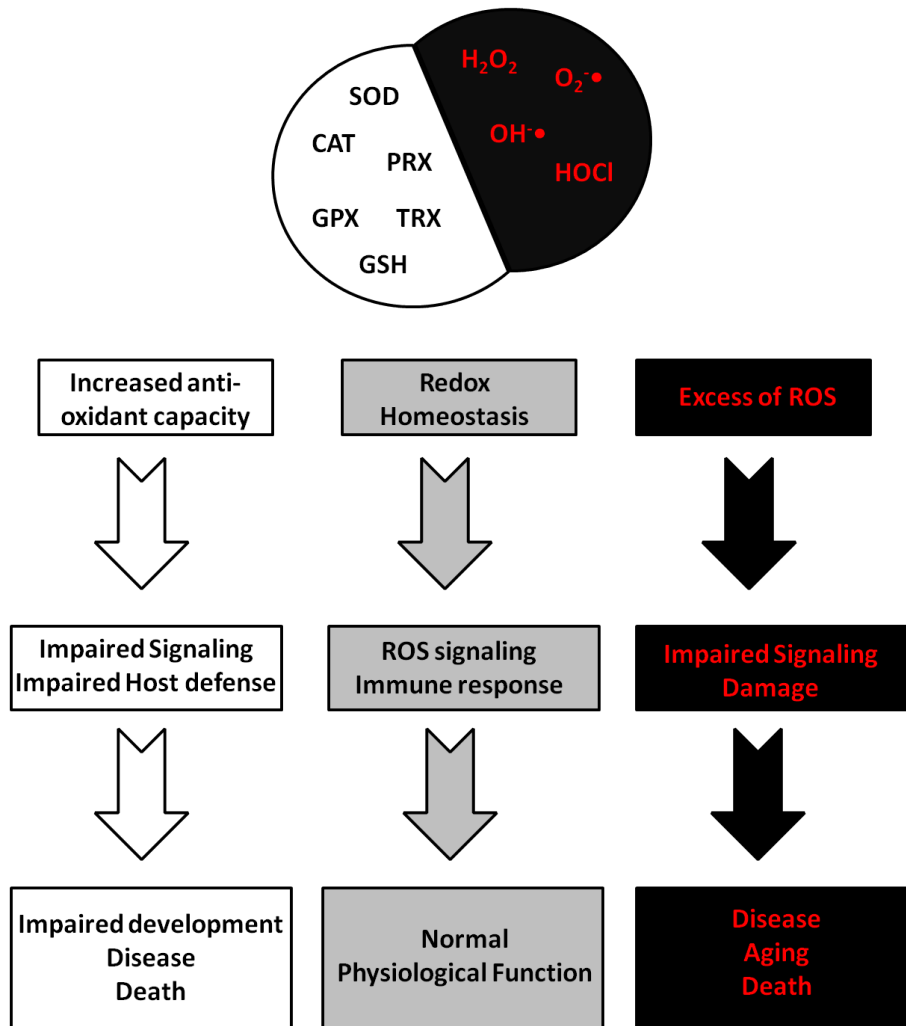


**Figure 2.1. Redox Homeostasis.** Maintaining the proper redox balance between oxidants, such as hydrogen peroxide (H<sub>2</sub>O<sub>2</sub>), superoxide (O<sub>2</sub><sup>•-</sup>), hydroxyl radicals (OH<sup>•</sup>), hypochlorous acid (HOCl), and antioxidants, like catalase (CAT), peroxiredoxin (PRX), glutathione peroxidase (GPX), superoxide dismutase (SOD), thioredoxin (TRX), glutathione (GSH), is essential for correct physiological processes. A shift towards more oxidizing conditions (i.e., oxidative stress) as well as an increase in the antioxidant capacity of the organism will result in pathophysiological conditions.

## 2.2 Sources of Reactive Oxygen Species

### 2.2.1 ROS generation in the mitochondrial electron transport chain

The fusion of a prokaryotic and a eukaryotic cell millions of years ago marked the beginning of a powerful symbiosis as the bacteria-turned-organelle enabled the eukaryotic cell to efficiently generate energy. The caveat, however, is that the electron transport chain (ETC) in the mitochondria is generally considered to be the major source for reactive oxygen species in eukaryotic cells (Cadenas

and Davies, 2000). Mitochondria produce the energy to oxidatively phosphorylate ADP, utilizing an electrochemical proton gradient, which is generated by a series of redox reactions located in the inner membrane. In a stepwise reaction catalyzed by four enzyme complexes (I-IV), electrons are passed from NADH to the more electronegative electron acceptor oxygen. Three of the complexes (I, III, and IV) also function as proton pumps, which utilize the energy released from the electron transport chain to transfer protons from the matrix into the intermembrane space. The proton gradient is subsequently utilized by complex V (ATP synthase) to drive ATP production. To maintain ATP production, it is necessary to pass all four electrons from complex IV onto the more electronegative molecular oxygen, a process estimated to require over 95% of the inhaled oxygen (Cadenas and Davies, 2000). Although very efficient and tightly regulated, the electron transport chain can lead to mono- or bivalent reduction of oxygen under physiological conditions, giving rise to superoxide anions and hydrogen peroxide, respectively (Cadenas and Davies, 2000; Klotz and Sies, 2009) (Figure 2.2). It is estimated that up to 2% of the molecular oxygen used in mitochondria escapes in form of superoxide anion radicals (Chance and Williams, 1956), with complex I and III considered to be the main superoxide producers (references within (Turrens, 1997)).

### 2.2.2 Oxidant generation by NADPH oxidases and dual oxidases

NADPH oxidases (NOX) and dual oxidases (DUOX), which are universally distributed in cells and organisms, generate ROS upon exposure to a variety of stimuli, including growth factors, cytokines or bacterial invasion (Lambeth, 2004). During the innate immune response, invading microorganisms are engulfed by phagocytes, and NADPH oxidases located in the inner membrane of the cells are quickly activated to produce large quantities of superoxide anions by transferring electrons from NADPH to oxygen (i.e. respiratory burst). Superoxide radicals are then converted to hydrogen peroxide, which is either directly released into the phagosome of phagocytes or used by myeloperoxidases in neutrophils (a subgroup of phagocytes) to form the potent antimicrobial hypochlorous acid (the active ingredient of household bleach) (Figure 2.2). Dysfunction of phagocytic NADPH oxidases has been implicated in a number of inheritable immunodeficiencies, such as chronic granulomatous disease (Bedard and Krause, 2007), which is characterized by the inability of the innate immune system to kill invading pathogens due to a failure to produce sufficient amounts of ROS (Lambeth, 2004). An increased susceptibility towards infections has also been observed in

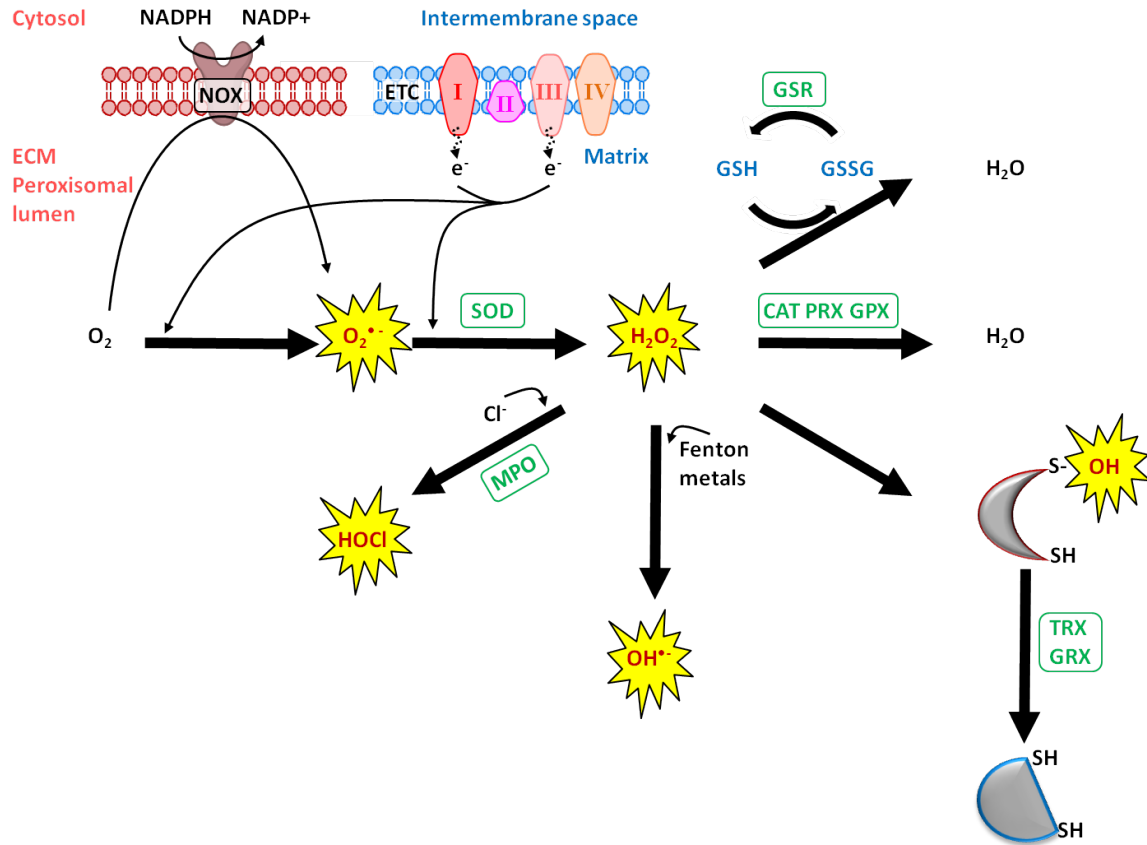


**Figure 2.2. Sources of ROS and their removal by antioxidants.** ROS are produced by the electron transport chain (ETC), located in the inner membrane of the mitochondria, and by transmembrane NADPH oxidases (NOX), located in plasma and peroxisomal membranes. Electrons, which constantly leak during the ETC, react with molecular oxygen to form superoxide ( $O_2^{\bullet -}$ ) or hydrogen peroxide ( $H_2O_2$ ). NADPH oxidases utilize cytosolic NADPH to generate  $O_2^{\bullet -}$  either in peroxisomes or the extracellular matrix (ECM). Superoxide is rapidly dismutated to the slow-acting  $H_2O_2$  in a process that is catalyzed by superoxide dismutase (SOD).  $H_2O_2$  can react with chloride ions to generate the very potent oxidant hypochlorous acid (HOCl), in a process that is catalyzed by myeloperoxidases (MPO) within phagocytes. In the presence of Fenton metals (i.e., iron, copper), peroxide rapidly forms highly reactive hydroxyl radicals ( $OH^{\bullet}$ ), which react with and potentially destroy all cellular macromolecules in their vicinity. To detoxify  $H_2O_2$ , cells utilize a combination of enzymatic clearance systems, consisting of catalase (CAT), peroxiredoxin (PRX), and glutathione peroxidase (GPX), as well as non-enzymatic small molecule scavengers. One of these scavengers is the small tripeptide glutathione (GSH), which becomes oxidized to GSSG in the process. Regeneration of GSH is achieved by glutathione reductase (GSR). Other peroxide scavengers are surface thiols in proteins, which undergo sulfenic acids (SOH) formation (Hansen *et al.*, 2009; Murphy, 2011). Sulfenates are either directly reduced by the thioredoxin (TRX) system or undergo S-glutathionylation, which is reversed by the glutaredoxin (GRX) system.

*C. elegans* upon reducing the levels of dual oxidase in the nematodes (Chavez *et al.*, 2009).

In addition to NADPH oxidases in phagocytic cells, isoforms of NADPH oxidases are involved in a host of other physiological processes. Growth factors, such as angiotensin II, platelet-derived growth factor (PDGF), or vascular endothelial growth factor (VEGF) utilize NOX-mediated ROS signaling to regulate angiogenesis and blood pressure, among other processes (Lambeth, 2004; Ushio-Fukai and Nakamura, 2008). Superoxide anions, generated by NADPH oxidases, can rapidly react with the anti-hypertensive nitric oxide (NO) thus depleting the NO pool and increasing blood pressure (Lassègue and Griendling, 2004). Thyroidal NADPH dual oxidases, in contrast, provide hydrogen peroxide for thyroid hormone synthesis (Nauseef, 2008; Dupuy *et al.*, 1991). Typically membrane-bound, NADPH oxidases utilize cytosolic NADPH to generate superoxide either in the extracellular matrix or the lumen of intracellular organelles (Figure 2.2). While superoxide itself is not membrane permeable, it is either transported to other cell compartments by ion channels or converted into the highly diffusible hydrogen peroxide. Many NADPH oxidases are ubiquitously expressed and are thought of being capable of generating higher ROS levels in a regulated manner than those continuously produced during respiration (Krause, 2007). It is thus not surprising that increased expression and/or activity of several NOX family members has been implicated to play a key role in a number of age-related diseases, including cancer, cardiovascular diseases and neurodegenerative disorders (Bedard and Krause, 2007; Krause, 2007).

### 2.2.3 Oxidants as by-products of biochemical reactions

In addition to reactions catalyzed by proteins of the ETC and by NADPH oxidases, many other cellular reactions have been shown to produce ROS. In peroxisomes, for example, electrons generated during the  $\beta$ -oxidation of long fatty acids are transferred onto molecular oxygen instead of components of the ETC, thereby producing hydrogen peroxide. Oxidative deamination of aromatic (dietary) amines and monoamine neurotransmitters, such as serotonin and dopamine, is catalyzed by monoamine oxidases (MAO) in a process that leads to the production of potentially neurotoxic by-products, including ammonia and hydrogen peroxide (Bortolato *et al.*, 2008). Other major endogenous ROS producers belong to the heme-containing cytochrome P450 protein superfamily. Members of this family are involved in oxidizing endogenous substrates as well as a broad range of exogenous compounds, including drugs, carcinogens and other xenobiotics. Since the monooxygena-

tion of these substrates is inefficiently coupled to the electron transfer from NADPH to cytochrome P450, it causes a continuous leakage of electrons, resulting in ROS formation even in the absence of substrates (Zangar *et al.*, 2004). Some xenobiotic compounds such as alcohol or drugs can further increase the P450-uncoupling reaction, thereby increasing ROS generation even more. The need to maintain low intracellular ROS level has apparently resulted in the development of feedback mechanisms as the presence of high ROS levels was recently found to decrease cytochrome P450 levels (Zangar *et al.*, 2004).

## 2.3 Antioxidants - Maintaining the balance

### 2.3.1 Detoxification systems and ROS scavengers

The aerobic lifestyle goes along with an inevitable generation of oxygen species. If oxidants are not properly removed, their high reactivity can cause oxidative damage to cellular macromolecules. While strictly anaerobic microorganisms have been shown to not possess superoxide dismutase or catalase activity, the oxygen-metabolizing species tested contain superoxide dismutase activity (McCord *et al.*, 1971). Superoxide anions are known to spontaneously dismutate to hydrogen peroxide at a slow rate. *In vivo*, this process is massively accelerated by the presence of superoxide dismutases (SODs) (Fridovich, 1972) (Figure 2.2), which are located in the cytosol, the mitochondrial intermembrane space and matrix, as well as in the extracellular space (Zelko *et al.*, 2002).

While H<sub>2</sub>O<sub>2</sub> is less reactive and more stable than other ROS (Giorgio *et al.*, 2007), it reacts rapidly with free ferrous (Fe<sup>2+</sup>) iron in the Fenton reaction, which generates hydroxyl radicals, one of the most reactive oxygen species known. Hence, removal of peroxide is of utmost importance to avoid widespread oxidative damage. Enzymatic clearance of hydrogen peroxide is performed by catalases, glutathione (GSH) peroxidases, and peroxiredoxins (Figure 2.2). Catalases are mainly found in the cytosol and peroxisomes, as well as in the mitochondrial matrix of some highly metabolically active tissues, such as heart and liver (Radi *et al.*, 1991; Salvi *et al.*, 2007). They catalyze the decomposition of two hydrogen peroxide molecules to oxygen and two water molecules, using one of the fastest turnover rates known for any enzyme (Nicholls *et al.*, 2000). While catalases contribute to hydrogen peroxide decomposition at high hydrogen peroxide concentrations, selenocysteine-containing GSH peroxidases work efficiently at low peroxide levels (Cohen

and Hochstein, 1963; Makino *et al.*, 1994), suggesting that they serve as the predominant peroxide scavengers under physiological  $H_2O_2$  concentrations (Makino *et al.*, 1994). GSH peroxidases catalyze the reduction of hydrogen peroxide to water by utilizing reduced glutathione (GSH) as electron donor. GSH, a highly abundant tripeptide is oxidized in this process to disulfide-bonded GSSG, and subsequently regenerated by GSH reductase, a NADPH-dependent oxidoreductase. The third group of peroxide-detoxifying enzymes is constituted by peroxiredoxins, which compensate for their slow reaction rates with extremely high cellular concentrations, making them one of the most abundant enzymes in many organisms (Wood *et al.*, 2003).

In addition to the various antioxidant enzymes that clear reactive oxygen species, organisms have also evolved various small molecules such as glutathione, metallothioneins and vitamins, which are capable of scavenging oxygen radicals. While the non-protein thiol  $\gamma$ -L-glutamyl-L-cysteinyl-glycine (glutathione) can act as reductant for peroxide (Figure 2.2) and free radicals (Orrenius and Moldéus, 1984), metallothioneins, which are low molecular weight metal-containing proteins, are capable of scavenging hydroxyl radicals and superoxide (Thornalley and Vařák, 1985). The water-soluble ascorbate (vitamin C) scavenges oxygen radicals in aqueous solution while  $\alpha$ -tocopherol (vitamin E) protects membranes from radical formation (Niki, 1987).

### 2.3.2 Maintaining and restoring the redox homeostasis

The “Free Radical Theory of Aging” postulates that accumulating reactive oxygen species can cause oxidative damage to cellular macromolecules such as DNA, lipids, and proteins. While oxidative damage to DNA and lipids ultimately can have dire consequences for the cell, oxidative inactivation of proteins probably has the most immediate effect on the fitness of an organism since one of the most ROS-sensitive and reactive cellular target is the sulfur-containing amino acid cysteine. Many cysteine thiols in proteins have been shown to rapidly react with peroxide, HOCl and/or NO, thereby forming a variety of different oxidative modifications, including sulfenic acid and disulfide bond formation, mixed disulfides with glutathione (S-glutathionylation) or S-nitrosylation (Winterbourn and Hampton, 2008). Because of their high sensitivity towards oxidation, cysteine thiols are also the amino acids of choice for those proteins, whose function is regulated by the redox conditions of the environment. Redox sensitive proteins are found to play roles in a majority of cellular functions, ranging from signal transduction (e.g., phosphatases and kinases) and gene expression



(e.g., p53) to metabolism (e.g., GapDH) and proteostasis (e.g., Cdc-48) (Brandes *et al.*, 2009; Kumsta *et al.*, 2011). Oxidative modification of redox sensitive cysteines leads to the transient activation (e.g., OxyR, Hsp33, Nrf2) or inactivation (e.g., phosphatases) of a protein's function, making thiol-modifications uniquely able to fine-tune cellular pathways and response systems to the cellular redox environment.

Two highly conserved enzymatic systems, the thioredoxin system and the glutaredoxin system are responsible for maintaining redox homeostasis and reducing most forms of oxidative thiol modifications in proteins. The thioredoxin system consists of the small oxidoreductase thioredoxin, which uses direct thiol-disulfide exchange reactions to reduce sulfenic acids, disulfide bonds or S-nitrosylated cysteines in proteins (Collet and Messens, 2010). Thioredoxins are then reduced by thioredoxin reductase, a selenocysteine-containing enzyme in eukaryotes, which utilizes NADPH as the ultimate electron donor (Figure 2.2). The second redox system consists of the small redox enzymes glutaredoxins, which directly interact with oxidized protein thiols. In contrast to thioredoxins, which are reduced by thioredoxin reductase, glutaredoxins are non-enzymatically reduced by reduced glutathione. Oxidized glutathione is subsequently regenerated by glutathione reductase, which, like thioredoxin reductase, uses NADPH as an electron donor (Holmgren *et al.*, 2005).

As outlined above, both thioredoxin and glutaredoxin systems depend on reduced NADPH as an electron source, making both systems and hence the cellular redox status ultimately dependent on the cellular NADPH/NADP<sup>+</sup> ratio (Schafer *et al.*, 2001). The major source of NADPH within the cell is the pentose phosphate pathway, which generates two molecules of NADPH for every oxidized glucose-6-phosphate molecule. The strict dependence of the cellular redox status on NADPH explains the need for efficient re-routing of glucose from glycolysis to the pentose phosphate pathway under conditions of oxidative stress (Godon *et al.*, 1998; Grant, 2008). Oxidative modification and inactivation of key enzymes of glycolysis seem to contribute to these changes in glucose flux, illustrating how redox-sensitive metabolic enzymes play an active part in the oxidative stress defense of organisms (Brandes *et al.*, 2011). Deficiency in glucose-6-phosphate dehydrogenase, which catalyzes the first step of the pentose phosphate pathway, results in lower intracellular NADPH/NADP<sup>+</sup> ratios and increased oxidative stress and has been associated with premature cell senescence and a number of different disease conditions (Ho *et al.*, 2007).

## 2.4 Levels of oxidants and antioxidants during the lifespan

Age-accompanying oxidative damage can either be caused by increased ROS production, decreased detoxification, or a combination thereof. To assess ROS levels over the lifetime of an organism, assays have been developed that directly measure the concentration of ROS, such as superoxide or peroxide. The obtained results were not always consistent with the “Free Radical Theory of Aging” as it was shown, for instance, that the concentration of hydrogen peroxide in *Drosophila* homogenates increases during the first trimester of their life but remains stable during the remainder of the lifespan (Sohal *et al.*, 1990). In contrast, mitochondrial matrix hydrogen peroxide was observed to increase during aging in *Drosophila* (Cochemé *et al.*, 2011). Peroxide levels also increased in aging *C. elegans* population as was recently demonstrated by using chromosomally encoded peroxide-specific sensor proteins (Back *et al.*, 2011) whereas microsomal superoxide anion production actually declined from reproductive to senescent age, with long-lived mutant animals (i.e., *age-1*) exhibiting higher superoxide anion levels than the age-matched control animals (Vanfleteren, 1993). In mice, both mitochondrial superoxide and hydrogen peroxide release from heart, brain and kidney tissues increased with the age of the animals (Sohal *et al.*, 1994).

Many studies have been conducted to assess the activity of ROS-detoxifying enzymes in young and old organisms, with the goal to either confirm or rule out the model that older animals have lower levels of ROS-detoxifying activity than young animals, hence the accumulation of oxidative damage. As exemplified below, while such correlation does seem to exist for certain antioxidant systems in some tissues and model systems, it does not generally apply to all ROS or model systems, making a more differentiated discussion necessary.

### *Superoxide dismutases*

Comparative analysis of superoxide dismutase activity in kidney, brain and heart tissue of young and old mice did not reveal any significant alteration in total SOD activity (Sohal *et al.*, 1994). Similarly, activity of Cu/ZnSOD in liver homogenates of mice between 4, 12, or 18 months of age appeared unchanged while analysis of MnSOD activity revealed even an increase of SOD activity with age (Andziak *et al.*, 2005). These results suggested that SOD activity levels in mice do not change with age. Cu/ZnSOD activity in brain tissues of aging rats, however, showed a gradual decline in activity, which appeared to be caused by a decrease in SOD expression levels (Semsei *et al.*,

1991). Studies in other model systems were consistent with the results obtained in mice and showed that SOD activity levels either remained unaltered during the lifespan (i.e., *C. elegans*) or linearly increased with age (i.e., *Drosophila lysates*) (Vanfleteren, 1993; Sohal *et al.*, 1990). Expression levels of Cu/ZnSOD, as determined by mRNA and steady state SOD protein analysis, remained relatively constant in aged flies (Radyuk *et al.*, 2004). These results ruled out the possibility that a significant decrease in SOD activity and/or level was directly responsible for the oxidative damage observed in aging organisms.

#### *Catalases, Glutathione peroxidases and Peroxidases*

Studies assessing the activity of peroxide-detoxifying enzymes during the lifespan revealed a relatively consistent trend, indicating that the peroxide detoxifying capacity of organisms does indeed decrease with age. Analysis of the catalase activity in liver samples of mice, for example, showed a decline with the age of the animals (Perichon and Bourre, 1995). A significantly decreased level of catalase and glutathione peroxidase activity was also observed in liver homogenates of 18 months old mice in comparison to 12 months old animals (Andziak *et al.*, 2005), a finding that was independently confirmed for catalase in heart tissue and for glutathione peroxidase in kidney (Sohal *et al.*, 1994).

Also brain samples of rats have been reported to exhibit a gradual decline of catalase activity coinciding with a decrease in catalase mRNA (Semsei *et al.*, 1991), although brain tissue of aged mice apparently exhibited increased catalase and glutathione peroxidase activity (Sohal *et al.*, 1994). Analysis of non-rodent model systems were overall also more consistent, revealing kinetics of catalase activity in *Drosophila* that seem to follow a bell-shaped curve with higher levels of catalase in young animals as compared to older animals (Sohal *et al.*, 1990; Durusoy *et al.*, 1995). In a subsequent more thorough analysis, catalase expression was shown to be both time- and tissue-specific, coinciding with pulses of ecdysteroid synthesis during development followed by a small decline as flies aged (Klichko *et al.*, 2004). Studies in young *C. elegans* adults revealed a similar initial increase in the catalase activity and a decline as the worms aged (Vanfleteren, 1993). Dramatic changes in expression level were also observed for peroxiredoxin 5 in *Drosophila*, which showed the highest expression level during embryogenesis, followed by a decline during aging (Radyuk *et al.*, 2009). These results are largely consistent with the idea that the activity levels of peroxide-

detoxifying enzymes decrease as animals age, potentially leading to the accumulation of peroxide in aging tissue.

#### *Glutaredoxin, Thioredoxin and NADPH*

Expression analyses were conducted to monitor the activity of the thioredoxin and glutaredoxin system to assess whether changes in the activity of the cellular redox systems contribute to the oxidative damage observed in aging organisms. An early study focusing on the thioredoxin system in rat kidneys reported decreasing levels of both thioredoxin and thioredoxin reductase with the age of the animals (Cho *et al.*, 2003). The same study also found decreased levels of reduced glutathione and glutathione reductase activity in older rat kidneys as compared to young animals. These results were independently confirmed in aged rat muscles, where expression levels of both mitochondrial thioredoxin reductase and cytosolic thioredoxin were significantly reduced (Rohrbach *et al.*, 2006). In contrast, however, levels of mitochondrial thioredoxin appeared to increase with age (Rohrbach *et al.*, 2006). Moreover, comparative analysis of the glutathione and thioredoxin system in the heart muscle of young and old rats did not reveal any significant changes but did reveal an increase in oxidized GSSG levels, indicative of a pro-oxidant shift in the glutathione reduction potential (Jacob *et al.*, 2010). A pro-oxidant shift in the glutathione pool has also been reported to occur in multiple other tissues of aging mice and rats, generally caused by an increase in oxidized glutathione and sometimes accompanied by a decrease in reduced glutathione. These changes tend to be most significant in liver tissues (Rebrin and Sohal, 2008). Given that both glutaredoxin and thioredoxin systems rely heavily on reduced NADPH to maintain redox homeostasis, this shift in redox potential might be partially explained by a decrease in cellular NADPH levels, which has been observed to occur in the neurons of aging rats (Parihar *et al.*, 2008). Studies in invertebrates confirmed some of the results obtained in rodents. It was shown, for instance, that the reduced glutathione pool sharply declines in older flies (Sohal *et al.*, 1990). Moreover, caloric restriction, one of the few near-universal life prolonging measures has been shown to partially reverse the detected changes in redox potential (Someya *et al.*, 2010; Cho *et al.*, 2003; Rohrbach *et al.*, 2006). In summary, these studies provide convincing evidence that a combined decline in the cellular anti-oxidant capacity occurs with the age of the animal, which likely contributes to the accumulation of oxidative damage.

## 2.5 Manipulation of the antioxidant capacity and the effect on lifespan

After years of correlative studies, big hopes were spawned with the development of methods that enable genetic manipulations of model organisms, as they should allow direct and unambiguous testing of the validity of the “Free Radical Theory of Aging”. If correct, modulating endogenous ROS levels either by deleting or overexpressing specific antioxidant systems should have clear effects on lifespan. An overview of the published studies conducted in mice, *Drosophila* and *C. elegans* can be found in Table 2.1 and 2.2. The many conflicting results obtained with genetic manipulations of antioxidant enzymes in a variety of different organisms over the last few years clearly illustrate the complexity of redox homeostasis and its role in lifespan. In general, deletion of antioxidant enzymes appears to have one of two outcomes. One being so serious that the organism is severely affected - thus decreased lifespan may not be a direct result of premature aging. The other one having little to no effect at all, suggesting either significant redundancy with other antioxidant enzymes or implying that their function is so highly specialized as to not affect longevity under “normal” conditions. Hence, it is probably unwise to draw significant conclusions from deletion studies. Overexpression studies could be viewed as a more direct approach to analyze the influence of antioxidant systems on aging. However, confusion arose from studies where the same genetic manipulations revealed different effects in different labs. This suggests that specific growth conditions, the design of experiment, and/or differences in the strain background might be additional factors that influence lifespan and need to be carefully controlled and monitored.

Antioxidant system	Species	Stress resistance	Lifespan	Ref
<b>Cu/Zn Superoxide dismutase</b>				
$\Delta sod1$	<i>Mm</i>		↓	1,2
$\Delta sod1$	<i>Dm</i>	↓	↓	3
$\Delta sod1$	<i>Ce</i>	↓	↓↔ <sup>a</sup>	4 - 7
$\Delta sod1 + \Delta sod2; \Delta sod3; \Delta sod4; \Delta sod5$	<i>Ce</i>	↓	↓↔	6, 7
$\Delta ECsod$	<i>Mm</i>	↓	↔	8, 9
<b>Mn Superoxide dismutase</b>				
$\Delta sod2$ <sup>Het, b</sup>	<i>Mm</i>	↓	↔	10, 11
$\Delta sod2$	<i>Dm</i>	↓ <sup>Het</sup>	↓ <sup>b</sup>	12
$\Delta sod2$	<i>Ce</i>	↓↔	↑↔	4, 6, 7
$\Delta sod2 + \Delta sod1; \Delta sod3; \Delta sod4; \Delta sod5$	<i>Ce</i>	↓	↑↔	6, 7
$\Delta sod1 \Delta sod2 \Delta sod3 \Delta sod4 \Delta sod5$	<i>Ce</i>	↓	↔ <sup>c</sup>	13
<b>Catalase</b>				
$\Delta cat$	<i>Mm</i>	↔	↔ <sup>d</sup>	14
$\Delta cat$	<i>Dm</i>	↓	↓	15, 16
$\Delta ctl1$	<i>Ce</i>		↔	17
$\Delta ctl2$	<i>Ce</i>		↓	17
<b>Peroxioredoxin</b>				
$\Delta prdx1$	<i>Mm</i>		↓	18
$\Delta prdx2$ <sup>e</sup>	<i>Dm</i>	↓	↓	19
$\Delta prdx2$	<i>Ce</i>	↓	↓	20 21
$\Delta prdx5$	<i>Dm</i>	↓	↓ <sup>f</sup>	22
<b>Glutathione peroxidase</b>				
$\Delta gpx1$	<i>Mm</i>	↓↔	↔	23 - 25
$\Delta gpx4$ <sup>Het, g</sup>	<i>Mm</i>		↑	26
<b>Thioredoxin</b>				
$\Delta trx1$	<i>Ce</i>	↓	↓	27, 28
$\Delta trx2$ <sup>Het, g</sup>	<i>Mm</i>		↔	2
$\Delta trx2$	<i>Dm</i>	↓	↓	29, 30

**Table 2.1. Effects of deletion of antioxidant genes on stress resistance and lifespan.**

1, (Elchuri *et al.*, 2004); 2, (Pérez *et al.*, 2009a); 3, (Phillips *et al.*, 1989); 4, (Yen *et al.*, 2009); 5, (Yanase *et al.*, 2009); 6, (Doonan *et al.*, 2008); 7, (Van Raamsdonk and Hekimi, 2009); 8 (Carlsson *et al.*, 1995); 9, (Sentman *et al.*, 2006); 10, (Van Remmen *et al.*, 2003); 11, (Van Remmen *et al.*, 2004); 12, (Duttaroy *et al.*, 2003); 13, (Van Raamsdonk and Hekimi, 2012); 14, (Ho *et al.*, 2004); 15, (Mackay and Bewley, 1989); 16, (Griswold *et al.*, 1993); 17, (Petriv and Rachubinski, 2004); 18, (Neumann *et al.*, 2003); 19, (Lee *et al.*, 2009a); 20, (Kumsta *et al.*, 2011); 21, (Oláhová *et al.*, 2008); 22, (Radyuk *et al.*, 2009); 23, (Ho *et al.*, 1997); 24 (Fu *et al.*, 1999); 25, (Zhang *et al.*, 2009); 26, (Ran *et al.*, 2007); 27, (Miranda-Vizuete *et al.*, 2006); 28, (Jee *et al.*, 2005); 29, (Tsuda *et al.*, 2010); 30, (Svensson and Larsson, 2007); **Abbreviations:** *Mm*, *M. musculus*; *Dm*, *D. melanogaster*; *Ce*, *C. elegans*; <sup>Het</sup> heterozygous; <sup>a</sup> *sod1* deletion reduces hypothermia-induced lifespan extension, <sup>b</sup> Homozygous deletion has severe health effects ; <sup>c</sup> Maximum lifespan extended; <sup>d</sup> Observation up to one year of age; <sup>e</sup> Null mutation or RNAi knockdown, stress resistance assessed in RNAi knock-down; <sup>f</sup> Accelerated death during development, maximum lifespan normal; <sup>g</sup> Homozygous deletion embryonic lethal.

Antioxidant system	Species	Stress resistance	Lifespan	Ref
<b>Cu/Zn SOD overexpression</b>				
<i>sod1 +/- sod2</i>	<i>Mm</i>		↔	1-3
<i>sod1</i> (motorneurons)	<i>Dm</i>	↑	↑	4
<i>sod1</i> (ubiquitous)	<i>Dm</i>	↑	↑	5
<i>sod1 +/- sod2</i>	<i>Dm</i>	↔	↔↑ <sup>a</sup>	6-8
<i>sod1</i>	<i>Ce</i>	↓	↑	9, 10
<b>Mn SOD overexpression</b>				
<i>sod2 +/- cat</i>	<i>Dm</i>	↑	↑↔↓ <sup>b,c</sup>	7, 11-14
<i>sod2</i>	<i>Ce</i>		↑	10
<b>Catalase overexpression</b>				
<i>cat</i> (mitochondria)	<i>Mm</i>		↑	15
<i>cat</i> (peroxisomes)	<i>Mm</i>		↔	2, 15
<i>cat</i>	<i>Dm</i>	↑	↓↔ <sup>d</sup>	6,11,16
<i>ctl1 + ctl2 + ctl3</i>	<i>Ce</i>		↓ <sup>e</sup>	9
<b>Peroxioredoxin overexpression</b>				
<i>prx2</i> (neurons)	<i>Dm</i>	↑	↑	17
<i>prx5</i>	<i>Dm</i>	↑	↑	18
<b>Thioredoxin overexpression</b>				
<i>trx1</i>	<i>Mm</i>	↑	↑↔ <sup>f</sup>	19, 20
<i>trx1</i> (neurons)	<i>Ce</i>		↑	21
<i>trx2</i>	<i>Dm</i>	↑	↑	22, 23

**Table 2.2. Effects of overexpression of antioxidant genes on stress resistance and lifespan.**

1, (Huang *et al.*, 2000); 2, (Pérez *et al.*, 2009b); 3, (Rando *et al.*, 1998); 4, (Parkes *et al.*, 1998); 5, (Reveillaud *et al.*, 1991); 6, (Sun and Tower, 1999); 7, (Sun *et al.*, 2004); 8, (Seto *et al.*, 1990); 9, (Doonan *et al.*, 2008); 10, (Cabreiro *et al.*, 2011); 11, (Mockett *et al.*, 2010); 12, (Mockett *et al.*, 1999); 13, (Bayne *et al.*, 2005); 14, (Sun *et al.*, 2002); 15, (Schriner *et al.*, 2005); 16, (Griswold *et al.*, 1993); 17, (Lee *et al.*, 2009a); 18, (Radyuk *et al.*, 2009); 19, (Mitsui *et al.*, 2002); 20, (Pérez *et al.*, 2011); 21, (Miranda-Vizueté *et al.*, 2006); 22, (Svensson and Larsson, 2007); 23, (Seong *et al.*, 2001); <sup>a</sup> Simultaneous overexpression of *sod1* and *sod2* increased the lifespan additively; <sup>b</sup> MnSOD has slightly decreased lifespan (4-5%); <sup>c</sup> Simultaneous overexpression of *sod2* and catalase in mitochondria decreased lifespan by 43%; <sup>d</sup> Two *cat*+ strains were tested; while one strain did not show a change in lifespan, the other strain had a significantly decreased lifespan; <sup>e</sup> Deaths by internal hatching; <sup>f</sup> While overexpression of *trx1* in male mice significantly extended earlier part of life (maximum lifespan was unaffected), female mice showed no significant change in lifespan.

## 2.6 A model organism for aging studies: *Caenorhabditis elegans*

In addition to vertebrate model organisms such as mice, established invertebrate model systems for aging research include the fruit fly *Drosophila melanogaster* and the nematode *Caenorhabditis elegans*. The nematodes exhibit age-accompanying physiological changes such as slowed motility or the accumulation of the pigment lipofuscin, which are found in other organisms as well (Olsen *et al.*, 2006; Wood, 1988). *C. elegans*, introduced by Sydney Brenner as model system (Brenner, 1974), can be easily cultivated on agar plates with bacteria as food source and has a life cycle of about three days (Wood, 1988). The development of *C. elegans* is characterized by four con-

secutive larval molts, after which the worms become fertile adults (Wood, 1988). Self-fertilizing hermaphrodites constitute the vast majority of animals within a wildtype population, which allows for the maintenance of an isogenic population (Wood, 1988). *C. elegans* is a multicellular organism and hence possesses distinguishable tissues and organs, such as nervous system, muscle tissue, intestine and reproductive system (White, 1988). The animals have a transparent cuticle, enabling the study of tissues and organs, and the use of genetically expressed fluorescent sensor proteins (Wood, 1988). Many genetic pathways or interventions that affect aging in *C. elegans*, such as the Insulin/IGF-1 signaling pathway or caloric restriction are evolutionary conserved and confer lifespan extension in *D. melanogaster* and mice as well (Kenyon, 2010).

## 2.7 Lifespan-extending interventions in *C. elegans*

### 2.7.1 Manipulation of the Insulin/IGF-1 signaling pathway

Genetic manipulation of the Insulin/IGF-1 signaling (IIS) pathway has been shown to reproducibly modulate lifespan in *D. melanogaster*, *C. elegans* and mice (Longo and Finch, 2003). Insulin/IGF-1 signaling is a highly conserved pathway, which has been implicated in a multitude of physiological processes, including stress response, diapause, reproduction, metabolism, growth, and aging (Tatar *et al.*, 2003). Signaling through the Insulin/IGF-1 receptor occurs via a phosphorylation cascade, which ultimately causes phosphorylation of the forkhead transcription factor FOXO, and prevents FOXO from its translocation into the nucleus. Conversely, lack of the IGF-1 receptor or disruption of the kinase cascade promotes FOXO's translocation into the nucleus and allows the transcriptional regulator to induce the expression of a variety of stress-related genes (Kenyon, 2005). FOXO-controlled genes encode for heat shock proteins, for proteins involved in pathogen resistance, metabolism (e.g.  $\beta$ -oxidation of fatty acids and gluconeogenesis), transcriptional repression and protein degradation as well as for antioxidant enzymes, such as superoxide dismutase, catalase and glutathione S-transferases (Murphy, 2006) (Figure 2.3). These findings suggested that the lifespan extension observed in mutants with compromised insulin signaling might be, at least in part, due to increased oxidative stress protection. Studies in *C. elegans* also revealed that mutants lacking the insulin/IGF-1 receptor *daf-2* or the phosphoinositide kinase PI<sub>3</sub>K (*age-1*) show increased level of SOD and catalase activity, significantly increased oxidative stress resistance and



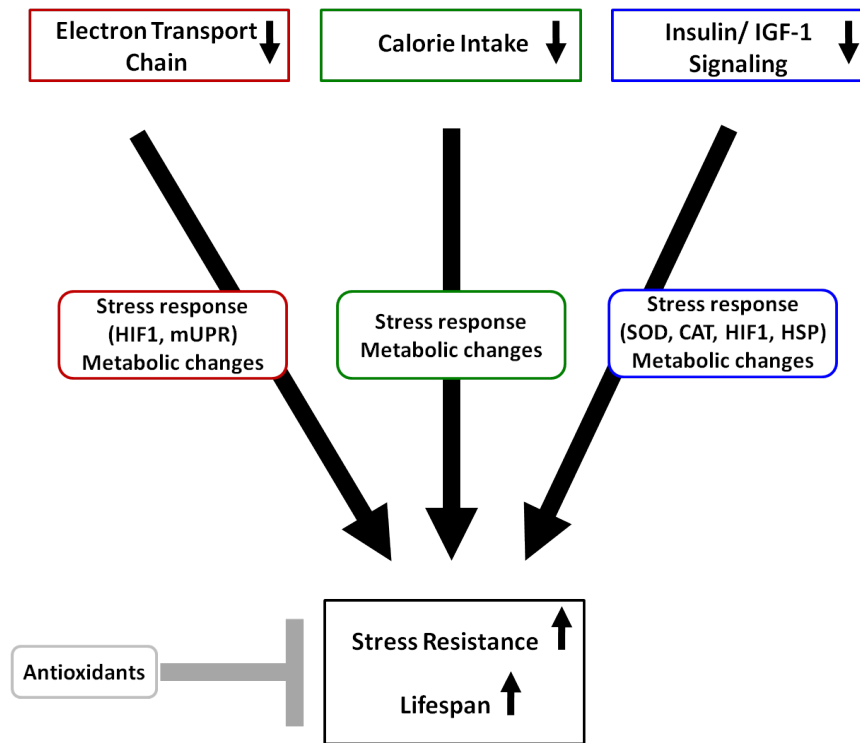


**Figure 2.3. Lifespan-extending interventions in *C. elegans*.** Reduction of components of the electron transport chain (ETC), a decrease in the caloric intake, or reduced Insulin/IGF-1 signaling extends lifespan in *C. elegans*. One factor that might contribute to the observed lifespan extension is an increased stress resistance. The role that oxidants play in these lifespan-extending interventions is not fully elucidated yet. However, it has been demonstrated that antioxidants typically interfere with the observed lifespan extensions. Note: Some ETC mutants can also be short-lived.

exhibit very extended lifespans (Honda and Honda, 1999; Johnson, 1990; Kenyon *et al.*, 1993; Brys *et al.*, 2007). The lifespan-extending features were found to strictly depend on the presence of the FOXO transcription factor DAF-16 as *C. elegans* mutants lacking DAF-16 show increased sensitivity towards paraquat-mediated oxidative stress and are severely short-lived (Yanase *et al.*, 2002; Lin *et al.*, 2001). *Daf-16* mutant worms also show significantly increased protein damage as measured by protein carbonylation, providing further confirmation that these animals experience increased levels of oxidative stress (Yanase *et al.*, 2002). At this point it is still unclear which of the many FOXO-regulated genes are ultimately responsible for the observed lifespan extension in worms and other organisms, and what exact role(s) ROS plays in the IIS-mediated lifespan regulation. A RNAi-mediated knock-down of FOXO-target genes, including glutathione transferase, cytosolic *ctl-1*, peroxisomal *ctl-2*, or mitochondrial superoxide dismutase *sod-3* was found to individually reduce the long lifespan of *daf-2* mutants while deletion of the cytosolic superoxide dismutase *sod-*

*I* had no effect on the lifespan of *daf-2* mutants. Moreover, loss of the extracellular superoxide dismutase *sod-4* further extended *daf-2*-mediated lifespan (Murphy *et al.*, 2003; Ayyadevara *et al.*, 2005; Doonan *et al.*, 2008). That lifespan-extension by compromised Insulin/IGF-1-signaling is not solely due to a reduction of oxidants and decreased oxidative damage became obvious when long-lived *daf-2* mutants were found to have higher respiratory rates, and exhibit increased levels of mitochondrial ROS level (Houthoofd *et al.*, 2005; Zarse *et al.*, 2012). When Insulin/ IGF-1 signaling was reduced during adulthood of worms, elevated respiration was observed that caused a transient increase in ROS, which eventually led to increased activity of catalase and SOD (Zarse *et al.*, 2012). The observed lifespan extension of IIS reduction was diminished upon treatment with antioxidants (Zarse *et al.*, 2012; Yang and Hekimi, 2010; Brys *et al.*, 2007). The observation that treatment of worms with the superoxide generator juglone caused nuclear translocation (i.e., activation) of DAF-16 while exposure to hydrogen peroxide lead to phosphorylation (i.e., inactivation) of DAF-16 (Weinkove *et al.*, 2006; Nemoto and Finkel, 2002) suggested that the type of oxidant and possibly its sub-cellular accumulation might affect signaling processes, oxidative stress resistance and ultimately the lifespan of organisms.

### 2.7.2 Caloric restriction

Reduction of the daily caloric intake by 30% (dietary or caloric restriction) routinely extends lifespan up to 50% in a variety of different model organisms, including yeast, flies, *C. elegans*, mice and primates (McCay *et al.*, 1935; Fontana *et al.*, 2010). Whereas earlier findings seemed to indicate that caloric restriction resulted in a lowered metabolic rate, more recent studies that were corrected for body mass suggested quite the opposite (Houthoofd *et al.*, 2002). In fact, caloric restriction appears to enhance mitochondria biogenesis (Lopez-Lluch *et al.*, 2006) and to increase the rate of respiration (Lin *et al.*, 2002; Nisoli *et al.*, 2005) (Figure 2.3). These results, although initially counterintuitive, are fully consistent with recent studies in *C. elegans*, which showed that 2-deoxyglucose (DOG)-mediated glucose restriction during adulthood increased mitochondrial respiration and ROS production, and significantly extended the lifespan (Schulz *et al.*, 2007) Interestingly pre-treatment of these animals with antioxidants, such as N-acetylcysteine (NAC) or vitamin E abolished the beneficial effect of glucose restriction on lifespan (Schulz *et al.*, 2007). These findings led to the model of mitohormesis, in which generation of slightly elevated levels of oxidants through increased res-

piration during a defined time in life enhances expression of antioxidant genes and with that, the capacity of organisms to detoxify ROS. Contrary to glucose-restriction, glucose-supplementation of *C. elegans*' diet prevented longevity of *daf-2* worms, and shortened the lifespan of wildtype animals by inhibiting the transcription factor DAF-16 (Lee *et al.*, 2009b; Schlotterer *et al.*, 2009). Interestingly, increased ROS generation was found at day 15 in worms fed on high-glucose-diet, suggesting that the duration of increased ROS level (or the magnitude) might make a difference in lifespan determination (Schlotterer *et al.*, 2009).

### 2.7.3 Impairment of the Electron Transport Chain

Screens for longevity genes mediated by RNAi found a ten-fold overrepresentation of genes involved in mitochondrial function (Lee *et al.*, 2002). The knock-down of those mitochondrial genes improved the H<sub>2</sub>O<sub>2</sub> tolerance of worms (although paraquat tolerance was reduced) and extended their lifespan (Lee *et al.*, 2002). Selective targeting of individual components of the electron transport chain (ETC), including proteins of complex I, III, IV and V caused a significant extension of the lifespan of *C. elegans* (Dillin *et al.*, 2002b). It is of note that reducing ETC function had to be initiated during *C. elegans* development to achieve lifespan extension whereas reduction of ETC components during adulthood of *C. elegans* resulted in lowered ATP level but no changes in lifespan (Dillin *et al.*, 2002b) (Figure 2.4). These results imply that the rate of mitochondrial respiration during development is at least partly responsible for adjusting *C. elegans*' growth rate, development, and adult lifespan. The developmental window during which the intervention seems to be successful ends by the third or early fourth larval stage of *C. elegans*, indicating that an event occurring during larval development might set the clock for lifespan (Rea *et al.*, 2007). One mechanism, which seems to play a role in the lifespan extension mediated by ETC reduction is the mitochondria-specific unfolded protein response (UPR), which can be induced in a cell-non-autonomous way, meaning that signals from one tissue can trigger or control processes in other tissues (Durieux *et al.*, 2011) (Figure 2.3).

Another mechanism might be ROS-mediated signaling since many long-lived strains with mutations in the ETC, such as *nuo-6*, *isp-1* and *clk-1*, showed elevated ROS level (Yang and Hekimi, 2010; Lee *et al.*, 2010). In fact, treatment of *nuo-6* and *isp-1* mutants with the antioxidant NAC abolished the observed lifespan extension, suggesting that (transient) accumulation of oxidants might ac-

tually be required for the lifespan-prolonging phenotype of those mutants (Yang and Hekimi, 2010), and speaking against the idea that accumulation of ROS is toxic per se. Observations in *C. elegans* suggested that compromised respiration could be involved in the ROS-mediated activation of HIF-1, which is indeed responsible for the lifespan extension observed in *C. elegans clk-1* and *isp-1* mutants (Lee *et al.*, 2010). Similarly, the treatment with low concentrations of the superoxide generator paraquat caused a transient increase in superoxide, which might result in a ROS-induced activation of HIF-1, and significantly increased the lifespan of *C. elegans* despite an apparent increase in oxidative protein damage (Yang and Hekimi, 2010; Lee *et al.*, 2010).

Taken together, these studies suggest that lifespan extension achieved by reducing mitochondrial respiration is not simply caused by minimizing the output of harmful reactive oxygen species and decreasing oxidative damage. It rather seems to involve the activation of complex pathways, including the unfolded protein response (UPR) (Durieux *et al.*, 2011), cell-cycle checkpoint control (Rea *et al.*, 2007), changes in HIF-1-mediated gene expression (Lee *et al.*, 2010) and possibly a switch in energy metabolism (Rea and Johnson, 2003) (Figure 2.3). That respiratory mutants do not mediate their longevity by one unifying feature was suggested by the finding that reduction of HIF-1 (either by mutation or RNAi) significantly reduced the extended lifespan of *isp-1* and *clk-1* mutants but only partially affected the long-lived phenotype of other mitochondrial mutants, such as *cyc-1* or *cco-1* (subunits of complex III and IV) (Lee *et al.*, 2010). This finding might also explain the apparently controversial results concerning the role of ROS in lifespan extension of mitochondrial mutants. While antioxidant treatment was found to not affect lifespan extension of some mitochondrial RNAi mutants (Durieux *et al.*, 2011), other studies reported that superoxide is in fact required to mediate lifespan extension (Yang and Hekimi, 2010).

## 2.8 Theoretical background

Redox proteomic analysis conducted over the lifespan of wildtype *C. elegans* revealed that protein thiol oxidation increases with the age of the worms (Knoefler *et al.*, 2012a). In addition, the unexpected finding was made that *C. elegans* also exhibits increased levels of oxidized proteins during larval development. Proteins were then rapidly re-reduced upon animals entering their reproductive period (Knoefler *et al.*, 2012a). Many of the proteins, which showed reversible oxidation during development have been previously shown to contain peroxide-sensitive cysteines (Kumsta *et al.*,

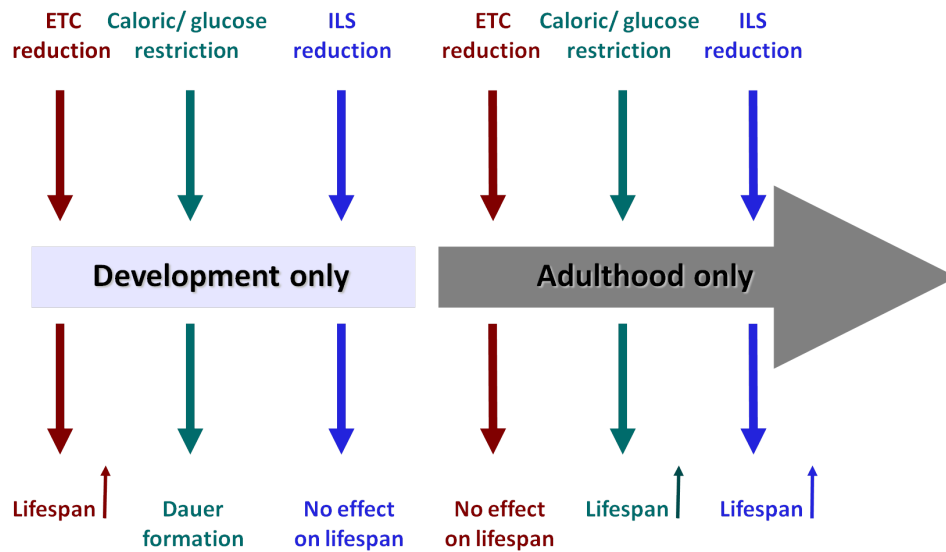


**Figure 2.4. Timing requirements for lifespan extension in *C. elegans*.** While a reduction of the electron transport chain (ETC) during development extends lifespan, the impairment of the Insulin/IGF-1 signaling (ILS) only during development does not have any effect on lifespan. In contrast, reduction of ILS during adulthood extends lifespan in *C. elegans*, while ETC reduction in adulthood has no effect on lifespan. Dietary restriction during adulthood extends lifespan in worms, while food limitation during development results in dauer formation of *C. elegans* larvae (Cassada *et al.*, 1975).

2011; Joe *et al.*, 2008; Maeda *et al.*, 2004), suggesting that the increased protein oxidation might be peroxide-mediated. The goal of this work was to determine to what extent levels of endogenous hydrogen peroxide fluctuate over the lifespan of *C. elegans*, and to assess whether changes in peroxide levels correlate with protein thiol oxidation and ultimately lifespan. To determine peroxide levels on an individual worm basis, probes needed to be established that could specifically detect *in vivo* peroxide level in a temporal and spatial resolution.

## 2.8.1 Measurement of intracellular reactive oxygen species

### 2.8.1.1 Fluorescent dyes

A common method for the measurement of intracellular reactive oxygen species utilizes the fluorescent properties of lipophilic molecules, such as dihydrodichlorofluorescein diacetate (H<sub>2</sub>DCF-DA) (Keston and Brandt, 1965). Once the membrane-permeable dyes enter the cells, intracellular esterases cleave the acetate moiety, thus retaining H<sub>2</sub>DCF inside the cell (Bass *et al.*, 1983). Intracellular reactive oxygen species then oxidize the non-fluorescent H<sub>2</sub>DCF yielding the fluorescent

dichlorofluorescein. Although commonly used in measuring  $\text{H}_2\text{O}_2$  or other reactive oxygen species, its specificity has been recently called into question (Karlsson *et al.*, 2010). Karlsson and co-worker suggested that induction of DCF-fluorescence depends less on peroxide but on cytosolic Fenton-type reactions involving iron and enzymatic oxidation by cytochrome c. DCF fluorescence thus does not necessarily indicate oxidative stress conditions but could result from lysosomal or mitochondrial membrane permeabilization as this leads to the release of lysosomal metals and cytochrome c into the cytosol (Karlsson *et al.*, 2010).

Another assay for the measurement of hydrogen peroxide is based on the reaction of peroxide with Amplex<sup>®</sup>Red (Molecular probes), a fluorogenic substrate of horseradish peroxidase. Amplex<sup>®</sup>Red becomes fluorescent specifically upon exposure to peroxide with a 1:1 stoichiometry (Zhou *et al.*, 1997). The excitation and emission spectra are in the far-red spectrum, thus avoiding interference with autofluorescence (Zhou *et al.*, 1997). An improved version of this fluorescent dye is Amplex<sup>®</sup>UltraRed (Molecular probes), as its fluorescence remains stable over a broader pH range, making the measurement of hydrogen peroxide in theory independent of the pH-value of the solution. Using the Amplex<sup>®</sup>UltraRed assay, the release of hydrogen peroxide into the surrounding media and the subsequent conversion from Amplex<sup>®</sup>UltraRed to the fluorescent Amplex<sup>®</sup>UltraRed can be measured. A disadvantage of this assay is that it cannot detect peroxide level in a tissue-specific manner.

### 2.8.1.2 Genetically encoded fluorescent sensor proteins

In recent years many genetically encoded redox-probes have been developed that allow specific detection of dynamic changes of the *in vivo* redox environment (Meyer and Dick, 2010). For the specific detection of peroxide levels, the HyPer (Hydrogen Peroxide) sensor can be utilized. HyPer is a fusion protein, consisting of a circularly permuted yellow fluorescent protein (cpYFP) and the regulatory domain of the *E. coli* hydrogen peroxide sensor OxyR (Belousov *et al.*, 2006). Cysteine 199 of OxyR, the redox center of the transcription factor, forms a sulfenic acid intermediate upon reaction with  $\text{H}_2\text{O}_2$  (Kullik *et al.*, 1995). A disulfide bond then forms between cysteine 199 and the nearby cysteine 208 (Zheng *et al.*, 1998). This disulfide bond formation changes the structural conformation of OxyR (Choi *et al.*, 2001), resulting in alterations in the fluorescent properties of the HyPer sensor. In its reduced state, the HyPer protein has two excitation maxima at 420 nm and

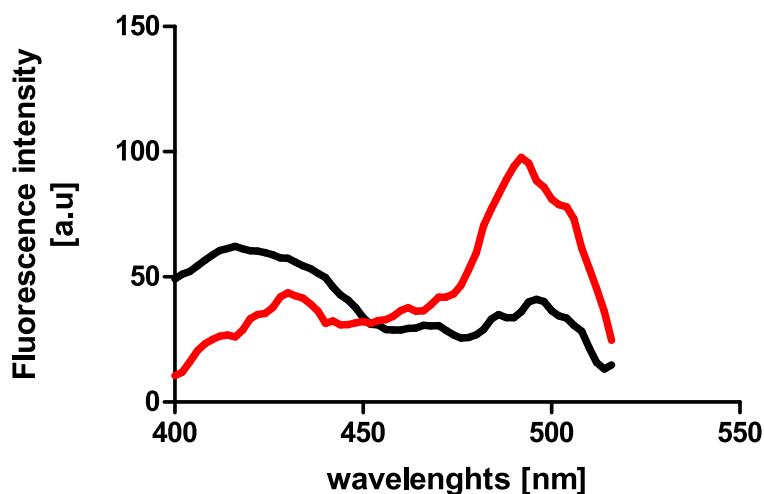


**Figure 2.5. Fluorescence emission spectra of the HyPer sensor.** HyPer fluorescence spectra (HyPer expressed in *E. coli* MG1655) of untreated bacteria (black line) and upon oxidation (20 mM diamide, red line) are displayed. Upon oxidation the emission after excitation with ~ 500 nm increases, while the emission upon excitation with ~ 420 nm decreases. The fluorescence spectra was measured with the Cary Eclipse Fluorescence Spectrophotometer (Varian) at an emission of 530 nm (slit: 10 nm) and excitation wavelengths 400 nm to 530 nm (slit: 2.5). Diamide has been shown to activate OxyR (Zheng *et al.*, 1998).

500 nm, with one single emission maximum at 530 nm. Upon exposure to peroxide, the emission upon excitation with 420 nm decreases while the emission after excitation with 500 nm increases proportionally (Figure 2.5). Thus, HyPer provides a ratiometric read-out of endogenous peroxide levels (Belousov *et al.*, 2006).





### 3 Objective of the thesis

The goal of my thesis was the establishment of peroxide-specific probes and their utilization as read-outs of endogenous H<sub>2</sub>O<sub>2</sub> level over the lifespan of *Caenorhabditis elegans*. A variety of independent techniques are utilized, such as the redox status of *C. elegans* peroxiredoxin as sensor of intracellular hydrogen peroxide, or the fluorescence-based AmplexUltra<sup>®</sup>Red assay to measure the release rate of H<sub>2</sub>O<sub>2</sub> from the animals.

The focus of my thesis was the hydrogen peroxide sensor HyPer, and the main aims were 1) the generation of transgenic *C. elegans* expressing the hydrogen peroxide sensor HyPer under a tissue-specific promoter, 2) the establishment of the HyPer detection method in worms, and 3) the determination of the HyPer ratio (i.e, peroxide level) over the lifespan of wildtype *C. elegans*.

Additionally, the effect of lifespan-modulating interventions, such as manipulation of the Insulin/ IGF-1 signaling, glucose restriction, or the influence of cultivation temperature on peroxide level and lifespan, was to be assessed to investigate the role reactive oxygen species could play in physiology and lifespan of *C. elegans*.



## 4 Results

### 4.1 *C. elegans* produce high concentrations of hydrogen peroxide during development<sup>2</sup>

#### 4.1.1 Redox state of peroxiredoxin 2 as read-out for endogenous peroxide level

Peroxiredoxins are enzymes responsible for the detoxification of intracellular peroxide. *C. elegans* peroxiredoxins 2 (PRDX-2) belong to the class of typical 2-cysteine peroxiredoxins, which contain two reactive cysteines: one peroxidatic and one resolving cysteine residue. Peroxide reacts with the peroxidatic cysteine residue of one peroxiredoxin molecule causing the formation of a sulfenic acid intermediate. The sulfenic acid then reacts with the resolving cysteine residue of another peroxiredoxin monomer, thereby forming a peroxiredoxin dimer connected by an intermolecular disulfide bond (Cox *et al.*, 2010). Oxidation of peroxiredoxin is fully reversible. The disulfide-bonded peroxiredoxin dimer is rapidly reduced by thioredoxin, which, in turn, is reduced by the NADPH-dependent thioredoxin reductase (Holmgren, 1985). The sulfenic acid intermediate of PRDX-2, however, can also get overoxidized by an excess amount of hydrogen peroxide. Overoxidation leads to the formation of sulfinic acid, which is unable to form a disulfide bond with another PRDX-2 molecule, thus remaining monomeric (Figure 4.1). *C. elegans* peroxiredoxin 2 has been shown to form a second disulfide upon exposure to H<sub>2</sub>O<sub>2</sub>, which is distinguishable from the other PRDX-2 disulfides (Oláhová *et al.*, 2008) (Figure 4.2 A). The fraction of peroxiredoxin dimers (i.e., PRDX-2 disulfide and peroxide-induced PRDX-2 disulfide) can be separated from the fraction of reduced or overoxidized peroxiredoxin monomer on a non-reducing SDS-PAGE. The oxidation state of peroxiredoxin can thus be determined as a function of endogenous peroxide level (Cox *et al.*, 2010). *C. elegans* peroxiredoxin 2 is expressed in a wide range of tissues, including pharynx, intestine, specific neurons and reproductive system<sup>3</sup>, thus providing a ubiquitous read-out of endogenous peroxide level.

<sup>2</sup>Majority of these results are going to be published in Knoefler *et al.* (2012a)

<sup>3</sup>[http://www.wormbase.org/species/c\\_elegans/gene/WBGene00006434?query=PRDX-2#04-9e\\${1}\\$-10](http://www.wormbase.org/species/c_elegans/gene/WBGene00006434?query=PRDX-2#04-9e${1}$-10)

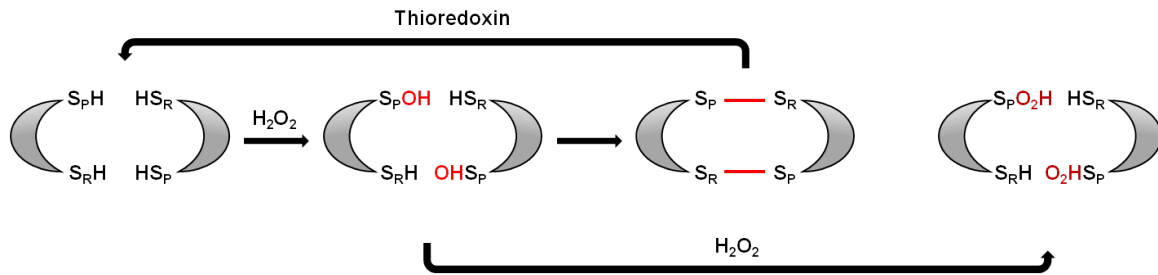


**Figure 4.1. Redox cycle of 2-cysteine peroxiredoxins.** In the presence of peroxide, the reduced peroxidatic cysteine (S<sub>P</sub>H) of a peroxiredoxin monomer becomes oxidized to a sulfenic acid intermediate (S<sub>P</sub>OH), which can react with the resolving cysteine (S<sub>R</sub>H) of a second peroxiredoxin monomer, thus forming a peroxiredoxin disulfide-bonded dimer (S<sub>P</sub>-S<sub>R</sub>). Thioredoxin is able to reduce the dimeric peroxiredoxin. When peroxide is in excess, the peroxidatic cysteine can get overoxidized to a sulfinic acid (S<sub>P</sub>O<sub>2</sub>H), which is unable to form a dimer with another peroxiredoxin monomer. Figure modified from (Cox *et al.*, 2010).

#### 4.1.1.1 Peroxide-induced peroxiredoxin 2 dimers increase upon peroxide treatment

The formation of peroxide-induced disulfide bonds in PRDX-2 was tested by treating a synchronized population of wildtype worms at L4 stage with a sublethal dose of H<sub>2</sub>O<sub>2</sub> (1 mM) for 30 minutes. This concentration of peroxide has been previously shown not to kill the worms but to induce significant behavioral and physiological changes, which are fully reversible (Kumsta *et al.*, 2011). After trapping PRDX-2's redox state with alkylating agents, such as N-ethylmaleimide (NEM) or 4-acetoamido-4'-maleimidylstilbene-2,2'-disulfonic acid (AMS), peroxiredoxin 2 monomers and dimers were separated on a non-reducing SDS-PAGE. The quantification of the bands showed that the fraction of peroxide-induced PRDX-2 disulfides increased upon H<sub>2</sub>O<sub>2</sub> exposure, confirming the hydrogen peroxide-sensitivity of PRDX-2 (Figure 4.2).

#### 4.1.1.2 Peroxide-induced peroxiredoxin 2 dimers are increased during development

The redox state of peroxiredoxin 2 was used as a read-out for endogenous peroxide level during development and adulthood of wildtype *C. elegans*. A population of worms was synchronized and raised at 15°C and aliquots of worms for trapping of the PRDX-2 redox state were taken during development (i.e., L3 and L4 larval stage) and adulthood (i.e., 2-day-old adults). Monomeric (i.e., reduced, overoxidized) and dimeric PRDX-2 were separated on non-reducing SDS-PAGE and subsequently quantified. The fraction of peroxide-induced peroxiredoxin 2 disulfides over the total PRDX-2 amount was determined. As shown in Figure 4.3, we found that the fraction of peroxide-

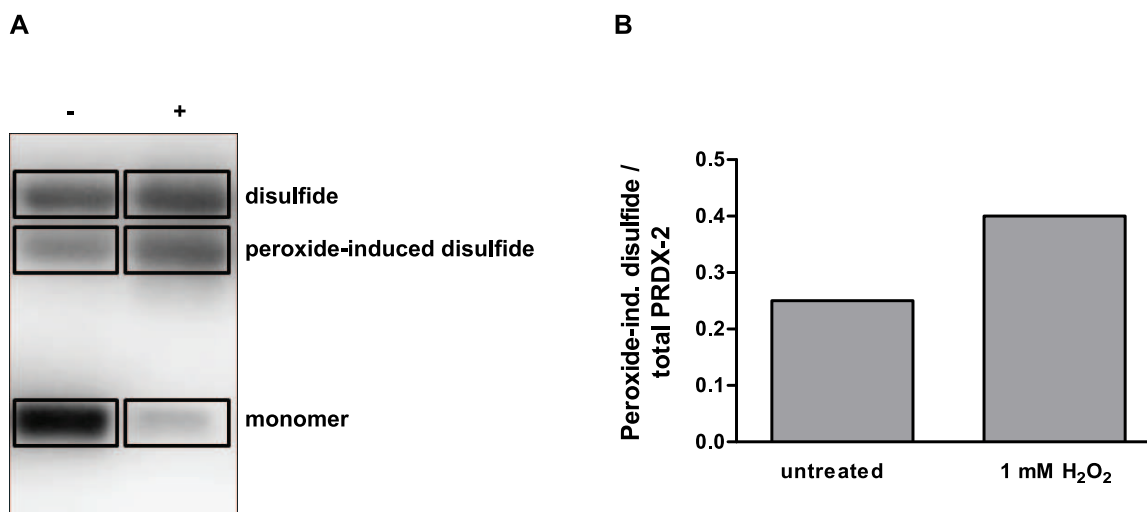


**Figure 4.2. Redox status of *C. elegans* PRDX-2 as a read-out for H<sub>2</sub>O<sub>2</sub> levels.** (A) PRDX-2 monomers, PRDX-2 dimers and peroxide-induced PRDX-2 dimers can be trapped in their redox state, separated on non-reducing SDS PAGE and visualized by immunoblotting. The treatment of living *C. elegans* with 1 mM H<sub>2</sub>O<sub>2</sub> for 30 minutes (+) resulted in increased levels of the peroxide-induced PRDX-2 disulfide fraction compared to the untreated worms (-). (B) Quantification of the PRDX-2 redox state was performed using the Kodac Gel Logic 2200 Imaging System and the Carestream Molecular Imaging Software (v.5.0.2.30).

induced peroxiredoxin 2 was significantly ( $p < 0.05$ ) higher in developing worms in comparison to two-day-old adult worms.

#### 4.1.1.3 Levels of overoxidized peroxiredoxin 2 are higher in early development

The lysis of worms in the absence of alkylating agents causes disulfide bond formation in all those cysteines in peroxiredoxin that are still reduced at the time of lysis (Cox *et al.*, 2010). In contrast, the overoxidized fraction of peroxiredoxin remains monomeric. Thus, quantification of the monomeric fraction in non-thiol trapped preparations can be used as a read-out for the level of overoxidized peroxiredoxin (Cox *et al.*, 2010). The fraction of overoxidized peroxiredoxin 2 of synchronized wildtype *C. elegans* was determined during development (L2, L3, L4 larval stage) and adulthood (1-day-old adults), and was found to be higher at L2 larval stage than in L4 and in one-day-old adults, although differences were not significant due to the small sample size (Figure 4.4). Although these results need to be reproduced, they do suggest the presence of increased levels of hydrogen peroxide during early development.

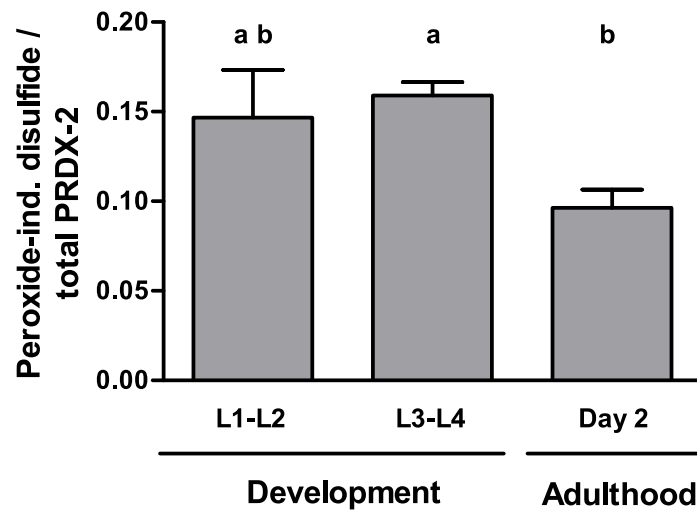


**Figure 4.3. Utilization of the PRDX-2 redox state as read-out for endogenous peroxide levels in *C. elegans*.** A synchronized wildtype population was cultured at 15°C, and worm aliquots were taken during early (L1-L2 larvae) and late development (L3-L4 larvae) and in adulthood (2-day-old adults). The average fraction of peroxide-induced PRDX-2 disulfides over total PRDX-2 amount and the SEM (n= 3-5) are depicted. The fraction of peroxide-induced PRDX-2 disulfides is increased during development than during adulthood. One-way ANOVA and Tukey's multiple comparison test were performed; means which are not significantly different share the same letter ( $p > 0.05$ ).

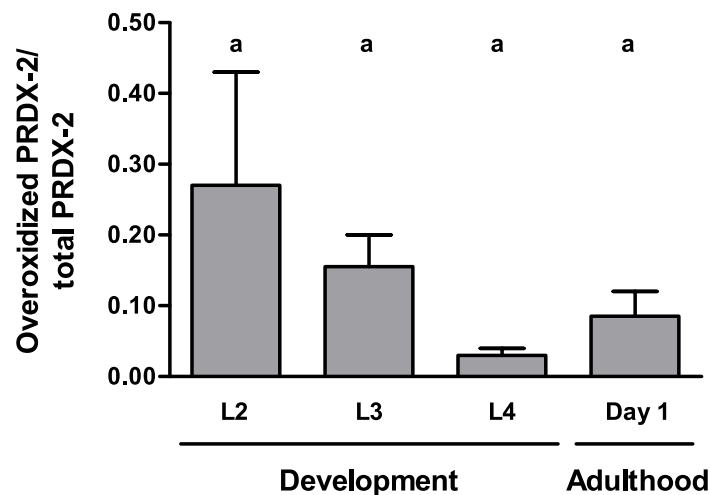


**Figure 4.4. Overoxidized PRDX-2 as read-out for endogenous peroxide level.** The average fraction of overoxidized PRDX-2 at different time points during development (L2, L3 and L4) and adulthood (day 1) and the SEM (n= 2) are presented. Especially in early larval development (L2) higher amounts of overoxidized PRDX-2 are detected. Experiments were performed at 20°C. One-way ANOVA followed by Tukey's multiple comparison test was performed; means which are not significantly different share the same letter ( $p > 0.05$ ).

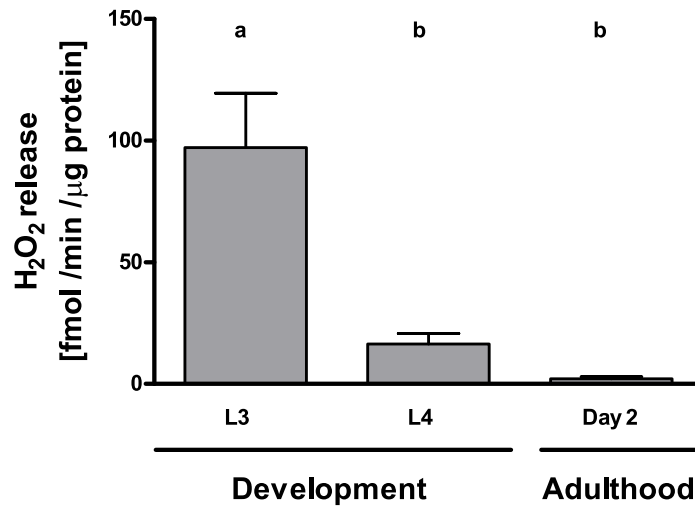


**Figure 4.5. Determination of H<sub>2</sub>O<sub>2</sub> release rates.** The release of hydrogen peroxide from developing (L3 and L4) and two-day-old adult wildtype worms was measured using the AmplexUltra<sup>®</sup>Red reagent. The average H<sub>2</sub>O<sub>2</sub> release and the SEM (n = 7) are displayed. L3 larvae exhibit significantly higher release rates than L4 larvae and young adults. One-way ANOVA followed by Tukey's multiple comparison test was performed on data derived from seven independent experiments.

#### 4.1.2 Measurement of hydrogen peroxide release from live worms

Since hydrogen peroxide has a low reactivity and diffuses rapidly (Giorgio *et al.*, 2007), its generation and subsequent secretion by living worms can be detected using the non-fluorescent compound AmplexUltra<sup>®</sup>Red (Molecular Probes), which turns into the fluorescent AmplexUltrox<sup>®</sup>Red in the presence of hydrogen peroxide (Manual AmplexUltra<sup>®</sup>Red, Molecular Probes). To measure the H<sub>2</sub>O<sub>2</sub> release rates from wildtype *C. elegans* during their development and adulthood, wildtype worms were synchronized and arrested at L1. Development was resumed in a timed manner, so that developing animals (i.e., L3 and L4 larval stage) and two-day-old worms of the same population could be measured simultaneously. A H<sub>2</sub>O<sub>2</sub> standard curve was used to calculate the hydrogen peroxide release rate, which was normalized to the total protein amount. The H<sub>2</sub>O<sub>2</sub> release from developing animals was significantly higher than the release rate from young adult worms ( $p < 0.05$ ) as shown in Figure 4.5.

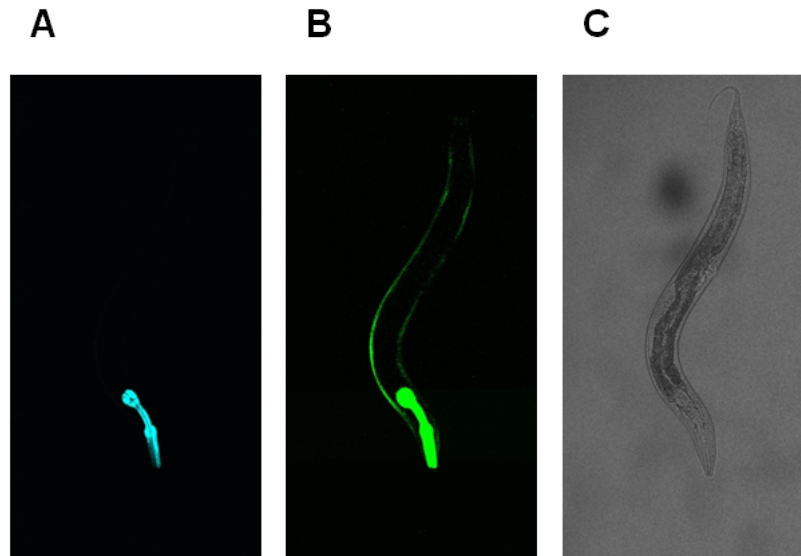


**Figure 4.6. Fluorescence of *C. elegans* expressing *myo-2::GFP* and *unc-54::HyPer*.** (A) Fluorescence of *myo-2::GFP* co-injection marker (pharynx), (B) fluorescence of *unc-54::HyPer* (body wall muscle), (C) and Differential Interference Contrast (DIC) image.

### 4.1.3 Determination of tissue-specific hydrogen peroxide level over the lifespan of *C. elegans*

#### 4.1.3.1 The H<sub>2</sub>O<sub>2</sub> sensor HyPer

The reversibly oxidized proteins that were identified in our OxICAT analysis and initiated these studies were found to be expressed in various tissues and sub-cellular locations of *C. elegans*. We thus set out to study hydrogen peroxide levels on a tissue and cell type-specific basis, which was achieved by using the genetically encoded H<sub>2</sub>O<sub>2</sub> sensor HyPer (Belousov *et al.*, 2006) (see also section 2.8.1.2). The H<sub>2</sub>O<sub>2</sub> sensor protein was cloned under the control of the *C. elegans unc-54* (heavy myosin chain) promoter<sup>4</sup>, which leads to its expression in the body wall muscle cells of *C. elegans*. The DNA was injected into wildtype N2 animals forming extrachromosomal arrays (Mello *et al.*, 1991), and the identification and selection of transgenic progeny was facilitated using the co-injection marker *myo-2::GFP*, which results in the strong expression of a green fluorescent protein in the pharynx as shown in Figure 4.6 A.

A stable transmitting line of worms carrying the HyPer gene (and the co-injection marker) as an extra-chromosomal array was exposed to  $\gamma$ -radiation, which causes chromosomal breaks and the random integration of transgenes into the genome of *C. elegans*. After a homozygous integrated line

<sup>4</sup>Cloning was performed by Caroline Kumsta (University of Michigan).



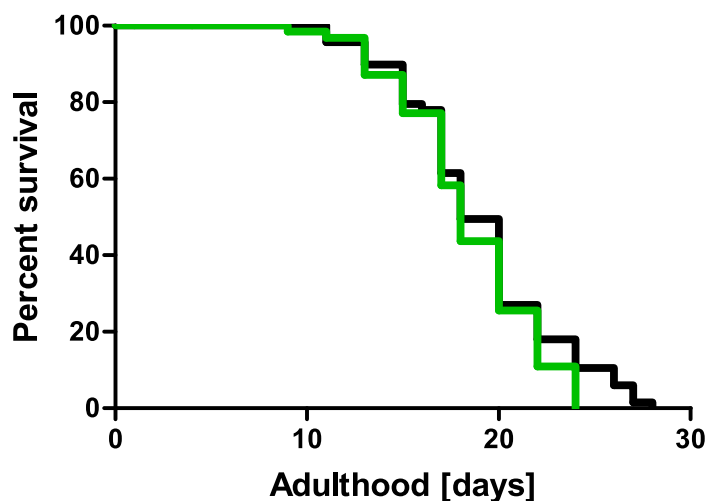


**Figure 4.7. Lifespans of transgenic and wildtype *C. elegans*.** The median survival of wildtype N2 (black line; n = 69 animals) and the transgenic N2 [*unc-54::HyPer*] (green line; n = 65 animals) is not significantly different (18 days);  $p = 0.1956$  (Log-rank Mantel-Cox test) and  $p = 0.4882$  (Gehan-Breslow-Wilcoxon test). Worms that crawled off the plates were censored. The lifespan was assessed at 15°C.

was identified, we backcrossed the line three times with the wildtype strain to minimize background mutations. The presence of the transgenes did not affect development or lifespan of *C. elegans* (Figure 4.7).

The ratiometric nature of the HyPer sensor makes the read-out of the HyPer ratio in principle independent of HyPer protein expression (Belousov *et al.*, 2006). To verify that this was indeed the case, we excited synchronized HyPer transgenic animals with 510 nm and sorted them by their emission strength into three groups using a COPAS SELECT worm sorter. The subsequent determination of the emission intensity after excitation with the 488 nm laser using a confocal microscope confirmed that the sorted groups had indeed different emission intensities (Figure 4.8 A). This finding showed that even in a synchronized isogenic worm population, expression levels of proteins differ significantly between individuals. Hence, a biosensor, whose read-out is unaffected by the amount of protein expressed is a necessity for lifespan studies in *C. elegans*. Next, we determined the HyPer ratios of the different groups (Figure 4.8 B). These studies revealed that all groups had indeed a very similar HyPer ratios, regardless of the HyPer expression level. This confirmation was crucial for our subsequent analyses, in which the HyPer sensor was utilized to determine endogenous hydrogen peroxide level throughout development and adulthood of live *C. elegans*.

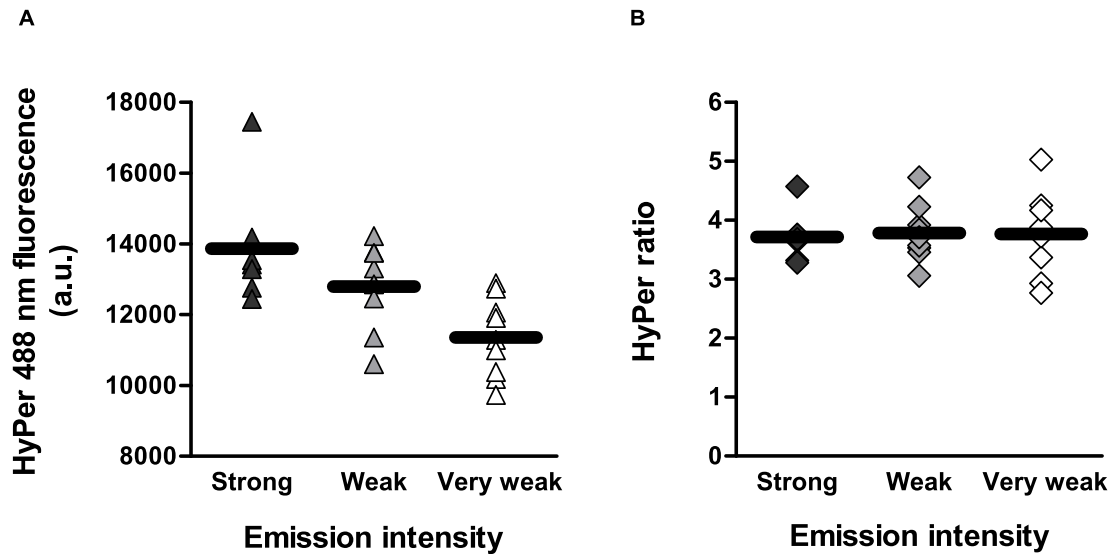


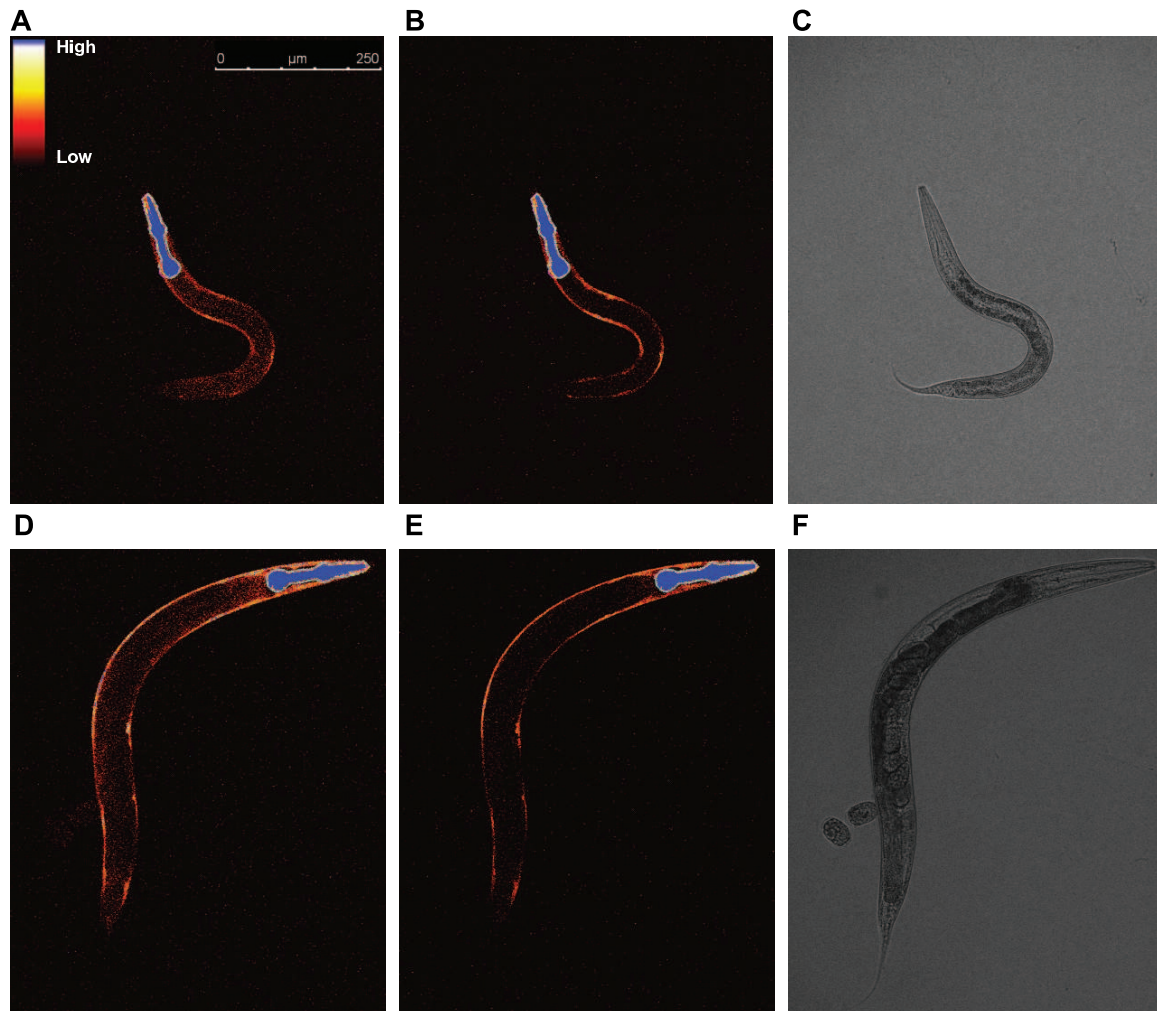
**Figure 4.8. The HyPer ratio is independent of HyPer fluorescence (i.e., HyPer protein expression).** (A) Using the COPAS SELECT worm sorter synchronized L2-L3 larval N2 [*unc-54::HyPer*] worms were sorted according to the emission intensities upon excitation with a 510/10 nm band pass filter into three different groups: strong, weak and very weak. The following day the worms were imaged with a confocal microscope and the sorting for HyPer fluorescence was confirmed using the 488 nm confocal microscope laser (Emission 505 nm to 530 nm). (B) The determination of the HyPer ratio showed that the ratio is independent of HyPer fluorescence.

#### 4.1.3.2 Determination of endogenous $H_2O_2$ level in living wildtype worms

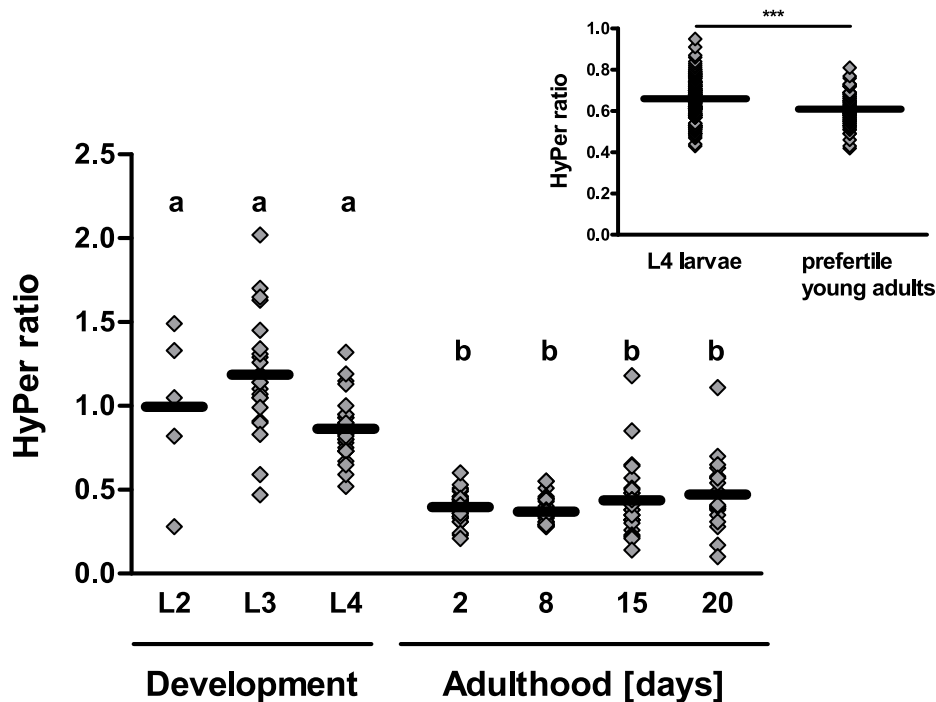
The HyPer sensor was used to determine endogenous hydrogen peroxide level in wildtype *C. elegans*, which express the HyPer sensor in the body wall muscle cells. Worms were synchronized and grown at 15°C, and aliquots of living worms were taken during development (i.e. L2, L3 and L4 larval stage) and during the adult lifespan (day 2, 8, 15 and 20) to determine the HyPer ratio (i.e. level of  $H_2O_2$ ) of individual worms. Representative images of a larval worm and an adult worm are shown in Figure 4.9. The comparison of the emission intensities, represented on a LUT scale, showed that in developing worms, the emission intensity upon 488 nm excitation (i.e., oxidized HyPer) is higher than the emission after excitation at 405 nm (i.e., reduced HyPer), suggestive of increased hydrogen peroxide level in developing worms. In contrast, in two-days-old adults the emission intensity after excitation with 405 nm was found to be higher than the emission upon excitation with 488 nm, suggesting lower amounts of peroxide in young adults.

Image quantification<sup>5</sup> revealed that developing worms (L2, L3 and L4 larvae) had on average

<sup>5</sup>Martin Konieczek (University of Michigan) conceived and implemented the analysis script “wormsuite” for the image quantification and analysis of the HyPer ratio in *C. elegans*



**Figure 4.9. HyPer fluorescence in the body wall muscle cells of larval and adult wildtype *C. elegans*.** Fluorescence (left and center column) and DIC (right column) images of N2 [*unc-54::HyPer*] larvae (L4, upper row) and young adults (Day 2, bottom row) are shown. The fluorescence emissions (505 nm to 530 nm) upon excitation with 405 nm laser (A, D) and with 488 nm laser (B, E) are displayed on a LUT scale. High emission intensities are shown in blue (oversaturated) and white; whereas low intensities are represented in shades of red (see scale in image A). DIC images are shown in C and F. (A, B) In L4 larvae the emission intensity at 488 nm is higher than the emission intensity at 405 nm, (D, E) whereas young adults show higher emission intensity at 405 nm than at 488 nm. The same microscope settings were used. The fluorescence in the pharynx (cyan outline) is the co-injection marker *myo-2::GFP* and was excluded from the HyPer ratio determination.



**Figure 4.10.** Hydrogen peroxide level in the body wall muscle cells of HyPer transgenic *C. elegans*. Aliquots of synchronized wildtype N2 [*unc-54::HyPer*] were imaged and the individual HyPer ratios (rhombus symbol) and the average HyPer ratios (bar) at specific time points during development and adulthood are displayed. Developing N2 [*unc-54::HyPer*] animals have significantly higher HyPer ratios than young adults, which drop to a minimum when worms mature. One-way ANOVA followed by Tukey's multiple comparison test were performed on the log-transformed HyPer ratios, and means that are not significantly different from each other ( $p > 0.05$ ) share the same letter. Experiments were performed at 15°C and repeated at least three times. A representative graph is shown. Inset: The drop in HyPer ratio occurs rapidly when worms transition from L4 larval stage to young adults. The mean HyPer ratios of L4 larvae and pre-fertile young adults are significantly different ( $p = 0.0005$ , unpaired t-test). Experiment was performed at 20°C.

higher HyPer ratios than adult worms, suggesting that the body wall muscle cells (where the HyPer sensor is expressed) of wildtype *C. elegans* are exposed to higher levels of hydrogen peroxide. When worms matured to young adults, the HyPer ratio was found to drop to a minimum, suggesting that reducing redox conditions are restored and less peroxide is present (Figure 4.10). That the drop in the HyPer ratio seems to occur rapidly upon transition from development to adulthood was suggested by the finding that the average HyPer ratio of worms that had just passed the L4-adult molt (prefertile young adults) was significantly lower ( $p = 0.0005$ ) than that of L4 larvae (Figure 4.10, Inset).

To generate a synchronized *C. elegans* population a potent bleach (hypochlorite) solution is used, which lyses the adult worms and releases the eggs. This oxidative stress could theoret-

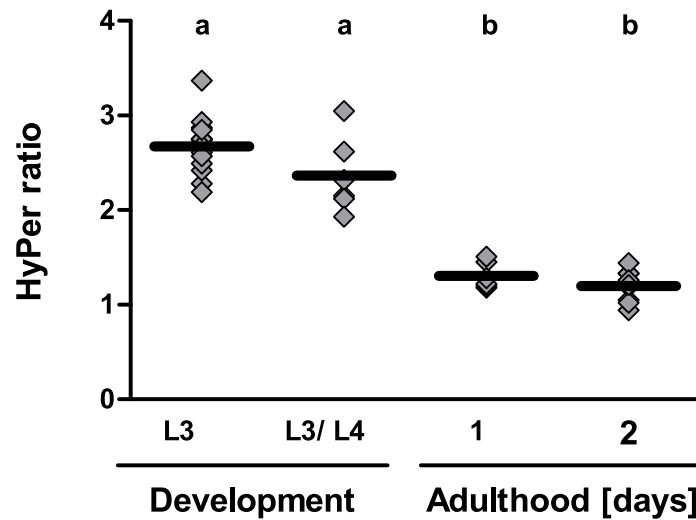


**Figure 4.11. HyPer ratios of unbleached developing and adult animals.** Endogenous hydrogen peroxide level were determined using the  $H_2O_2$  sensor HyPer. Wildtype N2 [*unc-54::HyPer*] worms, which were synchronized without bleaching procedure, exhibit higher HyPer ratios during development than adulthood indicating that elevated HyPer ratios occur independent of the synchronization procedure. One-way ANOVA followed by Tukey's multiple comparison test were performed on the log-transformed HyPer ratios, and means that are not significantly different from each other ( $p > 0.05$ ) share the same letter.

cally contribute to the increased HyPer ratios observed during development. To test whether this might be the case, we synchronized a population of HyPer transgenic worms without the use of the hypochlorite/sodium hydroxide based lysis solution, and subsequently compared the HyPer ratios of developing worms and adult worms (Figure 4.11). As shown before, the average HyPer ratio of larval worms was higher than that of young adults, indicating that it is unlikely that the high HyPer ratio observed during development in our previous experiments are caused by the synchronization procedure.

The experiments using worms expressing the HyPer ratio in the body wall muscle cells had shown that developing worms encounter increased levels of hydrogen peroxide in at least one distinct tissue. To determine the HyPer ratio in other tissues as well, we utilized worms expressing the HyPer sensor ubiquitously under the control of the ribosomal promoter *rpl-17*<sup>6</sup>. Determination of the HyPer ratio in the head region of wildtype worms (i.e., pharynx and neurons) revealed that also these tissues of *C. elegans* encounter high levels of peroxide during development (Figure 4.12). As before, the peroxide levels were found to drop to a minimum when animals matured and reached

<sup>6</sup>N2 (jrIs1[*P<sub>rpl-17</sub>::HyPer*]) animals were kindly provided by Patricia Back (University of Ghent).

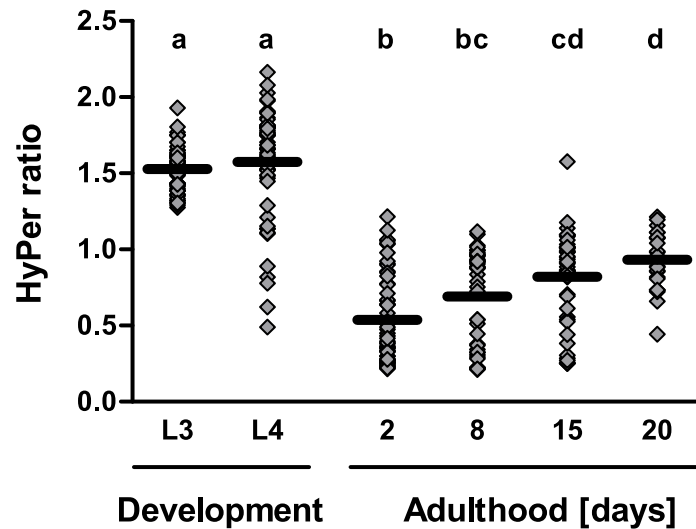


**Figure 4.12. Endogenous hydrogen peroxide level in the head region of HyPer transgenic wildtype *C. elegans*.** Aliquots of synchronized wildtype N2 jrIs1[*Prpl-17::HyPer*] were imaged and the individual HyPer ratios (rhombus symbol) and the average HyPer ratios (bar) at specific time points during development and adulthood are displayed. The HyPer ratio in the head region (neurons, pharynx) of developing worms is significantly higher than that of young adults, while an age-accompanying increase in HyPer ratio is observed as well. One-way ANOVA followed by Tukey's multiple comparison test were performed on the log-transformed HyPer ratios, and means that are not significantly different from each other ( $p > 0.05$ ) share the same letter. Experiments were performed at 15°C, and repeated at least three times. A representative graph is shown.

their reproductive period.

We also observed an age-accompanying increase of the HyPer ratio suggesting that a second surge of peroxide is produced as worms age<sup>7</sup>. A significant increase of the HyPer ratio in aged worms was not detected in worms expressing the HyPer sensor in the body wall muscle cells. This might be due to tissue-specific differences in hydrogen peroxide kinetics over the lifespan. Another, more likely reason, however, is that the decrease in HyPer protein expression observed in the body wall muscle cells of older worms excludes many worms from image quantification due to an insufficient signal. This might have biased the average HyPer ratio of an aged population towards healthier, mobile worms. For this possibility also argues the finding that a mutant strain, which expresses higher levels of HyPer in the body wall muscle cells, also exhibited an increase in peroxide upon aging (see Figure 4.15).

<sup>7</sup>Experiments were mainly performed by Nicholas Niemuth (University of Michigan).

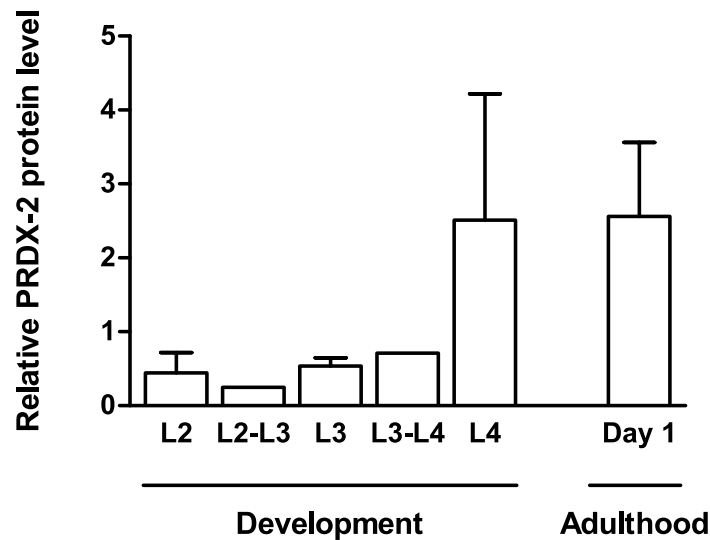


**Figure 4.13. Peroxiredoxin 2 protein level during development and adulthood.** The protein expression level of peroxiredoxin 2 was determined using quantitative western blot. PRDX-2 expression levels were normalized with the Coomassie-stained proteins on the membrane. Experiments were performed at 20°C, and the average PRDX-2 protein level and the SEM (n = 1-3) are depicted.

#### 4.1.3.3 The H<sub>2</sub>O<sub>2</sub> detoxifying system seemed to be lowered during development

The previous experiments indicated that endogenous peroxide levels are increased during *C. elegans* development as compared to early adulthood. This boost of H<sub>2</sub>O<sub>2</sub> could either be due to increased generation of peroxide or to decreased antioxidant capacity or a combination thereof. *C. elegans* does not possess glutathione peroxidases, leaving peroxiredoxins and catalases as the major enzymes for the detoxification of hydrogen peroxide. Aliquots of a synchronized population of wildtype worms were taken at different stages during development (L2, L2-L3, L3, L3-L4 and L4) and at day 1 of adulthood. As shown in Figure 4.13, we found that the protein expression levels of PRDX-2, which represents the most highly expressed peroxiredoxin homologue in *C. elegans*, was lower during early development in comparison to late development (L4) and adulthood. This decrease in PRDX-2 level likely contributes to the increased peroxide level observed during development. Levels of catalase could not be determined because all tested antibodies directed against catalase failed to detect the *C. elegans* isoforms. Future experiments will focus on quantitative RT-PCR to determine expression level of detoxifying enzymes such as peroxiredoxin, catalase, and superoxide dismutases during *C. elegans* development and adulthood.



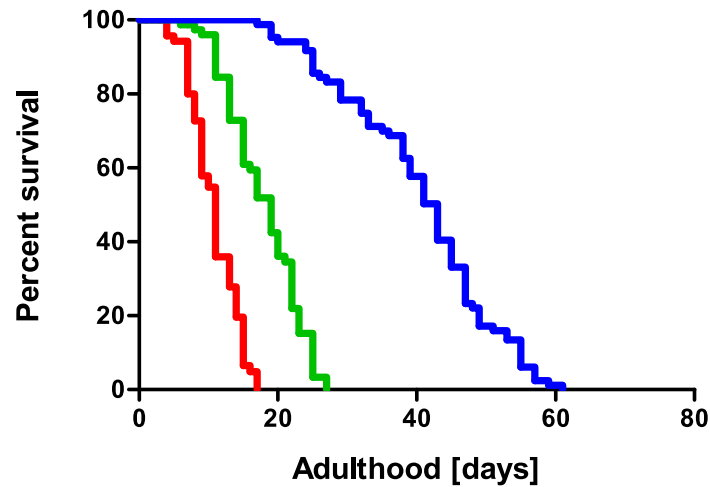


**Figure 4.14. Mutants of the IIS pathway differ in lifespan.** *Daf-16* [*unc-54::HyPer*] worms (red) have a shortened lifespan compared to wildtype N2 [*unc-54::HyPer*] (green) and the long-lived *daf-2* [*unc-54::HyPer*] (blue). Comparison of the survival curves was performed using the Log-rank test and the Grehan-Breslow-Wilcoxon Test ( $p < 0.0001$ ).

## 4.2 Hydrogen peroxide as signaling molecule in *C. elegans* development and lifespan

### 4.2.1 $H_2O_2$ level in mutants of the Insulin/ IGF-1 signaling pathway

The Insulin/ IGF-1 signaling (IIS) pathway is conserved, and has been shown to be involved in a variety of different processes, including stress response, dauer formation, reproduction, and lifespan (Longo and Finch, 2003; Tatar *et al.*, 2003). Signaling through DAF-2, the *C. elegans* homolog of the Insulin/IGF-1 receptor results in the phosphorylation of the FOXO transcription factor DAF-16. Phosphorylation prevents FOXO's translocation into the nucleus and thus the induction of DAF-16 responsive genes. In *daf-2* deletion animals, DAF-16 is constitutively in the nucleus and induces gene expression. These animals have a significantly longer lifespan than wildtype worms. *Daf-16* deletion worms, in contrast, are severely short-lived (Figure 4.14).

Since important DAF-16 responsive genes include antioxidant enzymes such as catalase and superoxide dismutase, we wanted to investigate whether differences in endogenous peroxide level are present in mutants of the IIS. We found significantly higher levels of peroxide release in wildtype and short lived *daf-16* mutants as compared to *daf-2* mutant, which were particularly pronounced during late development (Figure 4.15 A). These results indicated that peroxide level differ in mutants of the IIS pathway, presumably because antioxidant enzymes such as catalase are up-regulated by DAF-16. It also suggested that differences in endogenous peroxide level in late development and



early adulthood could correlate to the lifespan of these mutants (Figure 4.14).

To test more accurately the level of endogenous peroxide load in the IIS mutant animals, we mated wildtype N2 [*unc-54::HyPer*] males with *daf-2* or *daf-16* hermaphrodites to generate mutant strains expressing the H<sub>2</sub>O<sub>2</sub> sensor HyPer in the body wall muscle cells<sup>8</sup>. As before, aliquots of a synchronized population of wildtype, *daf-2* and *daf-16* expressing HyPer were imaged at different time points during development (L2, L3, and L4 larval stage) and adulthood (Day 2, 8, 15 and 20), and the average HyPer ratio of each individual animal was determined over its lifespan (Figure 4.15 B). For all three genotypes, we observed higher HyPer ratios during development in comparison to young adults, suggesting that 1) increased peroxide levels might be required during development, and that 2) the Insulin/IGF-1 signaling pathway does not affect formation and/or clearance of endogenous peroxide level during early development. In fact, while reproducible differences became apparent as early as late development (L4 larval stage), no consistent differences in the HyPer ratio were detectable between mutants of the IIS and wildtype during early development (L2 and L3 larval stage, see also L3 in Figure 4.15 A). Starting at L4 larval stage, however, the long-lived *daf-2* mutant showed much lower HyPer ratios than either wildtype or the *daf-16* mutant strain. These low levels were maintained at least until day 20 of adulthood. In contrast, the short-lived *daf-16* mutant showed significantly higher HyPer ratios than wildtype and *daf-2* mutants throughout its adult life. These findings indicate that differences in endogenous peroxide levels are present in short- and long-lived mutants of the IIS pathway, which become apparent as early as in late development. Note, that an age-accompanying increase in HyPer ratio was detected in *daf-16* [*unc-54::HyPer*] worms indicative that age-induced increases in the peroxide levels are also observed in body wall muscle cells and not only in neurons and pharynx (Figure 4.12).

#### 4.2.2 Developmental cultivation temperature influences H<sub>2</sub>O<sub>2</sub> level and lifespan

The nematode *C. elegans* is a poikilothermal organism, and its development and lifespan is influenced by the environmental temperature (Klass, 1977) (see Table 4.1). Worms raised at 15°C have a significantly longer lifespan than cohorts grown at 20°C or 25°C, as shown in Figure 4.16.

<sup>8</sup>Generation and genotyping of the *daf-16* [*unc-54::HyPer*] animals was performed by Ann-Kristin Diederich (University of Michigan).

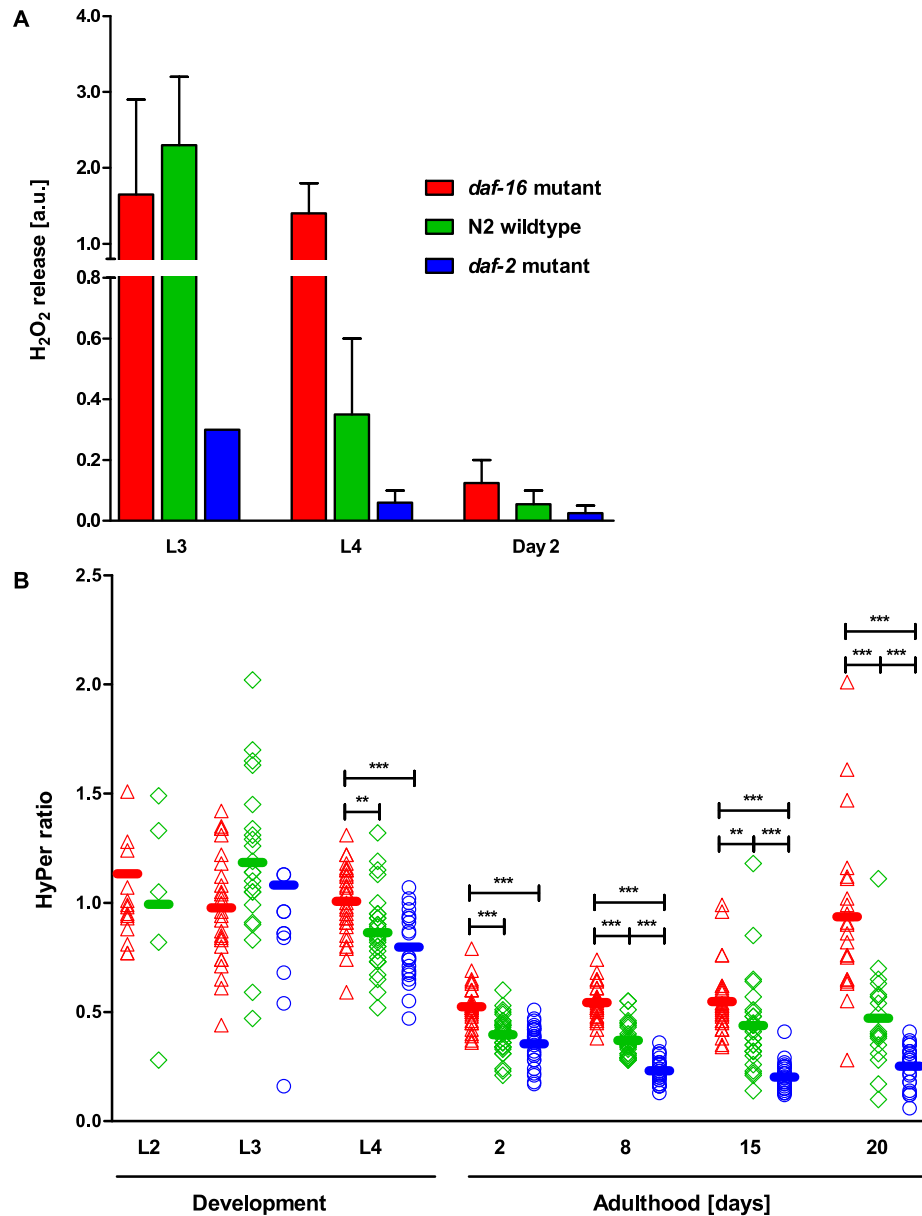


**Figure 4.15. Mutants of the IIS pathway differ in endogenous peroxide level.** (A) The H<sub>2</sub>O<sub>2</sub> release of *daf-16* mutant worms (red bar) is higher than that of wildtype (green) and *daf-2* mutants (blue) in late development (L4) and early adulthood (day 2), while in earlier stages (L3) no clear correlation was detected. The average peroxide release and the SEM (n=2) are displayed. (B) Endogenous peroxide level of transgenic [*unc-54*::HyPer] IIS mutants did reveal a correlation between lifespan and HyPer ratio starting as early as late development (L4 larvae), while no clear correlation was detected in early development (L2 and L3). One-way ANOVA followed by Tukey's Multiple Comparison test were performed on the log-transformed HyPer ratios; \*\*: p < 0.01; \*\*\*: p < 0.001. The experiment was repeated at least three times, and a representative graph is shown.

Temperature	Larval molts (hours after hatch)			
	(L1)-L2	L2-L3	L3-L4	L4-adult
16°C	24	39	54.5	74.5
20°C	15	24	34	46
25°C	11.5	18.5	26	35.5

**Table 4.1. Larval development is influenced by the cultivation temperature.** The transition between larval molts is dependent on the growth temperature (modified from “*Caenorhabditis elegans*: Modern Biological Analysis of an Organism” (p.9).

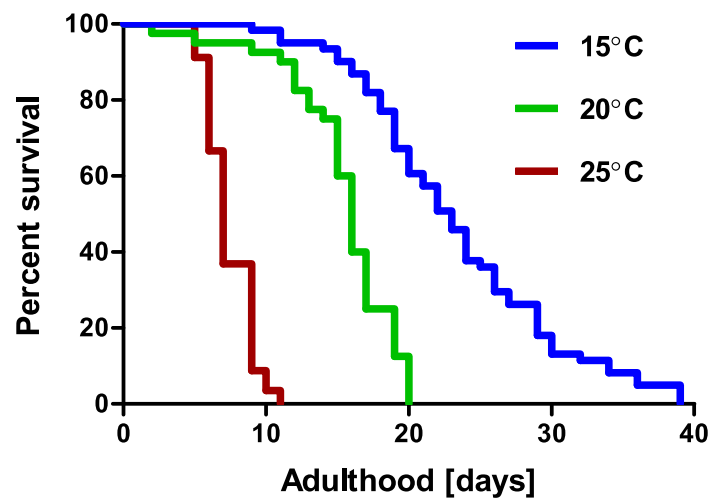


**Figure 4.16. The lifespan of wildtype *C. elegans* depends on the cultivation temperature.**

#### 4.2.2.1 Elevated temperatures result in low HyPer ratios in early development

To evaluate the role of cultivation temperature on the peroxide levels of wildtype *C. elegans*, populations of wildtype worms expressing HyPer in the body wall muscle cells were maintained at low (i.e., 15°C) or high (i.e., 25°C) temperature, synchronized and arrested at L1 larval stage at the respective temperature. Since the rate of development depends on the temperature (Table 4.1), L1 larvae were allowed to resume development in a time-controlled manner so that the same stages could be imaged at the same day, regardless of cultivation temperature. Aliquots of L1, L2, L3/L4 and L4 larvae were used to determine the developmental HyPer ratio of worms raised at different temperatures. During early development (i.e., L1 larvae and L2 larvae), the HyPer ratio of worms raised at 15°C was found to be higher than that of worms grown at 25°C ( $p < 0.05$ ), indicative of higher peroxide levels in worms raised at lower temperatures (Figure 4.17). This was surprising as lower cultivation temperatures are thought to decrease metabolism and hence should decrease ROS production in the electron transport chain. In later stages of development (i.e., L3/L4 and L4 larvae), no statistically significant difference in the HyPer ratio was found between worms grown at 15°C and worms cultivated at 25°C, suggesting that in older larvae the temperature might not effect endogenous peroxide level.

#### 4.2.2.2 Developmental growth temperature influences adult lifespan

Fluctuations in peroxide level occur during development and adulthood, and seem to be influenced by the cultivation temperature. To investigate whether the temperature experienced during development affects adult lifespan, synchronized wildtype populations were grown at 15°C and 25°C until day 1 of adulthood, after which worms were shifted to the other temperatures. Worms raised at 15°C were switched to 25°C, and animals grown at 25°C were transferred to 15°C. Their subsequent lifespan was compared to control groups, which were continuously maintained at either 15°C or 25°C. Animals, which had been raised at the lower temperature during their development and were switched to higher temperatures at day 1 of adulthood, had a significantly longer lifespan than the control group, which had been maintained at elevated temperatures throughout their development and adult life (Figure 4.18 A). Accordingly, worms that were exposed to elevated temperature only during development did not have the same long lifespan as worms continuously

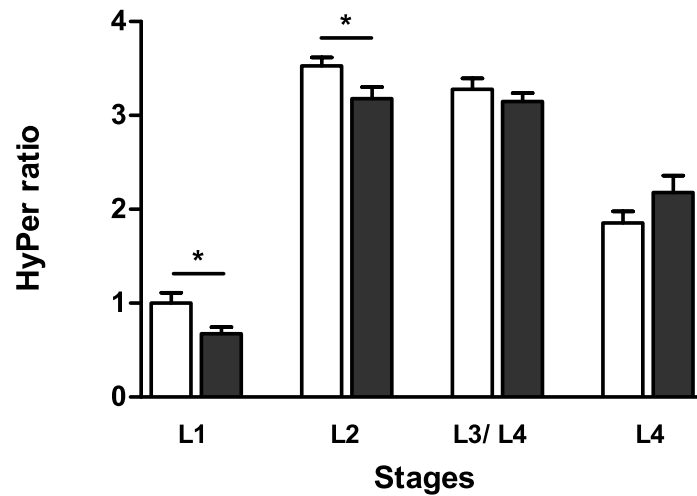


**Figure 4.17. Peroxide level in development are influenced by the growth temperature.** The average HyPer ratios of N2 [*unc-54::HyPer*] animals grown at 15°C (open bar) or 25°C (filled bar) were determined at larval stages L1, L2, L3/L4 and L4. The average HyPer ratios and the SEM (n = 17 – 48 worms from different experiments combined) are depicted. In early development (L1 and L2 larvae), the HyPer ratios of worms raised at lower temperature are higher than that of worms grown at high temperature (unpaired t-test, L1: p=0.0107; L2: p=0.0220). In later stages of development, no significant difference in the HyPer ratios of worms raised at different temperatures was detected (L3/L4: p=0.4179; L4: p=0.4458).

maintained at lower temperatures (Figure 4.18 B). These results were intriguing because they suggested that exposure to high or low temperatures during development influences the lengths of adult life, even though the developmental window is very short in comparison to the whole lifespan. They also indicated that events during adulthood contribute to the observed lifespan since the lifespan of worms that experienced low temperatures in development was not the same as the lifespan of worms that were maintained at lower temperature throughout their whole life.

### 4.2.3 Glucose restriction and its effect on H<sub>2</sub>O<sub>2</sub> level and lifespan

#### 4.2.3.1 Glucose restriction during adulthood extends lifespan

Young adult wildtype *C. elegans* grown on 2-Deoxy-D-glucose (DOG), an inhibitor of glycolysis, show an extended mean lifespan, which has been proposed to be mediated by a process termed mitohormesis (Ingram *et al.*, 2006; Schulz *et al.*, 2007) (see also section 2.7.2). Schulz *et al.* suggested that DOG-mediated glucose restriction results in increased respiration, which causes a transient increase of mitochondria-derived reactive oxygen species. This in turn, increases the antioxidant capacity of *C. elegans* and contributes to the extended lifespan of DOG-treated worms

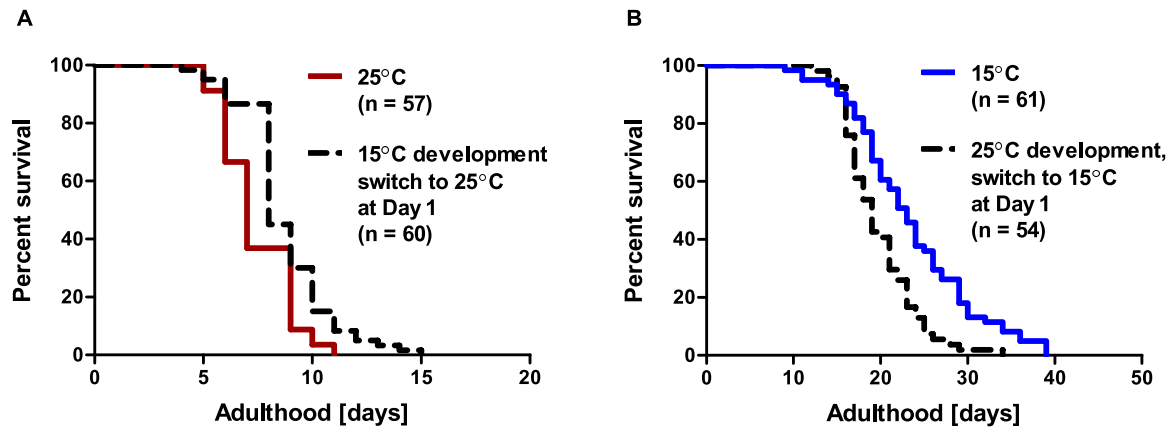


**Figure 4.18. Developmental growth temperature affects adult lifespan of wildtype *C. elegans*.** (A) Synchronized wildtype worms, which were raised at 15°C and shifted to 25°C at Day 1 of adulthood, had a significantly longer adult lifespan than animals continuously grown at 25°C ( $p = 0.0003$ ). (B) Animals reared at 25°C and shifted to 15°C at Day 1 of adulthood had a much shorter adult lifespan than the group continuously grown at 15°C ( $p=0.0009$ ).

(Schulz *et al.*, 2007). To determine whether glucose restriction indeed increases endogenous hydrogen peroxide levels, synchronized N2 [*unc-54::HyPer*] animals were transferred as young adults onto NGM plates containing 5 mM DOG. After 30 and 96 hours on DOG, the HyPer ratio was determined as a read-out for *in vivo* H<sub>2</sub>O<sub>2</sub> levels. After 30 hours, the DOG-treated worms exhibited elevated HyPer ratios (Figure 4.19 A), suggesting increased levels of peroxide upon glucose restriction. After 96 hours on DOG, no difference in HyPer ratio was detected between the DOG-treated worms and the control group. Animals which experienced glucose restriction during adulthood had an extended lifespan as shown in Figure 4.19 B), which was in agreement with results published by Schulz *et al.*

#### 4.2.3.2 Developmental Glucose restriction seems to be harmful

DOG-mediated glucose restriction has been shown to induce ROS formation and extend lifespan when administered during early adulthood (Schulz *et al.*, 2007) as shown in Figure 4.19. Next, we wanted to investigate whether a potential imbalance of glucose metabolism and increased respiration present during development, a period which has been found to have already increased peroxide level (Figures 4.10 and 4.12), had effects on physiology and lifespan of *C. elegans*. We, therefore, grew synchronized populations of N2 [*unc-54::HyPer*] on regular NGM plates or on NGM plates supplemented with 5 mM DOG either only during development or during development and adult

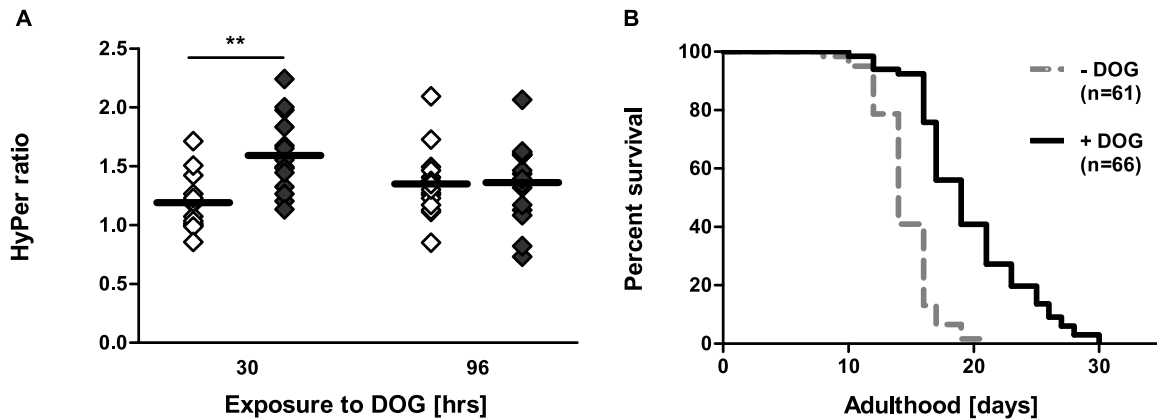


**Figure 4.19. DOG exposure of adult wildtype worms transiently increases HyPer ratio and extends lifespan.** (A) A synchronized adult population of N2 [*unc-54::HyPer*] animals was cultured on 5 mM DOG and the HyPer ratio was determined after 30 and 96 hours. DOG-exposed animals (filled symbols) exhibited an increased HyPer ratio after 30 hours compared to untreated animals (open symbols). After 96 hours on DOG no difference in HyPer ratio was detected. One-way ANOVA and Tukey's Multiple Comparison test were performed on the log-transformed data; \*\*:  $p < 0.01$ . (B) Worms maintained on DOG during their adulthood exhibited an extended lifespan. Survival curves were compared using Log-rank test ( $p < 0.0001$ ) and Gehan-Breslow-Wilcoxon test ( $p < 0.0001$ ).

lifespan. Following exposure to DOG, we observed a delay in the progression between larval molts compared to the untreated animal (Figure 4.20), suggesting that glucose restriction might induce the dauer stage, which is known to occur in *C. elegans* at times of food starvation (i.e., dietary restriction), crowded population, or otherwise adverse environmental factors (Riddle *et al.*, 1981). The fact that the DOG-treated worms eventually progressed to adults even when continuously grown on DOG, however, argues against dauer formation but instead suggests a delay in development potentially caused by glucose restriction.

The comparison of the HyPer ratio of stage-matched DOG-treated and control N2 [*unc-54::HyPer*] worms revealed that the HyPer ratios of DOG-treated worms were not significantly different from untreated animals in early development (L2/L3 larval stage). At later stages (L3/L4), however, the HyPer ratio of worms grown on DOG was significantly lower (Figure 4.21 A), suggesting that those animals either produced less peroxide or increased the activity of detoxifying systems. Surprisingly, worms which were exposed to DOG during development had a significantly shortened lifespan (Figure 4.21 B), which was in contrast to the lifespan extension observed when worms were treated with DOG during early adulthood (Figure 4.19). Continuous exposure to DOG during adulthood was unable to rescue the mortality caused by developmental DOG treatment, sug-

A

Post synchronization [hrs]	Larval development	
	Control group	DOG group
16	L1	L1
39	L2/ L3	L2
63	L3/ L4	L2/ L3
92	Day 1 of Adulthood	L3/ L4

B

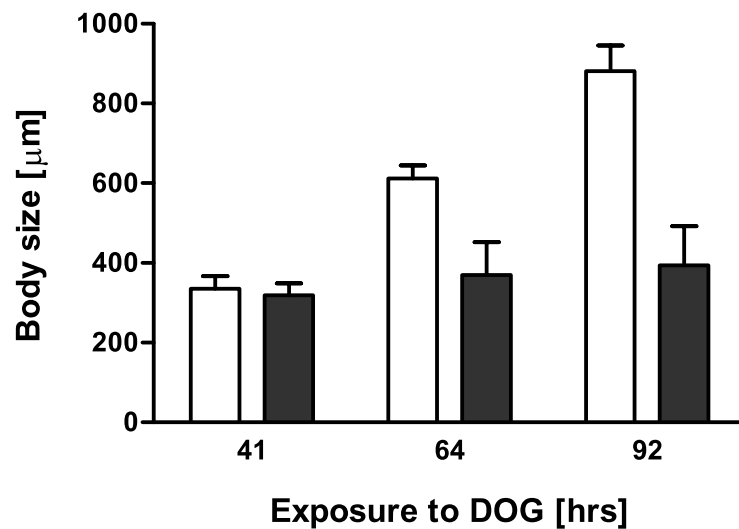


**Figure 4.20. Developmental DOG exposure retards development of wildtype worms.** (A) DOG exposure of larvae N2 [*unc-54::HyPer*] animals caused a delay in developmental molts, and (B) a reduced body size. The average body size (plus SD) of DOG-treated animals (filled bar) are smaller in comparison to untreated worms (open bar).



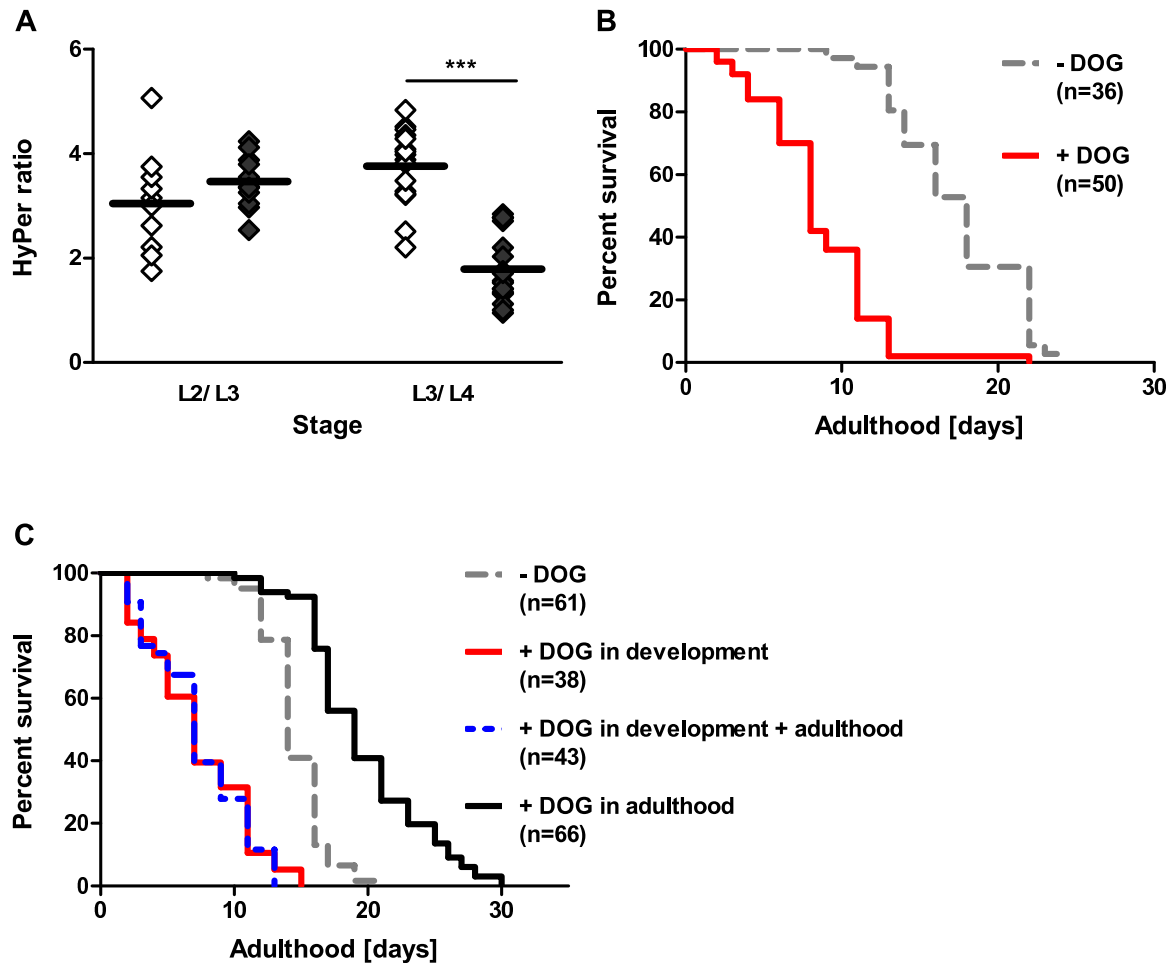


**Figure 4.21. Developmental DOG exposure reduces HyPer ratios during development and shortens lifespan.** (A) In early development (L2/L3) the HyPer ratio of DOG-treated animals (filled symbols) seems to be slightly increased compared to untreated worms (open symbols). In late development (L3/L4) the HyPer ratio of DOG-treated animals was significantly reduced. One-way ANOVA followed by Tukey's Multiple Comparison test were performed on the log-transformed HyPer ratio. (B) The lifespan of worms raised on DOG during development was shorter than the lifespan of the control group. Log-rank test and Gehan-Breslow-Wilcoxon test ( $p < 0.0001$ ) were performed. (C) The subsequent incubation on DOG during adulthood could not rescue the mortality caused by developmental DOG exposure.

gesting that any beneficial effect caused by DOG exposure during adulthood was diminished when worms were already exposed to DOG during their development (Figure 4.21 C). These results indicate that a disruption of glucose metabolism and/or peroxide homeostasis during development might have adverse outcomes while similar changes during early adulthood might be beneficial in terms of lifespan.

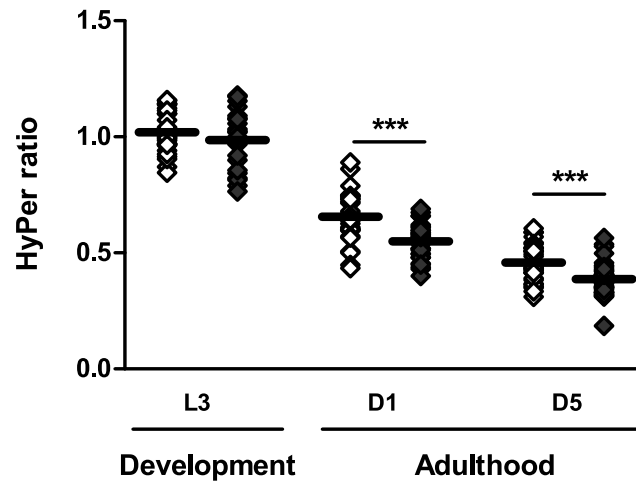


**Figure 4.22. Catalase 2 deletion animals have lower HyPer ratios during adulthood.** Aliquots of synchronized wildtype N2 [*unc-54::HyPer*] (open symbols) and *ctl2; him-8* [*unc-54::HyPer*] (filled symbols) were imaged during development (L3) and adulthood (Day 1 and Day 5), and the HyPer ratios were determined. A One-way ANOVA and a Tukey's Multiple Comparison test were performed on the log-transformed HyPer ratios. The experiments were performed at a minimum three times (at 15°C and at 20°C), and a representative graph is shown.

### 4.3 Manipulation of the oxidant homeostasis in *C. elegans*

#### 4.3.1 Manipulation of antioxidant capacity through catalase 2 deletion

##### 4.3.1.1 Lower HyPer ratios and shorter lifespans in catalase 2 deletion worms

The major catalase isoform in *C. elegans* is catalase 2 (CTL-2), which is expressed in the peroxisomes. Deletion of *ctl-2* has been shown to reduce overall catalase activity by 80% and shortens the lifespan of *C. elegans* by 16% (Petriv and Rachubinski, 2004). Transgenic *ctl-2* mutant worms expressing the HyPer sensor in the body wall muscle cells were generated by crossing *ctl-2; him-8* males (*him-8* results in a higher frequency of males in the hermaphrodite population) with HyPer-expressing wildtype N2 [*unc-54::HyPer*] hermaphrodites<sup>9</sup>. Synchronized populations of catalase 2 and wildtype worms were imaged during development and adulthood. The HyPer ratio of wildtype and *ctl-2; him-8* animals did not differ significantly at L3 larval stage, while the HyPer ratio of *ctl-2; him-8* [*unc-54::HyPer*] was found to be reduced during adulthood (day 1 and day 5) as shown in Figure 4.22.

These results were surprising considering that catalase 2 deletion worms have only 20% of

<sup>9</sup>Generation and genotyping of *ctl-2, him-8* [*unc-54::HyPer*] animals were performed by Sebastian Brandhorst (University of Michigan).

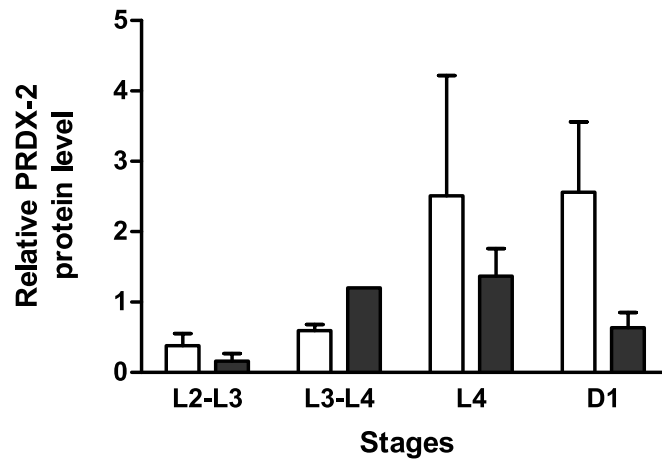


**Figure 4.23. Peroxiredoxin 2 protein level of catalase 2 deletion animals.** The average peroxiredoxin 2 protein level seemed to be slightly lower in *ctl-2; him-8* [*unc-54::HyPer*] worms (filled bars) than of N2 [*unc-54::HyPer*] (open bars). Peroxiredoxin 2 expression was determined using quantitative western blot, and the average PRDX-2 protein level and the SEM (n = 1-3) are displayed (experiment performed at 20°C).

wildtype's catalase activity (Petric and Rachubinski, 2004). Consistent with our HyPer results, however, Petric *et al.* also observed that *ctl-2* deletion strains exhibit reduced levels of oxidative damage compared to wildtype, as assessed by protein carbonylation. To determine whether peroxiredoxin 2 might compensate for the loss of catalase 2, we tested the steady state levels of PRDX-2 by westernblot in wildtype and *ctl-2* mutant strains. As shown in Figure 4.23, if at all, *ctl-2* deletion strains might in fact have lower levels of PRDX-2 than the wildtype strain. It remains to be determined whether other systems involved in cellular redox homeostasis might compensate for *ctl-2* deletion. The HyPer ratio (which is the level of reversible oxidation of peroxide-sensitive cysteines within HyPer) depends on the reducing capacity (i.e., thioredoxin) of the organism (Meyer and Dick, 2010). Lower HyPer ratios are hence either due to lower peroxide levels, or higher levels of reduced thioredoxins. It is therefore an intriguing question how expression and activity levels of thioredoxin compares in *ctl-2* deletion strains versus the wildtype and how this might be connected to changes in lifespan.

It is of note that we found the lifespan of *ctl-2; him-8* [*unc-54::HyPer*] to be only slightly shorter than the lifespan of the corresponding N2 [*unc-54::HyPer*] strain (Figure 4.24). It might be that the N2 wildtype strains used in the Petric *et al.* study and in our lab are not 100% identical, as mutations are known to accumulate over many generations. Furthermore, environmental parameters

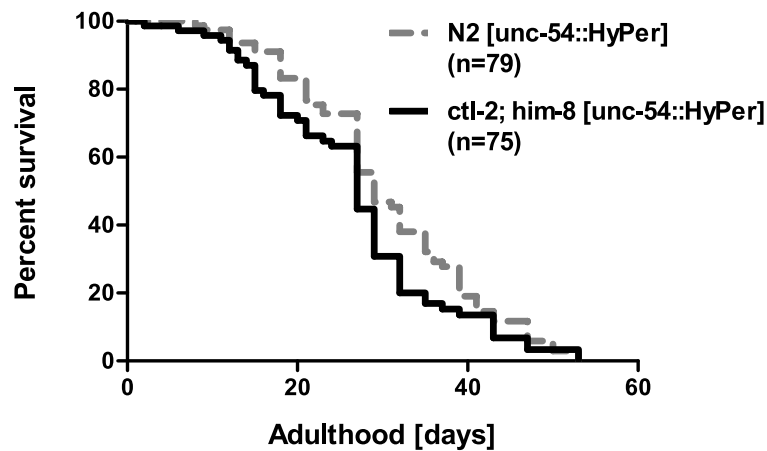


**Figure 4.24. Lifespan of catalase 2 deletion and wildtype animals.** The mean lifespan of *ctl-2; him-8 [unc-54::HyPer]* worms is only slightly shorter than the lifespan of N2 [*unc-54::HyPer*] animals at 15°C;  $p = 0.1061$  (Log-rank Mantel Cox) and  $p = 0.0468$  (Gehan-Breslow-Wilcoxon Test).

(synchronization, maintenance, lifespan assay) might influence the outcomes. The crossing to our N2 [*unc-54::HyPer*] strain might have removed or introduced background mutations, that could have affected the lifespan as well. Also, the n-numbers used by Petriv *et al.* are much higher than the ones used in our experiments (wildtype  $n=717$ ; *ctl-2*  $n=365$ ), which might have been required to detect a significant reduction in lifespan of 17%.

### 4.3.2 Induction of developmental oxidative stress

#### 4.3.2.1 Wildtype *C. elegans* can tolerate a short bolus of paraquat

In contrast to the deletion of *ctl-2*, which reduces the organism's antioxidant activity by genetic manipulation, treatment of worms with exogenous paraquat increases the oxidant load. The effects of a sublethal dosis of  $H_2O_2$  on *C. elegans* have been previously studied in our lab (Kumsta *et al.*, 2011). To induce oxidative stress in *C. elegans* the superoxide generator paraquat was used. Paraquat is a redox cyler, in which the paraquat di-cation is being reduced to the paraquat radical, which then reacts with oxygen generating superoxide. In mammals the paraquat di-cation gets reduced by the mitochondrial complex I, and superoxide generation takes place in the mitochondrial matrix (Cochemé and Murphy, 2008). To investigate the effects of the superoxide generator paraquat on wildtype *C. elegans*, we first had to determine the minimal dose of paraquat that affects behavior or physiology without killing the worms. Therefore, we treated a synchronized population

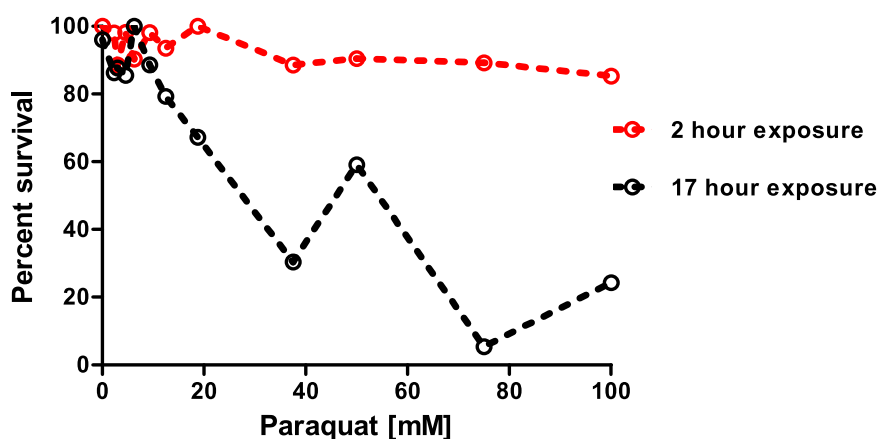


**Figure 4.25. Survival of paraquat-stressed wildtype *C. elegans*.** Animals were incubated with different concentrations of the superoxide-generator paraquat in a 96-well plate. The surviving worms were counted after two and 17 hours, respectively. The apparently improved survival of worms at 50 mM paraquat most probably represents a technical outlier, caused by the intrinsic error of the experiment in distinguishing live (moving) worms from dead (not moving) worms.

of wildtype worms with paraquat concentrations ranging from 2.3 mM to 100 mM for 2 hours, after which the number of surviving worms was assessed. Worms survived a two hour treatment with all tested paraquat concentrations. A longer treatment of 17 hours, however, killed worms at paraquat concentrations higher than 20 mM as shown in Figure 4.25.

Surprisingly, even a 2-hour exposure to 100 mM paraquat did not affect the motility of the worms (Figure 4.26) while 20 min treatment with 5 mM peroxide was sufficient to immobilize over 50% of worms (Kumsta *et al.*, 2011). For our subsequent studies, paraquat concentrations ranging between 10 mM and 50 mM and an incubation time of two hours were used.

#### 4.3.2.2 Paraquat treatment induces oxidative stress

To assess whether an exogenous administration of the superoxide generator paraquat increases endogenous hydrogen peroxide levels, synchronized wildtype L4 worms expressing the HyPer sensor in the body wall muscle cells were treated for 90 minutes with 30 mM paraquat. The HyPer ratio of the paraquat-treated animals was slightly elevated compared to the control group (Figure 4.27), indicating that exposure to paraquat could cause increase endogenous peroxide level.

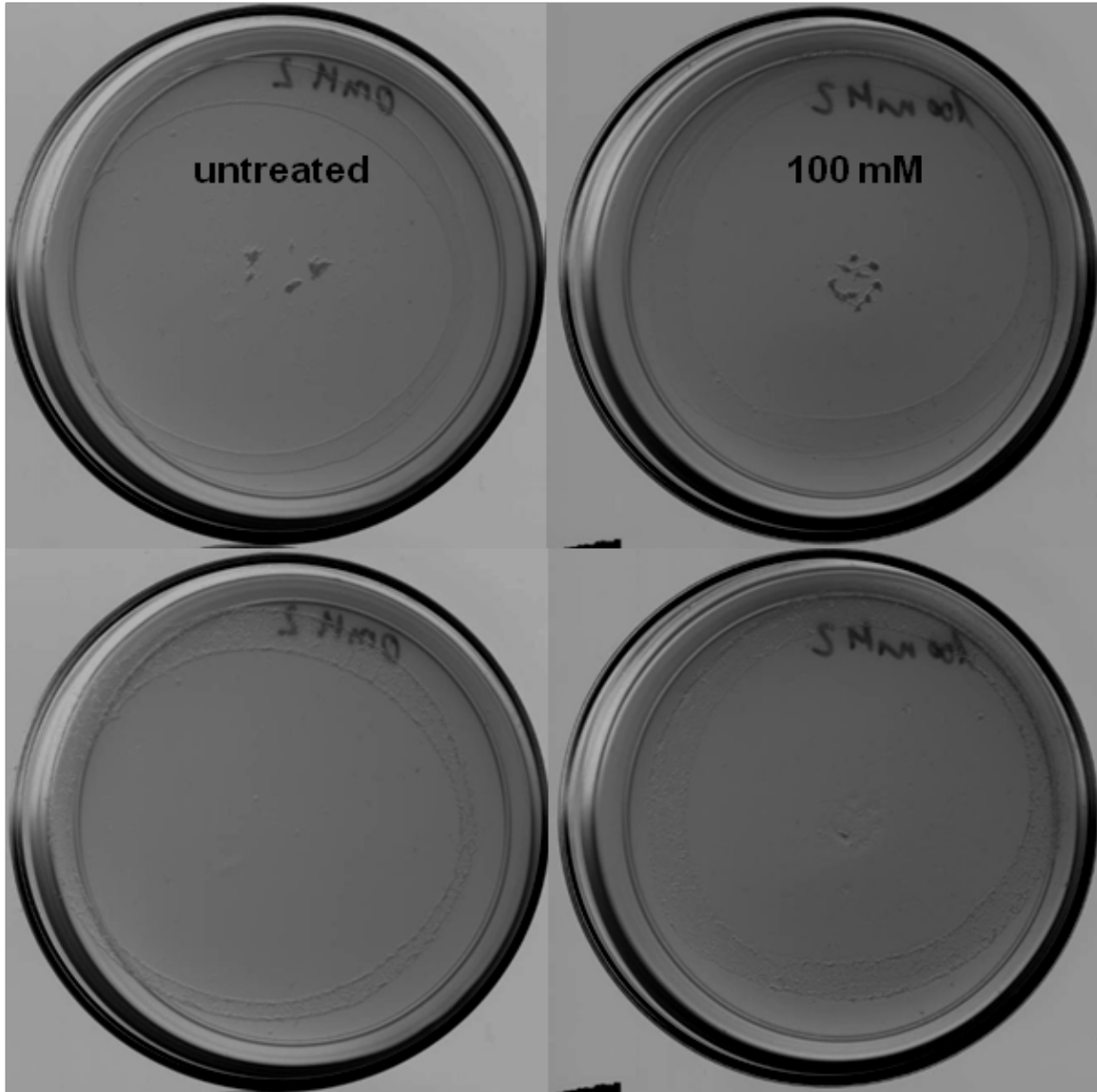


**Figure 4.26. Motility upon paraquat exposure of wildtype animals.** Synchronized wildtype worms were spotted in the middle of a motility plate after incubation for 2 hours with either M9 buffer (top row, left image) or 100 mM paraquat (top row, right image). After 1½ hours, the untreated worms (bottom row, left image) as well as the animals treated with 100 mM paraquat (bottom row, right image) had crawled to the outer OP50 ring, indicating that motility was not affected by paraquat stress.

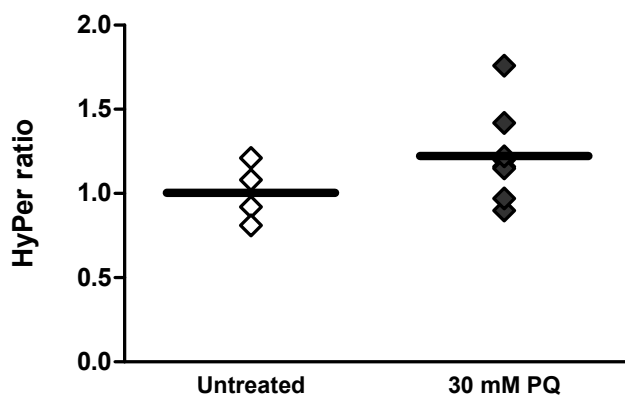


**Figure 4.27. HyPer ratio of paraquat-stressed animals.** Wildtype *C. elegans* expressing the HyPer sensor in the body wall muscle cells were treated for 90 minutes with 30 mM of the superoxide generator paraquat. The average HyPer ratio of untreated (open symbols) and treated (filled symbols) worms is represented by the bar.

#### 4.3.2.3 Paraquat treatment of L4 larvae shortens lifespan

Treatment of wildtype worms with a sublethal dose of  $H_2O_2$  decreased the worms' motility, pharyngeal pumping, and brood size but did not affect the lifespan of *C. elegans* (Kumsta *et al.*, 2011). To assess the physiological consequence of paraquat treatment, we synchronized wildtype worms and treated L4 larvae with 10 mM, 30 mM or 50 mM paraquat for two hours. Then, the PQ was removed and worms were cultivated at 20°C. As before, we did not observe any immediate motility defect. The lifespan of paraquat-treated worms, however, was significantly shortened compared to untreated animals (Figure 4.28 A, B). The reduction in lifespan was accompanied by an accelerated age-mediated decline in fast-movement-ability as shown in Figure 4.28 C. Neither a shortened lifespan nor an accelerated decline in fast-movement was observed in worms treated with hydrogen peroxide (Kumsta *et al.*, 2011), suggesting that intracellular targets of superoxide and peroxide might differ due to differences in the reactivity of the oxidants or the site of action. Worms treated with the superoxide generator paraquat showed reduced progeny production following the oxidative assault (Figure 4.28 D), which was also observed upon peroxide exposure (Kumsta *et al.*, 2011).

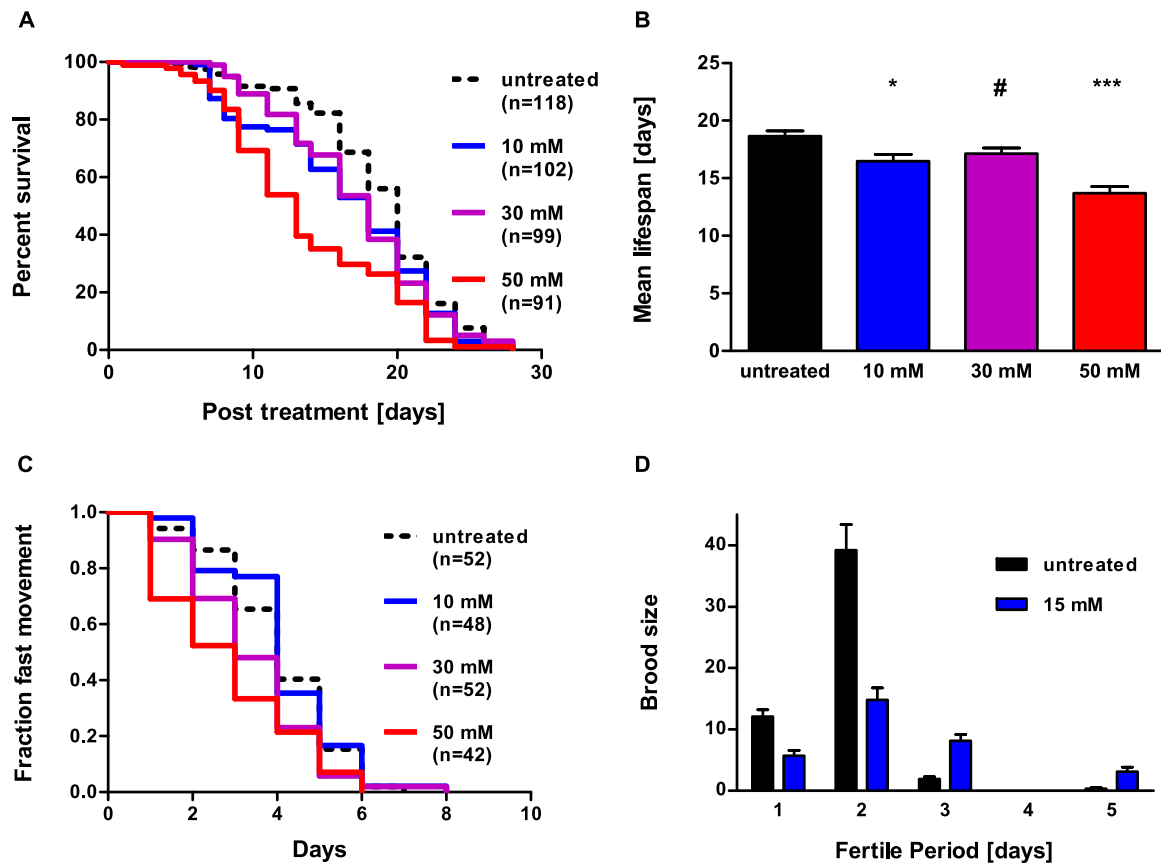


**Figure 4.28. Paraquat stress at L4 stage effects physiology and lifespan.** (A) Synchronized N2 L4 larvae were treated for two hours with 10 mM, 30 mM or 50 mM paraquat at 20°C. Survival upon paraquat treatment was reduced. The Log-rank test and the Gehan-Breslow-Wilcoxon test were performed: Untreated vs. 10 mM:  $p = 0.0305$  /  $p = 0.0106$ ; Untreated vs. 30 mM:  $p = 0.0467$  /  $p = 0.0127$ ; Untreated vs. 50 mM:  $p < 0.0001$  /  $p < 0.0001$ . (B) The mean lifespan (SEM is displayed) of untreated and paraquat-treated worms are different. A One-way ANOVA and a Tukey's Multiple Comparison test were performed; \*:  $p < 0.05$ ; \*\*\*:  $p < 0.001$ ; #: difference not significant. (C) Worms treated with paraquat exhibited an accelerated decline in fast movement ability (D) and a reduction in progeny number upon paraquat exposure. Brood size was assessed at 25°C.



Lifespan assays upon short-term administration of paraquat revealed that the effect on lifespan was dependent on the temperature (Figure 4.29). The treatment with 30 mM paraquat, which has only a modest effect on lifespan at 20°C resulted in a high mortality rate at 25°C in the very first days after paraquat exposure (Figure 4.29 B vs. C). Similarly, a paraquat concentration (15 mM) that shortened the lifespan at 25° had no effect on lifespan when worms were treated and grown at 15°C (Figure 4.29 C vs. A).

### 4.3.3 Induction of oxidative stress during adulthood

Superoxide exposure during development reduced the lifespan of *C. elegans*, suggesting that oxidant homeostasis during development might be fine-tuned and balanced. We also observed that glucose restriction resulted in opposing effects depending on the time point it was initiated. Thus we were wondering whether oxidant treatment during adulthood might result in a different outcome. Therefore, three-days-old adults (young fertile adult animals) were treated with 15 mM paraquat and the subsequent adult lifespan was assessed. A small beneficial effect upon paraquat treatment was observed although the maximum lifespan was not affected (Figure 4.30). This suggests that the effect of a short bolus of superoxide on mortality rate might be dependent on dosis, cultivation temperature and developmental stage of the worms. Further experiments are required to confirm those findings, and to narrow the potentially windows where oxidant exposure results in detrimental or beneficial outcomes, respectively.

## 4.4 Can developmental hydrogen peroxide level predict subsequent lifespan?

Our previous experiments have demonstrated that endogenous peroxide levels are elevated during development. The levels of oxidant seemed to be balanced as perturbations during development using oxidant exposure or glycolysis inhibitors resulted in a shortened lifespan. In our studies we also noticed variances in the HyPer ratio of individual worms. It has been previously shown that individuals of a synchronized isogenic worm population have different lifespans despite being maintained under the same environmental conditions. We were hence investigating whether the differences in the individual HyPer ratios in the early stages of life could correlate with the individual's lifespan. Synchronized wildtype worms expressing the HyPer sensor in the body wall muscle cells were re-

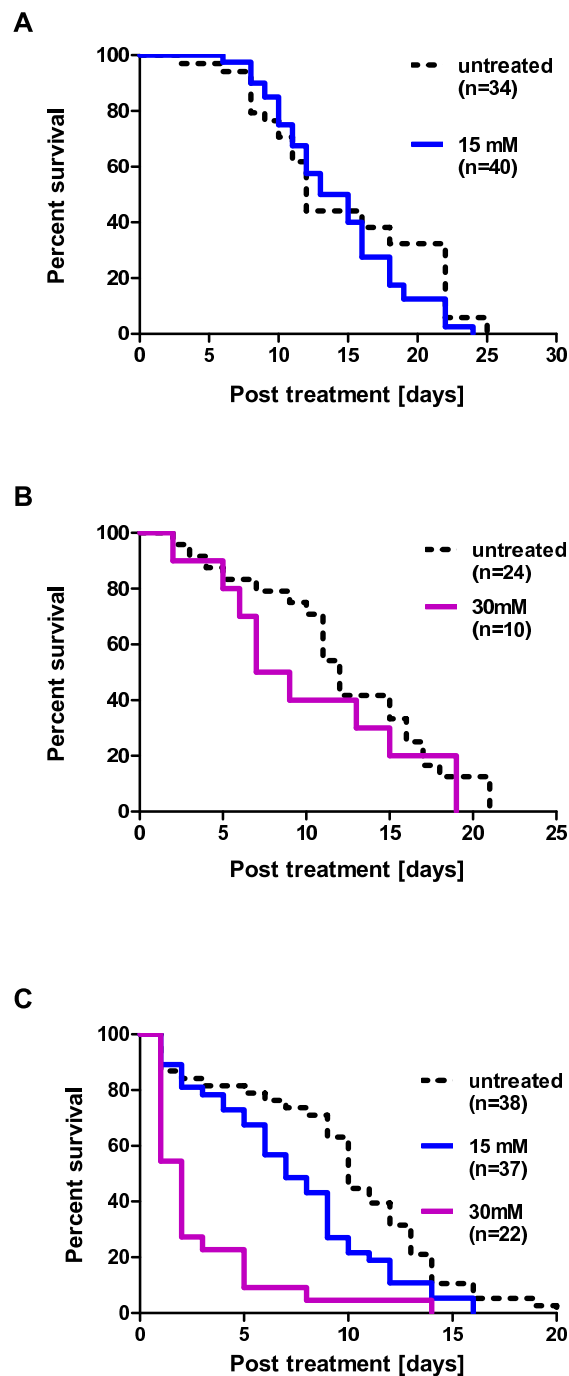


**Figure 4.29. Paraquat-mediated effect on lifespan is temperature-dependent.** Synchronized wildtype N2 worms grown at different temperatures were treated at L4 larval stage with paraquat and the lifespan was observed at (A) 15°C, (B) 20°C or (C) 25°C. The Log-rank (Mantel-Cox) test and the Gehan-Breslow-Wilcoxon test were performed. At 15°C there was no difference in lifespan observed between control and paraquat-treated group ( $p = 0.2425$  /  $p = 0.9434$ ), and the treatment with 30 mM paraquat did not affect lifespan at 20°C ( $p = 0.3596$  /  $p = 0.2973$ ). At 25°C, however, exposure to 15 mM paraquat ( $p = 0.0165$  /  $p = 0.0191$ ) and 30 mM ( $p < 0.0001$  /  $p < 0.0001$ ) shortened the lifespan of wildtype *C. elegans*.

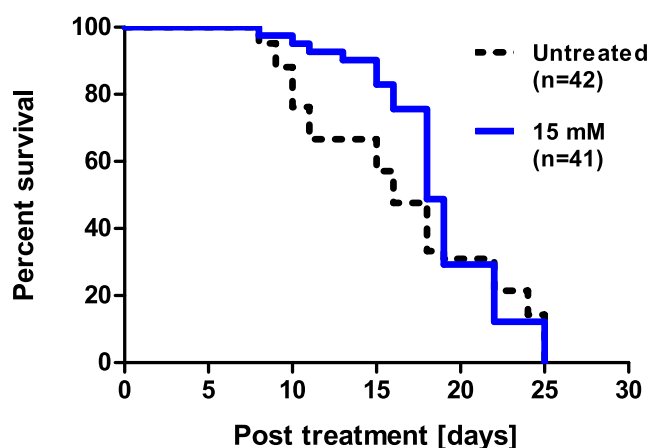


**Figure 4.30. Lifespan of young adults upon exposure to paraquat.** Three-days-old adults were treated for two hours with 15 mM paraquat and the subsequent lifespan was observed at 15°C. A log-rank (Mantel-Cox) test ( $p = 0.3502$ ) and a Gehan-Breslow-Wilcoxon test ( $p = 0.0694$ ) were performed.

versibly mounted on an agarose pad, imaged to determine their individual HyPer ratio, recovered from the objective slide, and transferred onto a single plate to assess their lifespan. The recovery rate was about 55% and deaths within the first days post recovery were excluded as mortality related to the mounting and recovery process. The histograms of the HyPer ratios of the remaining worms are displayed in Figure 4.31.

The worms were subdivided according to their HyPer ratio into fractions with very low HyPer ratios (the lower 15%), very high HyPer ratios (the upper 15%) and worms having intermediate HyPer ratios. Then, we determined their survival and their mortality rate (i.e. Gompertz curves). While the survival curve plots the surviving fraction of worms per day, the Gompertz curve displays the mortality rate on a logarithmic scale.

$$y(t) = ae^{bt} \quad (\text{Eq. 1})$$

With  $y(t)$  being the mortality rate at time  $t$ ,  $a$  describing the initial mortality rate,  $e$  being the Euler's number and  $b$  representing the rate of mortality increase with age. The intercept with the y-axis represents the initial mortality while the slope of the Gompertz fit shows the rate of mortality. Comparison of the survival curves of the three groups showed that the trends seem to depend on the exact stage at which the worms were imaged. While we always aimed for the L4 stage, exact stage matching was very difficult to achieve. Hence, in some experiments worms were already in late L4

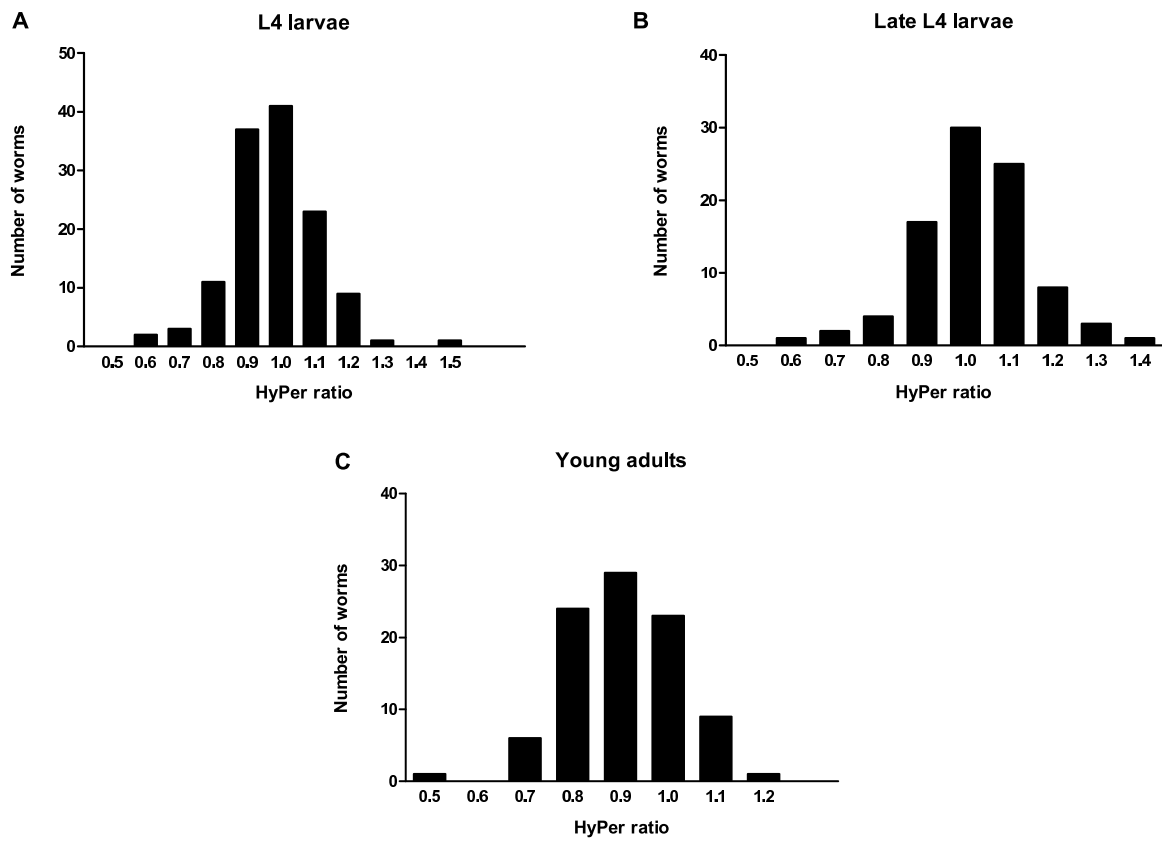


**Figure 4.31. Histogram of the HyPer ratios of a synchronized population.** (A) Frequency distribution of the HyPer ratio of L4 larvae, (B) late L4 larvae, (C) and young adults are displayed. A bin width of 0.1 was used.

stage and reached young adulthood in the course of the imaging and recovery process (which took usually a complete day). Since the HyPer ratios of L4 larvae and young adults differ significantly (see Figure 4.10), these worms were analyzed separately. The initial mortality of L4 larvae with lower HyPer ratios seemed to be elevated, suggesting that certain levels of peroxide might be required for a physiological function in late development and/or early adulthood (Figure 4.32 A). Yet, their increase of mortality rate was slightly lower. In contrast, worms that had high HyPer ratios at L4 stage showed a lower initial mortality rate (Figure 4.32 A), indicative of a beneficial effect of elevated peroxide level as larval worms. These results are intriguing since they suggest that elevated peroxide level are necessary and required for normal physiological function and subsequent adult lifespan of larval worms. These experiments, however, need to be confirmed aiming for higher n-numbers to allow adequate statistical analysis.

Late L4 larval worms, which had HyPer ratios that were either very low or very high, showed a higher initial mortality rate compared to the rest of the population (as shown in the Gompertz curves) as well as a shortened lifespan (see survival curves), suggesting that a fine tuned peroxide level is necessary for optimal survival (4.32 B). In young adults, no correlation between HyPer levels and lifespan were observed (4.32 C), suggesting that at this point in life the clock is already set. Additional experiments, however, are planned to confirm these exciting findings.

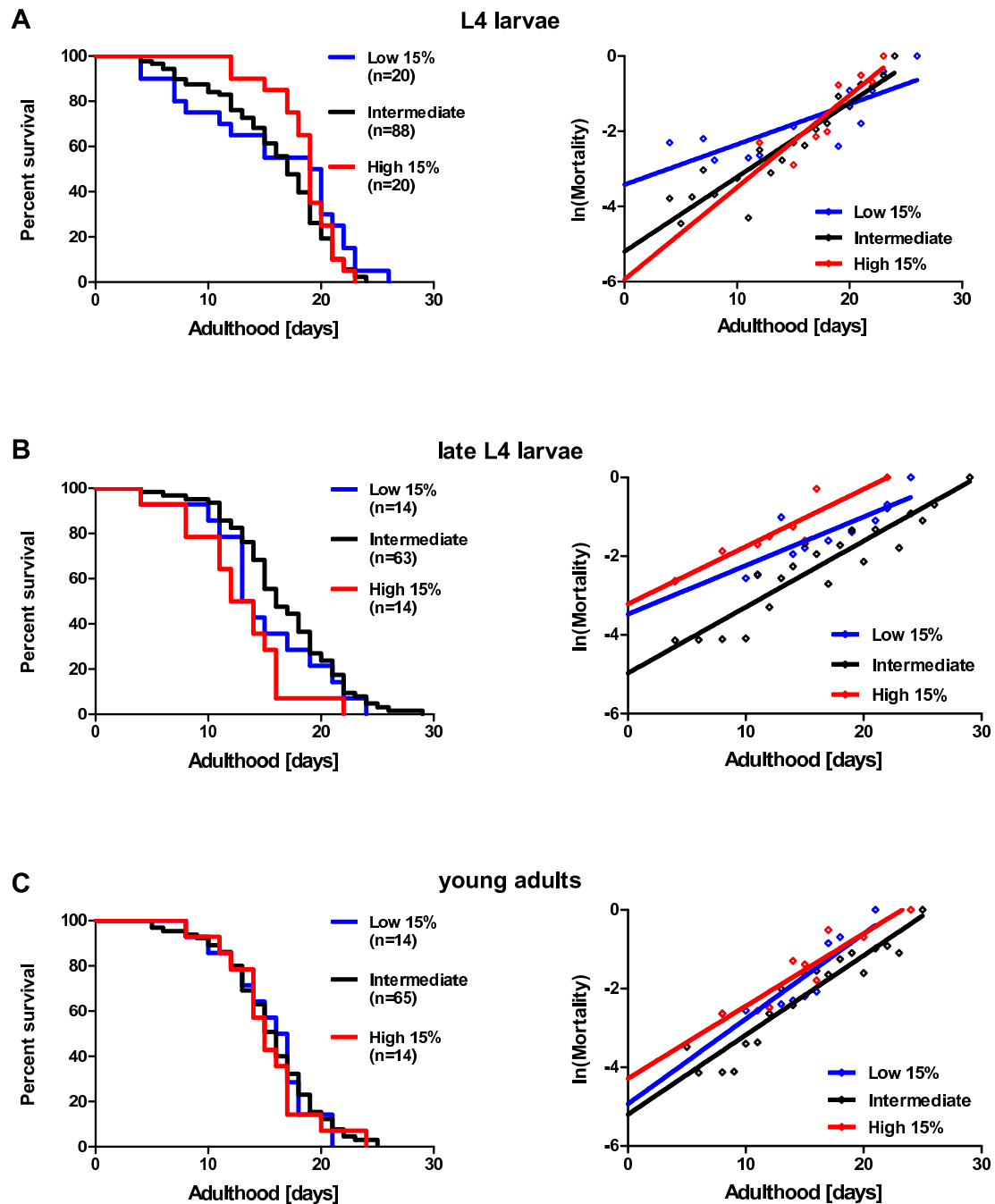


**Figure 4.32. Mortality and lifespan of *C. elegans* sub-populations which differ in their HyPer ratios.** The HyPer ratios in the body wall muscle cells of individual N2 [*unc-54::HyPer*] worm and their subsequent lifespans were determined. The survival curves are displayed on the left-hand side, while Gompertz curves are shown on the right side. The survival or mortality of worms that had HyPer ratios belonging to the 15% highest (red) or lowest (blue) distribution are compared to survival of worms that had intermediate HyPer ratios (black). The survival curves are not significantly different, but for (B) late L4 15% High vs. Intermediate population:  $p = 0.0051$  (Log-rank (Mantel-Cox) test) and  $p = 0.0032$  (Gehan-Breslow-Wilcoxon test). Similar trends for late L4 larvae were observed in two independent experiments (with lower n-numbers).

---

## 5 Discussion<sup>10</sup>

In this study, we used three independent techniques, including the AmplexUltra<sup>®</sup>Red assay, the H<sub>2</sub>O<sub>2</sub> sensor HyPer, and the peroxiredoxin redox state to determine *in vivo* peroxide level in *C. elegans*. We reproducibly found that wildtype animals encounter high amounts of peroxide during their development. Peroxide levels decrease when the animals mature and reach their reproductive age, after which an age-accompanying increase of peroxide sets in. Those findings were in excellent agreement with other studies from our lab which revealed that protein thiol oxidation was high during *C. elegans* development, decreased when animals matured and increased again as worms aged (Knoefler *et al.*, 2012a). Many of the peptides found to be reversibly oxidized during larval stages had previously been identified to be sensitive to peroxide-mediated oxidation. These results strongly suggested that elevated peroxide levels are present during the development of *C. elegans*. Furthermore, every mutant strain of *C. elegans* that we tested also showed transiently increased peroxide levels during development, suggesting that high ROS levels play an important part of larval development regardless of the lifespan of the animals. These findings were intriguing and argued for an important and crucial role of oxidants during development. They might also explain why increasing the organism's antioxidant capacity by either overexpressing antioxidant enzymes or administering mimetics in *C. elegans* did not result in beneficial outcomes, and in some cases, even had harmful effects on the organism (Doonan *et al.*, 2008; Keaney and Gems, 2003).

### 5.1 Peroxide generation during cuticle formation

The boost of oxidants during development most probably has various sources. One process that likely contributes to the elevated peroxide levels observed in *C. elegans* larvae is peroxide generated by the dual oxidase Ce-DUOX-1. This enzyme is expressed in the hypodermis peripheral to muscle cells and its peroxide production is critical for correct cuticle formation during larval molts (Edens *et al.*, 2001). Peroxide derived from Ce-DUOX-1 is used to cross-link tyrosines, which stabilizes collagens and other proteins in the extracellular matrix. Interestingly, immunostaining for Ce-DUOX-1 revealed higher levels of the enzyme in development than in adulthood (Edens *et al.*, 2001). From the localization of DUOX, it is conceivable that H<sub>2</sub>O<sub>2</sub> generation during larval molts is

---

<sup>10</sup>Parts of this discussion are going to be published in Knoefler *et al.* (2012a).

responsible for the high peroxide release rates measured with the AmplexUltra<sup>®</sup>Red reagent during development compared to adulthood (Figure 4.5). Many of the proteins found to be more oxidized during development, however, are expressed in tissues that are localized far away from the hypodermis, such as the intestine or neurons. This and the data derived from our HyPer measurements in neurons and pharynx argue against the idea that peroxide generated during larval molt constitutes the sole source of developmental ROS production.

## 5.2 Oxidant generation in metabolic processes

Another source of oxidants might be metabolic changes that occur in different stages of *C. elegans*' lifespan, such as elevated metabolic rates during development (Wadsworth and Riddle, 1989). The metabolic rate has been demonstrated to decrease from the L2 larval stage to young adult stage (De Cuyper and Vanfleteren, 1982), which correlates with the observed drop in peroxide level. After worms have consumed their lipid resources during embryogenesis, metabolism in worms shifts from the glyoxylate cycle towards the tricarboxylic acid (TCA) cycle in L2, L3 and L4 larval stages. This shift increases the metabolic rate and is accompanied by an increase in ATP levels in the last three larval stages (Wadsworth and Riddle, 1989). One of the proteins that we found to become more oxidized during L2 and L4 larval stages, is the bifunctional glyoxylate cycle protein isocitrate lyase/malate synthase (Knoefler *et al.*, 2012a), whose activity has been shown in an independent study to decrease during the L1 and L2 stages (Wadsworth and Riddle, 1989). It is tempting to speculate that ROS-mediated oxidation of this enzyme might constitute a feedback mechanism to reduce the flux of acetyl-CoA through the glyoxylate cycle.

## 5.3 Peroxide as mediator in ROS signaling

Another source of oxidants might come from developmental ROS signaling. Hydrogen peroxide, in particular, possesses unique features, which qualify the oxidant to act as a second messenger. In comparison to other reactive oxygen species, peroxide has a longer half-life, a lower reactivity and a higher intracellular concentration (Giorgio *et al.*, 2007).



### 5.3.1 Apoptosis

Studies in HeLa cells suggested that apoptosis is one process that involves increased hydrogen peroxide generation and/or peroxide signaling (Belousov *et al.*, 2006). It is of note that *C. elegans* goes through tightly regulated steps of programmed cell death, which results in the loss of about 10% of somatic cells during embryogenesis (Sulston *et al.*, 1983) and the L2 larval stage (Lettre and Hengartner, 2006). Neurons are the main types of cells that undergo apoptosis during early development in *C. elegans*, but muscle, hypodermal and pharyngeal cells are affected as well (Lettre and Hengartner, 2006). Another wave of apoptosis affects the germline in adult hermaphrodites (Gumienny *et al.*, 1999). Pre-apoptotic cells are characterized by a reduction of the mitochondrial membrane potential and increased ROS production due to increased uncoupling of mitochondria, which precedes nuclear fragmentation, DNA degradation and cell shrinkage (Zamzami *et al.*, 1995). Suppression of mitochondrial ROS production or administration of antioxidants prevents the shrinkage of apoptotic cells, (Zamzami *et al.*, 1995). Moreover, antioxidant enzymes appear to be down-regulated in regions where high ROS levels and apoptotic cells are present (Schnabel *et al.*, 2006). These results indicate that oxidants might play a role as mediators of programmed cell death (Zamzami *et al.*, 1995). Further studies are now needed to test whether the increased peroxide levels observed in early development in *C. elegans* take part in the initiation and/or mediation of programmed cell death, and whether the elevated thiol oxidation observed at the L2 larval stage might be a side-effect of pre-apoptotic ROS increase or might represent the selective oxidation of effector molecules involved in apoptosis.

### 5.3.2 Proliferation

In addition to programmed cell death, hydrogen peroxide also acts as a signaling molecule in other developmental processes, such as cell proliferation. In HeLa cells, proliferation is stimulated by the exogenous administration of low levels of hydrogen peroxide, while the addition of catalase and superoxide dismutase reduces cell growth (Burdon and Gill, 1993). In a similar way, hydrogen peroxide is required for platelet-derived growth factor (PDGF)-signaling, which can be inhibited by increased catalase activity (Sundaresan *et al.*, 1995). Peroxiredoxin 2 (PRDX-2) appears to work as a negative modulator of PDGF-signaling in mammals as absence of PRDX-2 was shown to

cause increased cell proliferation (Choi *et al.*, 2005). In our studies, we found protein expression levels of peroxiredoxin 2 to be lower during the development of *C. elegans*, suggesting that the antioxidant system might be reduced to enable redox signaling and cell proliferation. Future studies are necessary to determine whether other oxidant clearance systems, such as catalases or superoxide dismutases, are down-regulated as well.

#### 5.4 Evidence for developmental ROS signaling

An intriguing question is whether redox signaling occurs preferentially during development. Recent studies suggested that the development constitutes a period of active ‘programming’ as the reduction of components of the mitochondrial electron transport chain had to be initiated during development to promote lifespan extension (see also section 2.7.3). Dillin and co-workers showed that RNAi targeted against mitochondrial components of the ETC during the development of *C. elegans* led to a reduction of ATP level by 40 – 80 %, decreased body size and growth rate, and affected behavioral processes such as pharyngeal pumping and defecation. Most importantly, the mean lifespan of these worms was increased by an average of 60% (Dillin *et al.*, 2002b). Even when mitochondrial respiration was restored to normal levels during adulthood, reduced ATP levels and increased lifespan of the worms remained. In contrast, reducing mitochondrial components during adulthood did not alter the lifespan despite a decrease in ATP levels (see Figure 2.4). Another study narrowed down the window to the L3/ early L4 stage, in which respiratory RNAi needed to be applied to extend lifespan (Rea *et al.*, 2007). These findings strongly suggest that developmental events have the ability to influence subsequent behavioral processes and lifespan in adults.

##### 5.4.1 Effect of cultivation temperature on endogenous peroxide level

Cultivation temperature is known to influence developmental growth and the length of *C. elegans*’ lifespan (Klass, 1977; Hosono *et al.*, 1982). The higher the temperature is, the faster worms progress through the four different larval molts, and the shorter their lifespan. The reduced lifespan at elevated temperatures was originally thought to be caused by an increased ‘rate of living’, which means that the rate of chemical reactions are higher at elevated temperatures and hence the lifespan is shorter (Klass, 1977). Recent studies, however, presented evidence indicating that the temperature-

mediated lifespan of *C. elegans* is under active regulation (Lee and Kenyon, 2009). Lee *et al.* suggested that thermosensory neurons are involved in the regulation of lifespan at different growth temperatures. Genetic or laser ablation of specific neurons resulted in an even shorter lifespan at an elevated temperature (25°C) while the lifespan at lower temperatures was not affected. The authors proposed that the lifespan at higher temperatures might be actively regulated to be longer as it would be at this temperature. Interestingly, other temperature-dependent processes, such as feeding and reproductive timing, were not affected, indicating that thermosensory cues specifically address the rate of aging. In our studies we found that the HyPer ratios of developing worms reared at elevated temperatures were lower than that of worms grown at colder temperatures, indicating that worms produce less peroxide when raised at higher temperature. This finding is also inconsistent with the “rate of living” theory of aging as higher metabolic rates would predict higher peroxide level. But in light of the recent findings that the lifespan at higher temperatures is actively modulated, it is now tempting to speculate that increasing the levels of antioxidants enable animals to cope with these elevated temperatures. It has also been suggested that growth temperature is not only perceived but also memorized and that it can subsequently influence behavioral rates such as thermotaxis (Mori and Ohshima, 1995). That memory functions for past growth temperatures might exist that affect lifespan as well, concurs with our temperature-switch experiments. Animals which were grown at a low temperature during development and were transferred to a higher temperature as young adults had a significantly longer lifespan than worms that experienced elevated temperatures throughout their entire life. In the same way, worms accustomed to high temperatures during development and switched to low temperatures as young adults had shorter lifespans than worms constantly grown at the low temperature. These findings strongly suggest that the experience of high temperatures at early stages in life has an impact on lifespan. These results are in agreement with recent studies by Wu and co-workers, who showed that the initial mortality of *C. elegans* was influenced by past cultivation condition (i.e., temperature) while the present and future mortality was modulated by current environmental cues (Wu *et al.*, 2009). In contrast to our experiments, however, Wu *et al.* did not modulate developmental cultivation temperature but shifted temperatures exclusively during adult lifespan. Previous studies modulated the temperature either during growth (development), reproduction, or post-reproduction (Klass, 1977; Hosono *et al.*, 1982) and observed potential changes in the subsequent lifespan. While one study found that although a change in temperature always had

an effect on lifespan, in agreement with (Wu *et al.*, 2009), low cultivation temperature only significantly extended lifespan when applied during the reproductive period (Klass, 1977). Another study suggested that low temperature could increase lifespan only after maturation (Hosono *et al.*, 1982). In our experiments, animals were switched to different temperatures as mature, fertile young adults. Future experiments are needed to clarify whether the very short period of the transition of development to young adult could really be sufficient to influence the subsequent lifespan, or whether the developmental culture conditions contributed to the lifespan effect as well.

#### 5.4.2 Fluctuations in peroxide as modulator of reproduction

Gametogenesis in *C. elegans* might constitute another process that requires a fine-tuned redox balance, and might explain why the drop in peroxide level seems to appear within hours upon the L4 to young adult transition. In worms, spermatogenesis takes place by the late L4 larval stage and oogenesis begins shortly after the L4-adult-molt. Maximum brood size depends on the number of sperms produced before the hermaphrodites change from spermatogenesis to oogenesis (Shibata *et al.*, 2003; Gems *et al.*, 1998). Both oogenesis and spermatogenesis are delayed in the *C. elegans* *clk-1* (clock abnormality) mutants, apparently due to a disturbed redox signaling (Shibata *et al.*, 2003). In bovine oocytes, the expression of PRDX-6 has been found to be increased while overall transcription decreases and glutathione levels have been shown to be elevated during maturation (Leyens *et al.*, 2004; Tomek *et al.*, 2002; de Matos *et al.*, 1997). Right now, it can only be speculated whether a reduction in oxidant levels is necessary to allow oocyte maturation, and whether the drop in peroxide level observed in young fertile adults is crucial for a functional germline development. Interestingly, disruption of the Insulin/IGF-1 signaling during development through RNAi targeted against the IIS receptor DAF-2 caused a delay in reproduction (Dillin *et al.*, 2002a). These results suggest that reproduction is regulated during development, and that an imbalance in the IIS might interfere with reproduction as brood sizes of *daf-2* (e1370) have been found to be reduced by an average of 30 - 70 % (Gems *et al.*, 1998; Houthoofd *et al.*, 2005). It is now tempting to speculate that the reduced peroxide levels observed at L4 stage in *daf-2* [*unc-54::HyPer*] animals (Figure 4.15 B) could be an indication for reduced redox signaling, which might affect spermatogenesis in the germline and thus results in a reduced brood size.

### 5.4.3 Manipulation of the redox homeostasis

To assess whether perturbations in the peroxide homeostasis might affect physiology and lifespan in *C. elegans*, we tested a catalase 2 (CTL-2) deletion strain which lacks the peroxisomal catalase and exerts only 20 % of wildtype catalase activity (Petriv and Rachubinski, 2004). In addition, the *ctl-2* deletion animals exhibit a delay in egg-laying and a reduction in lifespan by 16 %, which is not observed in cytosolic catalase *ctl-1* deletion worms (Petriv and Rachubinski, 2004). We crossed the *ctl-2* deletion strain with our HyPer-expressing wildtype strain and expected higher HyPer ratios as compared to wildtype *C. elegans*. Surprisingly, however, we observed much lower HyPer ratios in adult *ctl-2* deletion worms in comparison to wildtype, suggesting that the deletion strain has actually lower peroxide levels. It is of note that Petriv *et al.* detected the upregulation of additional proteins with catalase activity and also noted lower levels of oxidative stress-mediated protein carbonylation in aged *ctl-2* worms, suggesting a compensatory up-regulation of other antioxidants with catalase activity in these worms (Petriv and Rachubinski, 2004). We compared the PRDX-2 expression level in *ctl-2* deletion worms and wildtype and did not find any significant differences in the expression levels between the two strains. It now remains to be tested which other enzyme systems are up-regulated in the *ctl-2* deletion strain that could account for the lower HyPer ratio. The use of the AmplexUltra<sup>®</sup>Red assay will serve as an additional probe to determine whether endogenous peroxide levels are indeed reduced in the *ctl-2* deletion strain. Alternatively, a lower HyPer ratio might reflect an increase in reduced HyPer protein (see 5.6), which would argue for a shift towards a more reducing capacity of the organism.

### 5.5 Can events early in life affect the lifespan of *C. elegans*?

Our findings that animals are exposed to elevated levels of endogenous peroxide during development from which they apparently recover when they reach the fertile period, and that differences in the recovery time exist between mutants of the Insulin/ IGF-1 signaling (IIS) pathway suggest that events early in life might influence adult lifespan in *C. elegans*. These results agree with previous reports by Morimoto and coworkers, who reported that the capacity to maintain a functional *C. elegans* proteome (i.e., proteostasis) decreases with age. Intriguingly, the onset of the proteostasis collapse becomes apparent as early as day 2 or 3 of adulthood and is particularly obvious in

muscle cells and neurons (Ben-Zvi *et al.*, 2009). The overexpression of stress transcription factors such as HSF-1 or DAF-16 delayed the collapse and in turn increased lifespan, whereas deletion of either of these factors accelerated the collapse and decreased lifespan. Proteins are one of the main cellular targets of reactive oxygen species and once oxidized, tend to form high molecular weight aggregates that require removal by the proteasome (Bader and Grune, 2006). If the removal of the protein aggregates fails, they can accumulate in the cell, interfere with basic cellular functions, and ultimately cause the death of the cell (Davies, 2001). Based on our results that high oxidative stress levels are generally present during development, it is now tempting to speculate that the observed failure of *daf-16* deletion mutants to restore low peroxide level and low protein thiol oxidation states (Knoefler *et al.*, 2012a) might contribute to the accelerated collapse of proteostasis and the shorter lifespan. Conversely, rapidly restoring the redox conditions and keeping peroxide levels low as observed in the *daf-2* mutants will reduce the load of oxidatively modified proteins and might delay the collapse of proteostasis thus extending the lifespan. A potential tradeoff, however, might exist in the reduced brood size (as discussed in 5.4.2).

### 5.5.1 Developmental glucose restriction

That early interventions could affect lifespan was suggested by recent studies with mice, in which caloric restriction (CR), when applied during the first three weeks of pre-weaning, was found to extend lifespan by a significant 18% (Sun *et al.*, 2009). Caloric restriction was achieved by increasing the litter size, thus reducing the food availability per pup. Although the molecular mechanism by which caloric restriction extends lifespan is not understood in detail, a correlation between CR and increased stress resistance has been proposed (Yu and Chung, 2001). Since caloric restriction was able to extend the lifespan in mice even when applied only during the first weeks of life, we were wondering if that might be true for *C. elegans* as well. We used a protocol of glucose restriction, which had been previously used in adult *C. elegans* (Schulz *et al.*, 2007). Schulz and co-workers have shown that 2-Deoxy-D-glucose (DOG), which is an inhibitor of glycolysis, caused an increase in respiration and an elevation of reactive oxygen species when given to adult worms. Interestingly, this transient increase in ROS levels appeared to be sufficient to extend the lifespan of these animals. The authors suggested that ROS, derived from respiration, induced a hormesis response, which leads to the up-regulation of the antioxidant response and with that to an increased stress resistance. That

reactive oxygen species were indeed involved in this process was demonstrated by the administration of antioxidants, which abolished the positive effects of caloric restriction on lifespan (Schulz *et al.*, 2007). These were interesting findings since they argued that ROS are important mediators in the lifespan-extending mechanism of glucose restriction. We tested HyPer-expressing wildtype *C. elegans* and applied DOG during the adulthood of the worms. We were able to confirm the results from Schulz *et al.* and found an increased HyPer ratio and an extended lifespan in DOG-treated adult worms. When DOG was applied during development of *C. elegans*, a decrease of the HyPer ratio was observed during the L3/L4 stage, indicative of reduced peroxide level. Furthermore, we found that the developmental growth rate was delayed, and that the subsequent adult lifespan was reduced irrespective of the remaining DOG-treatment. These results indicate that glucose-restriction during development has detrimental outcomes on growth rate and lifespan, which is in contrast to the beneficial effects observed when DOG was added during adulthood. One explanation might be that, while adult worms use their body fat to metabolically switch from glycolysis (which is inhibited by DOG) to  $\beta$ -oxidation (Schulz *et al.*, 2007), *C. elegans* larvae might not be able to change to lipid metabolism as lipids are used up during embryogenesis (see section 5.2). It can be speculated that this failure in switching to  $\beta$ -oxidation might account for the rapid dying. Another possibility might be that the reduced HyPer ratio observed in late development might be indicative of a hormetic up-regulation of antioxidant enzymes, which have been shown in adult animals (Schulz *et al.*, 2007). It is conceivable that increased level of catalase then interfere with early ROS signaling, necessary for development and lifespan. Future experiments have to be performed to distinguish between detrimental effects caused by developmental malnutrition and/or deregulated ROS signaling. It is tempting to speculate that the type(s) and expression level(s) of specific antioxidant enzymes (and thus the level of oxidants) are optimized for the needs of certain processes. It is interesting that an increased antioxidant capacity, which occurs in DOG-treated adults (Schulz *et al.*, 2007), can have beneficial effects in adulthood but has adverse outcomes in other stages of life. What should be kept in mind is that most antioxidant enzymes work very efficiently. In the case of catalase, very low levels of enzyme decompose high amounts of hydrogen peroxide (Nicholls *et al.*, 2000), suggesting that even a small deregulation in expression and/or activity of these enzymes might have major effects on peroxide level. Future experiments will determine whether catalase is indeed up-regulated upon glucose-restriction in development, and if that might be one explanation for the observed

shortened lifespan.

### 5.5.2 Developmental oxidant exposure

That the oxidant levels are indeed finely balanced during development was also suggested by our experiments using the superoxide generator paraquat. Wildtype L4 larvae were treated with a short bolus of sublethal paraquat concentrations, which significantly delayed reproduction confirming that reproduction is a sensitive process that can be easily perturbed. Furthermore, we found that the age-mediated loss in motility was accelerated in paraquat-treated worms and that the lifespan was significantly shortened upon paraquat exposure. These results were intriguing as two-hour incubation in paraquat as L4 larvae seemed insufficient to cause immediate changes but exerted effects as late as mid-adulthood (movement, mortality). These results further agreed with our previous conclusions that disruption of oxidant homeostasis during development results in the deregulation of physiological processes including reproduction and lifespan. A study using the ROS generator juglone found increased translocation of DAF-16 into the nucleus upon exposure to low concentrations of juglone (Heidler *et al.*, 2010), raising the question whether an increased activity of the FOXO transcription factor could have caused the delay in egg-laying (see also section 5.4.2).

In contrast to our studies, which showed that a short developmental oxidant bolus shortens the lifespan of the worms, Heidler *et al.* observed a lifespan extension when young adults were continuously treated with very low concentrations (40  $\mu$ M) of juglone (Heidler *et al.*, 2010). The observed differences in the effect on lifespan could be due to different types or doses of ROS generators, or to variations in the stage in life at which treatment was initiated. That the dose effect plays a role was suggested by studies that found that higher concentrations of juglone (250  $\mu$ M) had adverse (lifespan shortening) effects, which were partly prevented by ascorbic acid supplementation (Hartwig *et al.*, 2009). Another study conducted by Lee *et al.* observed that while worms treated with low concentrations of paraquat (0.125 mM – 1 mM) from L4 to day 3 of adulthood showed an extended lifespan, treatment with concentrations between 4 mM – 64 mM shortened lifespan, arguing for a dose effect as well (Lee *et al.*, 2010). It is of note that worms treated with 4 mM paraquat from the time of hatching arrested as larvae. Our studies agreed with these results and showed that concentrations of paraquat as well as the cultivation temperature affected the outcome on lifespan. The mortality rates were found to increase with higher concentrations of paraquat. We also observed



more severe effects when the paraquat treatment and the subsequent lifespan were performed at elevated temperatures. We can only speculate why elevated temperatures would increase mortality, but we think it might be an increased redox-cycling of paraquat within the mitochondria, or the temperature itself which might affect redox balance (as discussed in section 5.4.1). That the stage of treatment could also influence the effect of paraquat on lifespan was suggested in a preliminary lifespan experiment, where 3-day-old adults were treated with 15 mM paraquat, and slightly extended lifespan was observed upon oxidant exposure. This result suggests that an (transient) increase in oxidants in stages with low peroxide levels might have a beneficial effect, which would agree with the hormesis effect observed upon DOG treatment in adulthood. In the same way, increasing oxidant level during development might interfere with developmental and reproductive processes and might have adverse outcome on lifespan.

### 5.5.3 Could developmental variations in peroxide level affect lifespan?

Our studies strongly suggest that the oxidant levels during development are optimized for the need of the organism, and that either a drastic increase or a decrease in ROS level has detrimental effects. Yet, it is of note that synchronized wildtype worms exhibit highly variable HyPer ratios at any given time point during development. These results suggest that individual differences in peroxide (oxidant) levels exist. We were wondering whether these variances might account for the differences in individual lifespans observed in an isogenic *C. elegans* population. Recently a clear correlation was found between the expression level of a heat-inducible promoter driving GFP in 1-day old adults of a synchronized isogenic population and their lifespan (Rea *et al.*, 2005). These results suggest that intrinsic differences exist within young adults of an isogenic population raised under the same environmental conditions which affect lifespan. This study also agreed with recent findings that the aging process is not only influenced by genetic factors but also by stochastic events as well (Hernon *et al.*, 2002). We were curious whether the variances in HyPer ratio observed in an isogenic wildtype population could be used as an even earlier biomarker of aging. We thus analyzed the ROS levels in individual HyPer-expressing worms (L4 stage) of a synchronized *C. elegans* population and recovered the worms after the imaging process for subsequent lifespan analysis. Thus, the HyPer ratio and lifespan for each worm were determined. Our preliminary experiments suggest that low HyPer ratios during L4 stage substantially increased the initial mortality while high HyPer

ratios seemed to decrease the mortality in the first days. These results argue for the requirement for certain oxidant levels in early stages of life. These results need to be reproduced, however, as they were hampered by the low number of surviving worms, which made statistical analysis impossible. It is conceivable that the observed early deaths might have been caused by vulva malformation and internal hatching of the progeny. A recent study overexpressing all three catalases in *C. elegans* observed an increased mortality due to internal hatching, which could be suppressed by the simultaneous overexpression of superoxide dismutase 1 (Doonan *et al.*, 2008). These results, which might explain the increased initial mortality observed in worms with lower HyPer ratios, suggest that certain peroxide levels are required for reproductive processes in *C. elegans*. Late L4 larvae, which exhibited very low or very high HyPer ratios exhibited an increased initial mortality compared to worms with intermediate peroxide levels, suggestive of an “optimized” ROS level for “maximized” survival. Again, further experiments are required to reproduce these findings.

## 5.6 Conclusions

The “Free Radical Theory of Aging” proposes that an accumulation of reactive oxygen species causes damage to cells and macromolecules and ultimately leads to aging, disease and death. In an attempt to test this popular theory, a multitude of studies have been performed over the years, utilizing the deletion and/or overexpression of specific antioxidant systems in different model organisms. The results of these studies failed to ultimately show whether the FRTA is valid or not. In our opinion, however, the first step in evaluating this theory has not been taken. We need to first know whether oxidants are indeed accumulating, when their concentration increase, and what their roles are for development, growth and aging. With HyPer, we now have a tool to specifically detect hydrogen peroxide level in select tissues in living animals, and can thus evaluate and assess the effects of ROS on all these processes. The HyPer sensor has some drawbacks that need to be considered. First, a strong promoter is required to allow reliable fluorescence quantification throughout all stages during the lifespan. Second, the HyPer ratio has been shown to be affected by changes in pH (Belousov *et al.*, 2006). To exclude potential artifacts caused by pH alterations, alternative pH-insensitive yet hydrogen peroxide-specific probes such as the AmplexUltra<sup>®</sup>Red assay are needed to verify that a drop in peroxide level occurs indeed during the larval-adult transition. Third, although it has been demonstrated that the *E. coli* OxyR and the HyPer protein specifically react with

hydrogen peroxide *in vitro* (Zheng *et al.*, 1998) (Belousov *et al.*, 2006), the fluorescence read-out of HyPer does not respond to peroxide directly but depends on the formation of the disulfide bond within OxyR. It can thus also be affected by the reducing capacity of an organism (Meyer and Dick, 2010). It is noteworthy that other fluorescent H<sub>2</sub>O<sub>2</sub> sensors have been recently constructed including HyPer2, which has twice the dynamic range of HyPer (Markvicheva *et al.*, 2011). Another sensor, which could be used to detect *in vivo* hydrogen peroxide, consists of a redox-sensitive GFP fused to the peroxidase Orp1, which exhibited similar response and sensitivity as HyPer upon exposure to hydrogen peroxide (Gutscher *et al.*, 2009). In summary, HyPer and other redox sensor are the tools of the future to critically evaluate *in vivo* oxidant level and determine their effects on health and lifespan of organisms.



## 6 Materials & Methods

### 6.1 Cultivation of *C. elegans*

Nematode growth media (NGM) plates seeded with *E. coli* OP50 (uracil auxotroph) were used as food source for the cultivation of *C. elegans* (Brenner, 1974). A culture of OP50 bacteria was grown overnight in LB medium, adjusted to  $10^{10}$  cells per ml, and seeded on NGM plates. The bacteria were dried overnight at room temperature forming an OP50 lawn. The transfer of multiple worms onto fresh plates was achieved either by taking a chunk from a populated plate and place it face down onto a fresh plate, or by washing worms off their plates using M9 minimal media and plating the worm pellet after centrifugation onto fresh plates. Individual worms can be transferred using a worm pick, which is made of a platinum wire attached to a glass Pasteur pipette.

#### Nematode Growth Media (NGM) agar:

NaCl	3 g
Bacto-Peptide	2.5 g
Bacto Agar	19 g
Add 1 L ddH <sub>2</sub> O	
Autoclave and add sterile:	
Cholesterol (5 mg/ml in Ethanol)	1 ml
1M CaCl <sub>2</sub>	1 ml
1M MgSO <sub>4</sub>	1 ml
KH <sub>2</sub> PO <sub>4</sub> , pH 6.0	25 ml

#### LB medium (Lysogeny broth):

Tryptone	10 g
NaCl	5 g
Yeast Extract	5 g
Fill up to 1 L with ddH <sub>2</sub> O	
Autoclave	

M9 Minimal Medium:

Na <sub>2</sub> HPO <sub>4</sub>	5.8 g
KH <sub>2</sub> PO <sub>4</sub>	3 g
NaCl	0.5 g
NH <sub>4</sub> Cl	1 g
Fill up to 1 L with ddH <sub>2</sub> O	
Autoclave	

## 6.2 Synchronization of a worm population

### 6.2.1 Hypochlorite-NaOH Lysis

Gravid worms were washed off the plates with M9 buffer and pelleted in a centrifuge at 3 000xg. After removal of the supernatant, an equal volume of freshly prepared lysis solution was added. The lysis process, supported by frequent vortexing steps, was routinely checked under the microscope. When the worms started to break open and to release the eggs, the worms were quickly spun down at 3 000xg, and the lysis solution was removed. After the eggs were washed three times with M9 buffer, they were either put directly onto OP50-seeded NGM plates, where they would hatch and develop, or were incubated in M9 media under mild shaking, which allowed the eggs to hatch and arrested the worms at the L1 larval stage. To resume their development L1 larvae were transferred onto OP50-seeded NGM plates (Hope, 1999).

Lysis solution:

Clorox <sup>®</sup> Regular Bleach:	2 ml
10N NaOH:	0.25 ml
Fill up to 5 ml with ddH <sub>2</sub> O	

### 6.2.2 Synchronization without hypochlorite treatment

Synchronization of a *C. elegans* population can also be achieved by carefully washing off adult and larval worms from an NGM plate, hence allowing the embryos to remain on the agar. A chunk of NGM harboring the eggs can then be transferred onto a fresh OP50-seeded NGM plate, where embryos proceed with their development.

### 6.3 Assessment of physiological processes and lifespan

Animals were cultivated for several generations at the same temperature at which the experiment was going to be performed. Synchronization of the *C. elegans* population was maintained by transferring L4 larvae worms onto NGM plates, containing the chemical 5'-fluoro-2'-deoxyuridine (FUdR, 20 mg/l, Sigma-Aldrich) before the start of the fertile period. FUdR, an inhibitor of DNA synthesis, prevents the development of the progeny. For the lifespan analysis, the L4 molt stage was considered as time point zero and the survival was assessed every other day. Animals, which did not move, did not react to tapping of the plate, or did not respond to gentle prodding with the worm pick, were considered dead while animals that crawled off the plate were censored at the time of the event for the statistical analysis.

Motility was assessed by pipetting the worms in the center of a 6 cm NGM plate, which contained a ring of OP50 bacteria close to the outer edge of the plate. Motility of the worms towards the food source (i.e., OP50) was assessed every 15 minutes.

Movement was assessed over the lifespan of worms by judging the ability of the worms to move around the plate. While young animals usually exhibit a sinusoidal, coordinated and fast movement (A-Movement), aged worms did only move after prodded gently with the worm pick and have less coordinated movement ability (B-Movement). Very old worms do not move even after prodding and are just capable of moving their head or tail (C-Movement) (Herndon *et al.*, 2002).

Brood size was determined by maintaining the animals on NGM plates without FUdR, thereby allowing the eggs to hatch and develop. To distinguish the parents from the progeny generation, parent worms were transferred every other day onto a fresh plate using a worm pick, while the

remaining progeny (eggs and/or hatched larvae) on the other plate were counted.

## **6.4 Oxidative stress treatment**

### **6.4.1 Treatment of worms with the superoxide generator paraquat**

Synchronized L4 larvae were washed off their plates and pelleted at 3 000xg. Aliquots (100 – 400  $\mu$ l) of the worm solution were distributed into Eppendorf tubes and an equal volume of a 2-fold concentrated, (from a 500 mM frozen stock) freshly prepared paraquat solution was added to the worm solution. The worms were incubated in the presence of paraquat for two hours shaking at the same temperature at which the subsequent lifespan assay was performed. After the stress treatment, the worms were washed three times with M9 medium. The animals were pipetted onto an OP50-seeded NGM plates and individually transferred onto seeded 6 cm NGM plates for lifespan analysis (1-15 worms/plate).

### **6.4.2 Treatment with sublethal concentrations of hydrogen peroxide**

A synchronized population of *C. elegans* was washed off NGM plates and pelleted by centrifugation as in 6.4.1. To expose the animals to exogenous peroxide stress, the animals were incubated shaking for 30 minutes with sublethal concentrations of hydrogen peroxide (1 mM), after which the H<sub>2</sub>O<sub>2</sub> was either removed by washing with M9 buffer or treated worms were directly used for a subsequent experiment (Kumsta *et al.*, 2011).

## **6.5 Manipulation of *C. elegans* gene expression**

Gene expression in *C. elegans* can be manipulated by expressing transgenes from extrachromosomal arrays or upon chromosomal integration, or by silencing gene expression using RNA interference (RNAi).

### **6.5.1 Generation of transgenic animals**

The tissue specific expression of the hydrogen peroxide sensor HyPer in the body wall muscle cells of *C. elegans* was achieved by cloning the HyPer gene (Belousov *et al.*, 2006) into the plasmid pPD30.38 (Addgene plasmid 1443) using the restriction sites NheI and NcoI, generating the



Strain	Genotype	Description		Source
N2	<i>C. elegans</i> wild isolate			CGC
LB90	<i>ctl-2</i> (ua90) II; <i>him-8</i> (e1489) IV	Partly deletion <i>him-8</i> : increased frequency of males	outcrossed 6 times	CGC
CF1041	<i>daf-2</i> (e1370)	Base substitution: G→A Missense mutation: P1465S	Strain CF326 outcrossed 7 times	Allen Hsu
GR1307	<i>daf-16</i> (mgDf50) I	deficiency eliminates <i>daf-16</i> coding region	outcrossed 3 times	CGC

**Table 6.1. Overview of mutant *C. elegans* strains used in this thesis.**

plasmid pPD30.38::HyPer [unc54::HyPer]. *C. elegans* wildtype animals were transformed by gonad microinjection (Mello *et al.*, 1991), which generates transgenic animals carrying multiple extrachromosomal arrays of the injected DNA. The plasmid pPD30.38::HyPer [unc-54::HyPer] was co-injected with the plasmid pPD118.33 [*myo-2*::gfp] (Addgene plasmid 1596) into N2 wildtype animals at a concentration of 100 ng/μl for each plasmid using an injection scope. The progeny of the injected worms were monitored for *myo-2*::GFP-derived fluorescence in the pharynx using a fluorescent microscope (Olympus SZX16, GFP filter: EX460-480HQ; EM495-540HQ). A stable transmitting line was used to generate integrated chromosomal arrays by irradiating animals carrying the extrachromosomal arrays with 3000 rad of a Cs137 source. The homozygous transgenic strain was outcrossed three times with the wildtype strain N2 to minimize the mutations in the chromosome background. The integrated outcrossed wildtype strain [unc-54::HyPer; *myo-2*::GFP] is referred to as N2 [unc-54::HyPer].

## 6.5.2 Generation of transgenic mutant animals

### 6.5.2.1 Generating and maintaining a male *C. elegans* stock

Mutant animals expressing the hydrogen peroxide sensor HyPer in the body wall muscle cells were generated by crossing male transgenic N2 wildtype worms with mutant *C. elegans* hermaphrodites. Male nematodes occur at a frequency of 0.1 % in a population (Ward and Carrel, 1979), caused by the spontaneous non-disjunction of the X-chromosome during meiosis giving rise

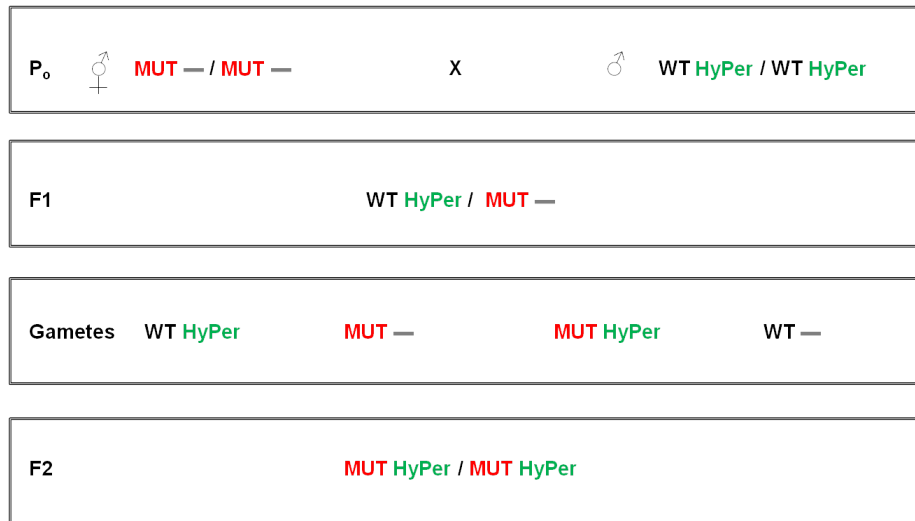


**Figure 6.1. Schematic overview of the cross between wildtype and mutant animals.** Mating of wildtype worms carrying the HyPer transgene (WT HyPer) and a mutant animal (MUT), which does not have the HyPer gene (-). Recombination of the F<sub>1</sub> genotype leads to a F<sub>2</sub> generation, where some members are both homozygous for the mutant allele and the HyPer gene.

to nullo-X gametes. The abundance of male progeny can be enhanced by incubating L4 animals at 30°C for five to six hours (Hodgkin, 1983), after which the male stock is maintained by continuously setting up matings between males and hermaphrodites.

### 6.5.2.2 Crosses and selection of transgenic mutants

Male N2 [*unc-54::HyPer*; *myo-2::GFP*] were crossed to GR1307 [*daf-16(mgDf50)* I], CF1041 [*daf-2(e1370)*] or LB90 [*ctl-2* (ua90) II; *him-8(e1489)* IV] hermaphrodites. This strategy was chosen to facilitate the selection of progeny derived from mating, because fluorescent progeny (*myo-2::GFP*) must be heterozygous by definition (Figure 6.1). Mating plates were typically set up with five males and three hermaphrodites on each plate. Hermaphrodites of the F<sub>1</sub> generation, which are heterozygous for the transgene and the mutation, gave rise to an F<sub>2</sub> generation, which includes a homozygous recombination of both transgene and mutation (Figure 6.1).

### 6.5.2.3 Genotyping

Individual progeny were transferred with a worm pick into 10  $\mu$ l of PCR worm lysis solution containing proteinase K, spun down shortly, and frozen at -80°C to promote lysis. After 15 minutes, the sample was transferred to 60°C and lysis was continued for 60 minutes. Then, proteinase K

was inactivated by a 15 minute incubation at 95°C. The lysed worms were then ready to use for genotyping.

PCR worm lysis solution:

5X GoTaq Buffer: 2  $\mu$ l

Proteinase K (10  $\mu$ g/  $\mu$ l) : 1  $\mu$ l

Fill up to 10  $\mu$ l with ddH<sub>2</sub>O

The chromosomal region of the mutant alleles of the GR1307 [*daf-16*(mgDf50) I], the LB90 [*ctl-2* (ua90) II; *him-8*(e1489) IV] or the CF1041 [*daf-2*(e1370)] mutation was amplified by PCR. The mutant alleles of the GR1307 [*daf-16*(mgDf50) I] and LB90 [*ctl-2* (ua90) II; *him-8*(e1489) IV] strains harbor gene deletions, which can be distinguished from the wildtype allele on a 1% agarose gel (Figure 6.2). The mutant allele of the CF1041 [*daf-2*(e1370)] strain contains a point mutation, which cannot be distinguished on an agarose gel. Therefore the amplified DNA was sent for sequencing, which enabled the differentiation between homozygous wildtype, as well as worms heterozygous or homozygous for the mutant *daf-2* allele (Figure 6.3). The presence of the HyPer gene was verified using the fluorescence of the co-injection marker *myo-2::GFP* since co-injection marker and gene of interest are theoretically transmitted jointly. Nevertheless, the HyPer DNA was amplified by PCR and visualized by DNA electrophoresis.

Primer:

<i>ctl-2</i> fwd:	aagtagcgacgctctggctgtg
<i>ctl-2</i> rev:	gttgaccggccttccacgg
<i>daf-2</i> PCR fwd:	agatgaacgagctggaggaa
<i>daf-2</i> PCR rev:	cgtatgatgcctgttcgatg
<i>daf-2</i> Sequencing:	tccagcacatttcatcacc
smd-1 <i>daf-16</i> fwd:	ttcccctttctctcgtctaattc
smd-1 <i>daf-16</i> rev:	catcatcatcatacagtcgcaaa
HyPer PCR fwd:	caactggacagcgcaaacctc
HyPer PCR rev:	ctgaactgttgccggttacg

PCR reaction:

GoTaq <sup>®</sup> DNA Polymerase (Promega)	1.25 U
5X Green GoTaq <sup>®</sup> Reaction Buffer	1X
Primer fwd	0.5 $\mu$ M
Primer rev	0.5 $\mu$ M
dNTP (Invitrogen)	0.2 $\mu$ M

50X TAE buffer:

Tris	242 g
Glacial Acetic Acid	57 ml
0.5M EDTA, pH 7.5	100 ml
Fill up to 1 L with ddH <sub>2</sub> O	

Genotyping	ctl-2	daf-2	daf-16	HyPer
Denaturation:	2 min @ 95°C 30 sec @ 95°C			
Annealing:	30 sec @ 65°C	30 sec @ 55°C	30 sec @ 60°C	30 sec @ 62.7°C
Elongation:	2 min @ 72°C	35 sec @ 72°C	75 sec @ 72°C	40 sec @ 72°C
Cycle numbers:	26	35	35	26
Final elongation:	5 - 10 min @ 72°C			
Expected PCR fragments:	N2: 1.9 kb; ctl-2: 0.9 kb	0.3 kb	N2: 0.9 kb; daf-16: no amplification	0.6 kb

**Table 6.2. PCR programs for the genotyping of mutant alleles and transgenes.**

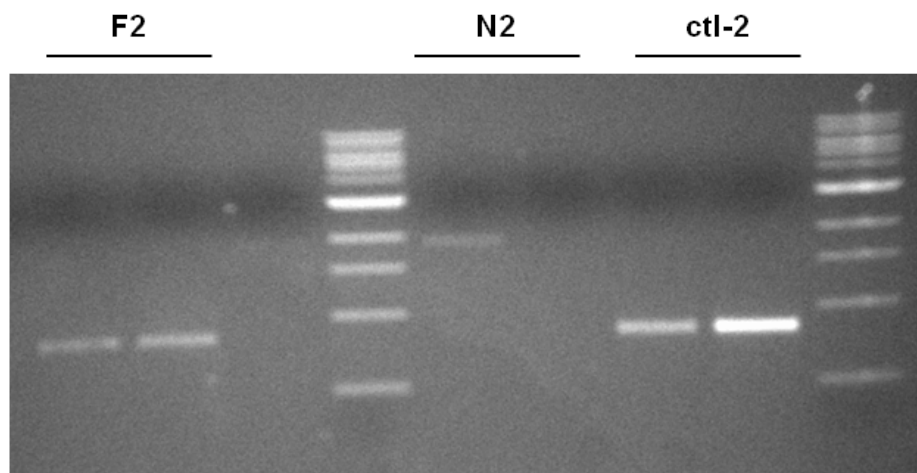


**Figure 6.2. Agarose gel electrophoresis after PCR genotyping of *ctl-2* deletion worms.** The deletion of catalase 2 results in a PCR fragment with the size of ~ 1kb (*ctl-2*, two right lanes), while the wildtype (N2, middle lane) has a PCR fragment of ~ 2kb. The F2 generations of a mating of *ctl-2*, *him-8* and N2 [*unc-54::HyPer*] was genotyped (F2, two left lanes). Both tested samples are homozygous for the catalase 2 deletion. 1% agarose gel in 1X TAE.

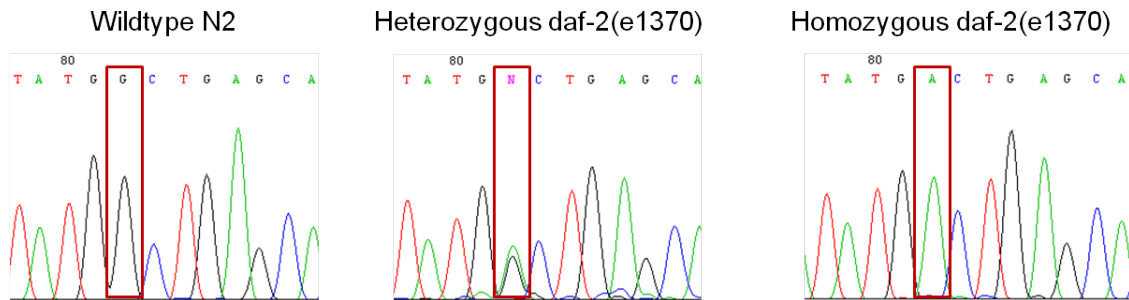


**Figure 6.3. Genotyping of *daf-2(e1370)* using DNA sequencing.** The genomic region of the *daf-2(e1370)* mutation was sequenced after PCR amplification. Sequencing spectra of wildtype, heterozygous *daf-2(e1370)* and homozygous *daf-2(e1370)* are shown and the mutated base is highlighted with the box. The *daf-2(e1370)* strain contains a G→A point mutation.

## 6.6 Imaging of HyPer fluorescence

The hydrogen peroxide sensor HyPer possesses two excitation maxima, at ~420 nm and ~500 nm, and a single emission maxima at 516 nm.

### 6.6.1 Confocal Microscopy

Worms were mounted on 2% agarose pads using a worm pick and immobilized with 2 mM levamisole hydrochloride. A Leica SP5 Confocal imaging system on a DM 6000B upright microscope body (Wetzlar, Germany) was used for image acquisition. Animals expressing the fluorescent sensor protein HyPer were excited sequentially with a 405 nm diode and a 488 nm argon laser, which are close to the published excitation maxima (Belousov *et al.*, 2006). Emission was measured at 505 – 530 nm using the same photo multiplier tube (PMT), set to zero offset and adequate gain. The RSP 500 dichroic beam splitter in conjunction with a 20x objective (NA 0.7 HC PL APO CS) was used. The resulting “405 image” and “488 image” had 1024 x 1024 pixels at 16-bit resolution. Additionally, a differential interference contrast (DIC) and a 405 nm excitation / 530-550 nm emission image were acquired to assist with image quantification. The laser and microscope settings were kept constant from day-to-day within one experiment. To account for fluctuations in laser power, a fluorescent reference slide (Ted Pella, Redding, California) was imaged before and after each group, and was used for normalization purposes in the image quantification.

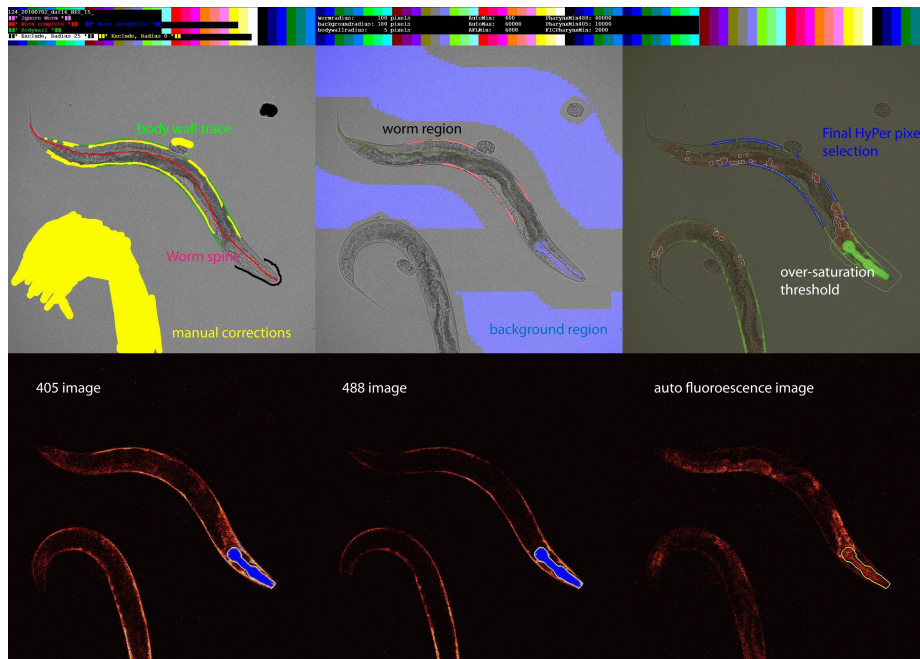


**Figure 6.4. ImageJ display of “wormsuite” image analysis.** ImageJ output of the automated calculations (e.g., background region, HyPer pixel selection) and the manual modifications (e.g., worm spine, body wall trace) using the Matlab script “wormsuite”. After a final check of the HyPer pixel selection, the HyPer ratio can now be calculated by the script.

## 6.6.2 Image quantification

A MATLAB (The MathWorks) script “wormsuite”<sup>11</sup> was used in conjunction with ImageJ (Rasband, 1997-2012) to perform the automated image quantification (a descriptive image is shown in Figure 6.4).

### 6.6.2.1 Tracing worm spine and body wall to define worm and background region

Initially, each worm was identified by tracing its center in the DIC image. This track is referred to as the worm spine. In a similar manner, the body wall was marked as the body wall trace.

The automated image analysis then dilated the worm spine to define a binary mask, called the worm region. The number of dilation iterations was set in a way that all worms lay completely within this worm region including a decent margin of about 100 pixels. The inverse of that worm region is referred to as the background region. Regions with very high signal in any channel (e.g., fluorescent particles or the pharyngeal co-injection marker *myo-2::GFP*) were identified by applying

<sup>11</sup>Implemented by Martin Koniczek (University of Michigan).

an over-saturation threshold, and were excluded from both the worm region and the background region (see Figure 6.4).

### 6.6.2.2 Defining the HyPer regions and obtaining the HyPer ratio

To correct for the channel backgrounds, the average signals of the background region in the 405 image and 488 image (i.e., background or offset) were subtracted from the value of each pixel in the worm region of the corresponding image. For each set of microscope and laser settings an appropriate minimum HyPer signal threshold was chosen for the 405 nm and 488 nm channel. Contiguous blocks of pixels above that threshold within the worm region and in proximity to the body wall trace defined preliminary HyPer regions. The result of this automated selection was then displayed in ImageJ and a manual check was performed. If necessary, corrections were applied (e.g., exclusion of obviously incorrectly identified preliminary HyPer regions) (Figure 6.4). The mean pixel intensities of the final HyPer selection in the background-corrected 405 and 488 images were then divided by each other to obtain the final HyPer ratio:

$$\text{HyPer Ratio} = \frac{\text{Background-corrected mean emission upon 488 nm excitation}}{\text{Background-corrected mean emission upon 405 nm excitation}} \quad (\text{Eq. 2})$$

### 6.6.2.3 Reference ratios for normalization

In parallel, the fluorescent reference slide was used to calculate a reference ratio with backgrounds defined as zero and the whole image treated as HyPer selection. This is acceptable since the fluorescent slide signal is very uniform and more than a magnitude higher than the (almost constant) dark signal of the imaging chain. Whenever comparisons between days were performed, the daily average of these reference ratios was used to normalize the actual HyPer ratios for each worm of that day (through dividing by the reference ratio).

### 6.6.3 Fluorescence microscopy

For the non-confocal fluorescence image acquisition, an Olympus BX61 (Olympus America Inc.) upright microscope was used, equipped with a Photometrics Coolsnap HQ2 cooled CCD (Charged-



coupled device) camera. Images of HyPer -transgenic *C. elegans* were taken with a UPlan S-Apo 20x objective (NA 0.75). For excitation, an external filter wheel was used with 420/40x and 500/20x excitation filters, a dual band pass dichroic T515LPXR and a 535/30x emission filter. For DAPI fluorescence, a quad filter set (DAPI/ FITC/ TRITC/CY-5) was utilized. A closed feedback-loop was enabled to keep the illumination of the X-Cite<sup>®</sup> exacte mercury lamp consistent within one experiment. The resulting “420 image” and “500 image” have 1344 x 1024 pixels at 14-bit resolution. Quantification of the HyPer ratio from these images was accomplished using the MATLAB script “wormsuite” and ImageJ as described in 6.6.2, limiting the worm spine and subsequent worm region to the head of each worm.

#### 6.6.4 Recovery of *C. elegans* after image acquisition

Worms were mounted reversibly as described in Fang-Yen *et al.* (2009). Briefly, worms were transferred into 0.4  $\mu$ l of 0.1  $\mu$ m diameter polystyrene microspheres (Polysciences) on a 10% w/v agarose (in M9) pad. For the image acquisition, an Olympus BX61 (Olympus America Inc.) upright microscope was used as described in 6.6.3. After image acquisition, the animals were recovered from the objective slide and transferred onto NGM plates. The duration on the slide and the image acquisition were kept as short as possible (< 5 min). The animals were scored daily for their movement quality and survival, and animals were considered dead when they did not move or did not respond to prodding.

#### 6.7 Determination of hydrogen peroxide release

The Amplex<sup>®</sup>UltraRed reagent (Molecular Probes, Invitrogen) was used to determine the release of hydrogen peroxide from living worms. The assay utilizes a nonfluorescent compound, Amplex<sup>®</sup>UltraRed, which in the presence of hydrogen peroxide and horseradish peroxidase is converted to the fluorescent Amplex<sup>®</sup>UltraxRed in a 1:1 stoichiometric ratio. The Amplex<sup>®</sup>UltraRed fluorescence is stable at pH values ranging from about 5 to 10 (manufacturer’s manual). Stock and working solutions were prepared based on the manufacture’s instruction.

#### Amplex<sup>®</sup>UltraRed 5X reaction buffer:

250 mM NaH<sub>2</sub>PO<sub>4</sub>, pH 7.4

### **6.7.1 Amplex<sup>®</sup>UltraRed assay**

Synchronized worm were washed off NGM plates with M9 with as little as OP50 bacteria as possible, and spun down at 200xg. The worm pellet was washed with M9 buffer, followed by a wash with 1X Reaction Buffer (Molecular probes, Invitrogen) supplemented with 0.05% Triton X-100, which decreased the adherence of worms to plastic (Davis *et al.*, 2010). The worms were finally resuspended in 1X Reaction Buffer/ 0.05% Triton X-100 in a final volume of 20  $\mu$ l in 390  $\mu$ l. 50  $\mu$ l of the worm solution were pipetted in triplicates into a 96-well solid black microtiter plate with transparent bottom, while 50  $\mu$ l were frozen at -80°C for subsequent determination of the protein concentration 6.7.2. For calculating the amount of hydrogen peroxide released, a H<sub>2</sub>O<sub>2</sub> standard curve was measured in parallel. For initiating the enzymatic reaction, 50  $\mu$ l of a working solution of Amplex<sup>®</sup>UltraRed and horseradish peroxidase was added to the wells containing either worms or the H<sub>2</sub>O<sub>2</sub> dilutions, and the fluorescence emission of Amplex<sup>®</sup>UltraRed was measured at 590 nm in a BMG FLUOstar Omega Microplate Reader after excitation with 544 nm. The average Amplex<sup>®</sup>UltraRed fluorescence of each sample was normalized with the respective protein concentration, which was determined using the DC protein assay (see 6.7.2).

### **6.7.2 Measurement of the protein concentration**

The frozen worm aliquots were allowed to thaw on ice. Then, samples were boiled for five minutes at 95°C to promote the lysis of the worms. After spinning down the worm debris for 10 minutes (13 000xg), the supernatant was used to determine the protein concentration using the Bio-Rad DC<sup>™</sup> Protein Assay according to the manufacturer's instructions. Shortly, the absorbance of a BSA standard curve was utilized as reference to determine the protein concentrations of the samples. The assay was prepared in a 96-well microplate, using 5  $\mu$ l of the protein sample in triplicates. 25  $\mu$ l of a working Reagent A' (Reagent A plus Reagent S) was added to each worm sample or the BSA standard curve, after which 200  $\mu$ l of solution B was added to initiate the reaction. After 15 minutes

incubation at room temperature, the absorbance was measured at 750 nm in a BMG FLUOstar Omega Microplate Reader.

## 6.8 Determination of Peroxiredoxin 2 redox state

The redox state of peroxiredoxins was used as read-out of endogenous peroxide level (Cox *et al.*, 2010). Upon reaction with H<sub>2</sub>O<sub>2</sub>, the peroxidatic cysteine residue of *C. elegans* peroxiredoxin 2 forms a sulfenic acid intermediate, which reacts with the resolving cysteine residue of another peroxiredoxin monomer leading to the formation of disulfide bonded peroxiredoxin dimer. Higher amounts of H<sub>2</sub>O<sub>2</sub> can cause the overoxidation of the sulfenic acid intermediate to sulfinic acid, which prevents disulfide bond formation (Cox *et al.*, 2010). Presence of low levels of peroxides therefore leads to disulfide-linked dimers while reduced or overoxidized peroxiredoxins will migrate as monomers on non-reducing SDS-PAGE. Thiol trapping of the reduced cysteine residues followed by the subsequent separation of the protein fraction on non-reducing SDS-PAGE thus enables the differentiation between reduced and oxidized peroxiredoxin as well as the identification of the peroxide-induced peroxiredoxin 2 disulfides (Oláhová *et al.*, 2008) (Figure 6.5). When worms are lysed in the absence of alkylating agents the reduced monomeric peroxiredoxin dimerizes, while the overoxidized fraction of peroxiredoxin remains to run at the monomer size (Cox *et al.*, 2010).

### 6.8.1 Lysis of worms and protein precipitation

Synchronized worm populations were washed off NGM plates and pelleted by centrifugation. 50 µl of the worm solution was then transferred into 2 ml Eppendorf tubes. The thiol-trapping steps were carried out on ice and cooled solutions and centrifuges were used. Chilled TCA was added to a final concentration of 10% (500 µl final volume) to prevent thiol-disulfide exchange reactions (Leichert and Jakob, 2004). Worms were lysed using the homogenizer Powergen 125 (Fisher Scientific) for 2 minutes (power level 6). Protein precipitation was carried out on ice for 30 minutes followed by a 30 minutes spin at 13 000xg in a pre-cooled tabletop centrifuge. The supernatant was carefully removed and the protein pellet was washed with ice-cold acetone to remove residual TCA.

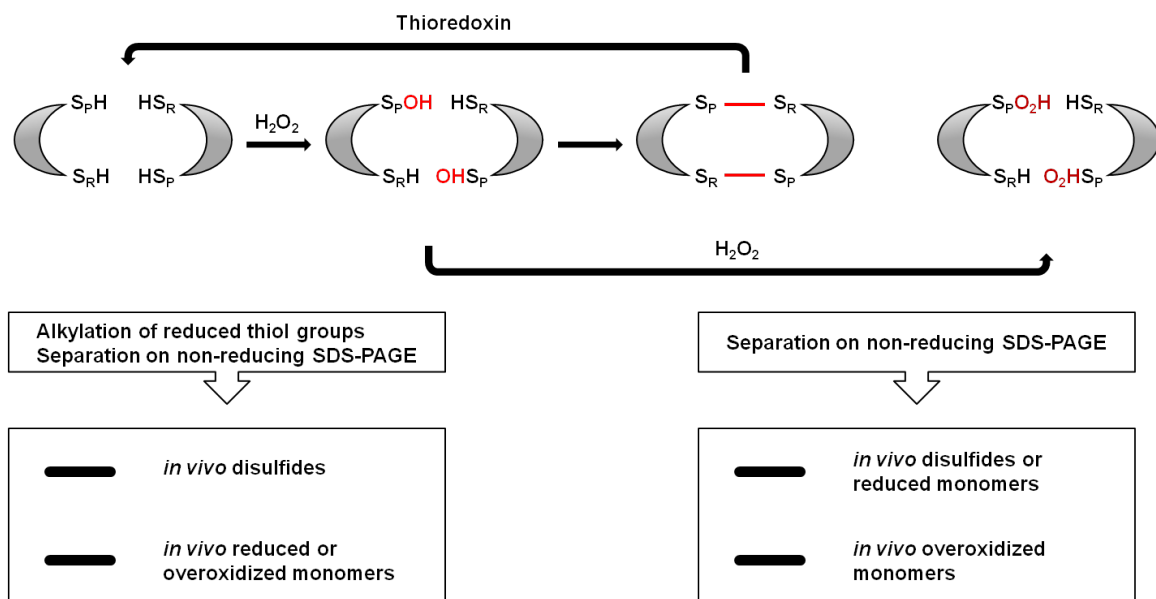


**Figure 6.5. Quantification of the redox state of PRDX-2.** The redox cycle of 2-cysteine peroxiredoxins is displayed. In the presence of peroxide, the reduced peroxidatic cysteine ( $S_P H$ ) of a peroxiredoxin monomer becomes oxidized to a sulfenic acid intermediate ( $S_P OH$ ), which can react with the resolving cysteine ( $S_R H$ ) of a second peroxiredoxin monomer thus forming a peroxiredoxin disulfide-bonded dimer ( $S_P - S_R$ ). Oxidized dimers can be reduced by thioredoxin (Trx). When peroxide is in excess the peroxidatic cysteine can get overoxidized to a sulfinic acid ( $S_P O_2 H$ ), which is unable to form a dimer with another peroxiredoxin monomer. The redox state of peroxiredoxin can be trapped by alkylating agents such as NEM or AMS, thus keeping reduced peroxiredoxin in its monomeric state. The dimer and monomer fraction can be distinguished on a non-reducing SDS-PAGE. Lysis of worms in the absence of alkylating agents results in the conformation of reduced monomers to disulfide-bonded dimers while overoxidized peroxiredoxin still runs as a monomer thereby allowing the determination of the overoxidized fraction. Figure modified from (Cox *et al.*, 2010).

### 6.8.2 Labeling of protein thiols

Reduced protein thiols were labeled with either 25 mM AMS (pH 7) or 100 mM (pH 8) in DAB buffer. N-Ethylmaleimide (NEM) and 4-acetoamido-4'-maleimidylstilbene-2,2'-disulfonic acid (AMS) are thiol-reactive reagents with AMS adding approximately 500 Da to every thiol group of a protein. The resuspended protein solution should have the optimal pH for the respective alkylating reagent, and was - if necessary - adjusted using 1 M Tris (pH not adjusted). The labeling was performed for one hour at 25°C shaking (1200 rpm), after which the debris was spun down and the soluble proteins were stored at -80°C until further use.

#### Denaturing Alkylation Buffer (DAB):

Urea	1.8 g
1 M Tris-HCl, pH 7	1 ml
500 mM EDTA	100 $\mu$
10% (w/v) SDS	250 $\mu$
Fill up to 5 ml with ddH <sub>2</sub> O	

### 6.8.3 Determination of the protein concentration

The protein samples were diluted ten times in ddH<sub>2</sub>O to avoid interference of the DAB buffer with the Bio-Rad DC<sup>TM</sup> Protein Assay, and the protein amount was measured as described in 6.7.2.

### 6.8.4 SDS-PAGE and Western Blot

The protein samples were adjusted to the same concentration, and supplemented with 1X non-reducing SDS-loading buffer. To separate the monomeric, reduced fraction of peroxiredoxin-2 from the disulfide bonded, dimeric fraction of PRDX-2 12% Mini-PROTEAN<sup>®</sup> TGX<sup>TM</sup> Gels (BioRad) were used. The separated proteins were transferred onto a methanol-activated Polyvinylidene fluoride (PVDF) membrane (Millipore), using a semi-wet blotting system. Rapid immunodetection was performed according to Millipore's protocol. Briefly, after the blotting process the membrane was dehydrated by soaking the membrane for 10 seconds in 100% methanol. After the methanol

evaporated the membrane was incubated with the primary anti-peroxiredoxin-2 antibody for one hour. The blots were washed two times with 1X PBS for 10 seconds, after which the membrane was incubated with the secondary anti-rabbit antibody for 30 minutes. The secondary antibody was conjugated to horseradish peroxidase, and the Enhanced Chemiluminescent Substrate (SuperSignal West Pico Chemiluminescent Substrate, Thermo scientific) was added after washing the blot twice with 1X PBS (10 seconds). Chemoluminescence was detected and imaged with the Kodac Gel Logic 2200 Imaging System and the Carestream Molecular Imaging Software (v.5.0.2.30).

SDS-Running Buffer:

Glycine	288 g
SDS	20 g
Tris	58 g
Fill up to 20 L with ddH <sub>2</sub> O	

5X Non-Reducing Loading Buffer:

SDS	5 g
Glycerol	30.5 g
1M Tris, pH 7.0	15 ml
Bromophenol Blue	0.025 g
Fill up to 50 ml with ddH <sub>2</sub> O	

Western Blot Buffer:

Tris	5.8 g
SDS	0.37 g
Methanol	200 ml
Glycine	2.93 g
Fill up to 1 L with ddH <sub>2</sub> O	

20X TBS:

NaCl	160 g
KCl	4 g
Tris	60 g

Adjust to pH 7.4 with HCl

Fill up to 1 L with ddH<sub>2</sub>O

10 X PBS:

NaCl	80 g
KCl	2 g
Na <sub>2</sub> HPO <sub>4</sub> *7H <sub>2</sub> O	22 g
KH <sub>2</sub> PO <sub>4</sub>	2 g

Adjust to pH 7.2 with liquid NaOH

Fill up to 1 L with ddH<sub>2</sub>O

Antibodies:

Rabbit  $\alpha$ -peroxiredoxin 2                      1:1000 in 1X TBS + 1% milkpowder  
(Alpha Diagnostics International)

Goat  $\alpha$ -rabbit IgG HRP conjugated      1:10000 in 1X TBS + 1% milkpowder  
(Thermo scientific)

**6.8.5 Quantification and Analysis**

Mean intensities of the bands corresponding to the peroxide-induced PRDX-2 dimer, the PRDX-2 dimer and the reduced/overoxidized PRDX-2 monomer were quantified using the Carestream Molecular Imaging Software (v.5.0.2.30). The monomeric band and the two dimeric bands were manually enclosed in a region of interest (ROI), with separate ROI's defining membrane regions used for background correction. The average mean intensity of the background regions were sub-

tracted from the mean intensities derived from ROI's corresponding to the monomeric or dimeric fractions. The background-subtracted values were then used to calculate the fraction of peroxide-induced PRDX-2 disulfide over total amount of PRDX-2 (sum of all bands).

## 6.9 Isolation of RNA and proteins from *C. elegans*

### 6.9.1 Sample preparation and lysis

Animals of a synchronized *C. elegans* population were washed off their NGM plates using 600  $\mu$ l ice-cold M9 buffer and transferred into a 1.5 ml Eppendorf tube. Then, an equal volume of ice-cold 60% sucrose was added. The worm – sucrose solution was centrifuged in a tabletop centrifuge at 100xg for 5 min. Then, the speed was increased to 1 000xg for another five minutes to separate worms from bacteria and agar debris. The floating worms were transferred into fresh 1.5 ml Eppendorf tubes and washed three times with M9 buffer. For isolating protein and RNA from the worm samples, 400  $\mu$ l Trizol<sup>®</sup> reagent was added to each 100  $\mu$ l worm solution. The mixture was vortexed for two minutes at room temperature, followed by three freeze-and-thaw-cycles (-80°C and 37°C) to promote lysis of the worms <sup>12</sup>.

### 6.9.2 Preparation of RNA using the TRIZOL<sup>®</sup> Reagent and the RNeasy Kit

To separate RNA from DNA and proteins, the TRIZOL<sup>®</sup> Reagent (Life technologies), a monophasic phenol and guanidine isothiocyanate solution, was used. The reagent, which inhibits RNases during sample homogenization and supports the isolation of RNA, is an improved version of the acid guanidinium thiocyanate-phenol-chloroform extraction by Chomczynski and Sacchi (Chomczynski and Sacchi, 1987). 200  $\mu$ l TRIZOL<sup>®</sup> Reagent was added to each of the lysed samples and samples were incubated for five minutes at room temperature. After adding 140  $\mu$ l chloroform, the samples were vigorously shaken for 15 seconds, and then incubated for two minutes at room temperature. Then, samples were spun down at 12 000xg for 15 minutes (4°C) to separate the top aqueous solution containing RNA from DNA and proteins. The RNA-containing aqueous phase was transferred into fresh 1.5 ml Eppendorf tubes, supplemented with an equal volume of 70% ethanol, and transferred into a Qiagen RNeasy spin column. The RNA isolation was carried out according to the

<sup>12</sup>Modified from the protocol from the Lamitina Lab, and the manuals from the TRIZOL<sup>®</sup> Reagent (Life technologies) and the RNeasy<sup>®</sup> Mini Kit (Qiagen)



manufacturer's instructions of the RNeasy<sup>®</sup> Mini Kit (Qiagen), and the RNA was eluted in 50  $\mu$ l RNAase-free water and stored at -80°C.

### 6.9.3 Isolation and precipitation of protein

To separate proteins from DNA, 180  $\mu$ l 100% ethanol was added to the interphase and the bottom phenol-chloroform layer. Mixing was achieved by inverting the sample several times. After incubating the samples for two to three minutes at room temperature they were centrifuged for five minutes at 2 000xg at 4°C to pellet the DNA. The phenol-ethanol supernatant, which contained the proteins, was transferred into a fresh 2 ml Eppendorf tube, and 900  $\mu$ l isopropanol was added to precipitate the proteins. After an incubation of ten minutes at room temperature the samples were centrifuged for ten minutes at 12 000xg at 4°C. The supernatant was discarded and the protein pellet was washed with 1.2 ml of 0.3 M guanidine hydrochloride in 95% ethanol for 20 minutes at room temperature, after which the pellet was spun down again at 7 500xg for 5 min at 4°C. The wash procedure with 0.3 M guanidine hydrochloride was repeated twice, then once with 2 ml 100% ethanol, vortexed and incubated at room temperature for 20 minutes. After a final centrifugation at 7 500xg for 5 min the ethanol wash was removed and the protein pellet was dried at room temperature for about 5 to 10 minutes, after which it was resuspended in 200  $\mu$ l of 1% SDS. To assist the complete dissolving of the protein pellet the samples could be incubated at 50°C. Insoluble material was sedimented by spinning the samples at 10 000xg for 10 min at 4°C, and the samples were stored at -20°C.

### 6.10 Analysis of protein expression level

Protein concentrations were measured using the Bio-Rad DC<sup>™</sup> Protein Assay, as described in 6.7.2. The samples were adjusted to the same protein concentration and the proteins were separated under reducing conditions on 12% Mini-PROTEAN<sup>®</sup> TGX<sup>™</sup> (Bio-Rad). The separated proteins were transferred onto PVDF membranes and immunodetection and quantification were performed as described in 6.8.4 and 6.8.5. After the immunodetection the PVDF membrane was washed twice with 1X TBS-T, stained with 0.1% Coomassie R-350 and destained. After the blot was washed with water and air dried (Welinder and Ekblad, 2011), the density of the stained proteins of one gel lane were visualized and quantified using the Kodac Gel Logic 2200 Imaging System and the

Carestream Molecular Imaging Software (v.5.0.2.30). The peroxiredoxin 2 protein level were normalized by dividing the mean intensity of the peroxiredoxin 2 protein bands by the mean intensity of the corresponding coomassie-stained gel lane.

5X Reducing Loading Buffer:

SDS	5 g
Glycerol	30.5 g
1M Tris, pH 7.0	15 ml
Bromophenol Blue	0.025 g
2-Mercaptoethanol	2.5 ml
Fill up to 50 ml with ddH <sub>2</sub> O	

20X TBS-T:

Tween <sup>®</sup> 20	20 ml
NaCl	160 g
KCl	4 g
Tris	60 g
Adjust to pH 7.4 with HCl	
Fill up to 1 L with ddH <sub>2</sub> O	

Coomassie staining:

0.1% Coomassie R-350 (GE healthcare) in methanol/ H<sub>2</sub>O (1:1)

Coomassie destaining:

Acetic acid/ ethanol/ H<sub>2</sub>O (1:5:4)

### **6.10.1 Statistical Analysis**

For statistical analysis the software GraphPad Prism 5 (Version 5.01) was used. Lifespan data were analyzed using the Log-rank test (Mantel Cox) or the Gehan-Breslow-Wilcoxon test. The p-value of 0.05 was used as significance level. While the log-rank test is more powerful when the ratio of hazard functions (deaths per time) does not change, the Gehan-Breslow-Wilcoxon test gives more weight to early deaths (GraphPad PISM Version 5.0 Statistics Guide).

Experimental data were analyzed either with the One-Way ANOVA followed by Tukey's multiple comparison test, or with the Student's t-test. The HyPer ratio values were log-transformed for the statistical analysis.



## 7 References

- Andziak, B., O'Connor, T.P., and Buffenstein, R. Antioxidants do not explain the disparate longevity between mice and the longest-living rodent, the naked mole-rat. *Mechanisms of ageing and development*, 126(11):1206–1212, 2005.
- Ayyadevara, S., Dandapat, A., Singh, S.P., Beneš, H., Zimniak, L., Reis, R.J.S., and Zimniak, P. Lifespan extension in hypomorphic daf-2 mutants of *Caenorhabditis elegans* is partially mediated by glutathione transferase CeGSTP2-2. *Aging Cell*, 4(6):299–307, 2005.
- Back, P., De Vos, W.H., Depuydt, G.G., Matthijssens, F., Vanfleteren, J.R., and Braeckman, B.P. Exploring real-time in vivo redox biology of developing and aging *Caenorhabditis elegans*. *Free Radical Biology and Medicine*, 2011.
- Bader, N. and Grune, T. Protein oxidation and proteolysis. *Biological chemistry*, 387(10/11):1351–1355, 2006.
- Barnham, K.J., Masters, C.L., and Bush, A.I. Neurodegenerative diseases and oxidative stress. *Nature Reviews Drug Discovery*, 3(3):205–214, 2004.
- Bass, DA, Parce, J.W., Dechatelet, L.R., Szejda, P., Seeds, MC, and Thomas, M. Flow cytometric studies of oxidative product formation by neutrophils: a graded response to membrane stimulation. *The Journal of Immunology*, 130(4):1910–1917, 1983.
- Bayne, A.C.V., Mockett, R.J., Orr, W.C., and Sohal, R.S. Enhanced catabolism of mitochondrial superoxide/hydrogen peroxide and aging in transgenic *Drosophila*. *Biochemical Journal*, 391(Pt 2):277, 2005.
- Bedard, K. and Krause, K.H. The NOX family of ROS-generating NADPH oxidases: physiology and pathophysiology. *Physiological reviews*, 87(1):245–313, 2007.
- Belousov, V.V., Fradkov, A.F., Lukyanov, K.A., Staroverov, D.B., Shakhbazov, K.S., Terskikh, A.V., and Lukyanov, S. Genetically encoded fluorescent indicator for intracellular hydrogen peroxide. *Nature methods*, 3(4):281–286, 2006.

- Ben-Zvi, A., Miller, E.A., and Morimoto, R.I. Collapse of proteostasis represents an early molecular event in *Caenorhabditis elegans* aging. *Proceedings of the National Academy of Sciences*, 106(35):14914–14919, 2009.
- Bortolato, M., Chen, K., and Shih, J.C. Monoamine oxidase inactivation: from pathophysiology to therapeutics. *Advanced drug delivery reviews*, 60(13):1527–1533, 2008.
- Brandes, N., Reichmann, D., Tienson, H., Leichert, L.I., and Jakob, U. Using quantitative redox proteomics to dissect the yeast redoxome. *Journal of Biological Chemistry*, 286(48):41893–41903, 2011.
- Brandes, N., Schmitt, S., and Jakob, U. Thiol-based redox switches in eukaryotic proteins. *Antioxidants & redox signaling*, 11(5):997–1014, 2009.
- Brenner, S. The genetics of *Caenorhabditis elegans*. *Genetics*, 77(1):71–94, 1974.
- Brys, K., Vanfleteren, J.R., and Braeckman, B.P. Testing the rate-of-living/oxidative damage theory of aging in the nematode model *Caenorhabditis elegans*. *Experimental gerontology*, 42(9):845–851, 2007.
- Burdon, R.H. and Gill, V. Cellularly generated active oxygen species and HeLa cell proliferation. *Free Radical Research*, 19(3):203–213, 1993.
- Cabreiro, F., Ackerman, D., Doonan, R., Araiz, C., Back, P., Papp, D., Braeckman, B.P., and Gems, D. Increased lifespan from over-expression of superoxide dismutase in *C. elegans* is not caused by decreased oxidative damage. *Free Radical Biology and Medicine*, 2011.
- Cadenas, E. and Davies, K.J.A. Mitochondrial free radical generation, oxidative stress, and aging. *Free Radical Biology and Medicine*, 29(3-4):222–230, 2000.
- Carlsson, LM, Jonsson, J., Edlund, T., and Marklund, SL. Mice lacking extracellular superoxide dismutase are more sensitive to hyperoxia. *Proceedings of the National Academy of Sciences*, 92(14):6264, 1995.
- Cassada, R.C., Russell, R.L., *et al.* The dauerlarva, a post-embryonic developmental variant of the nematode *Caenorhabditis elegans*. *Developmental biology*, 46(2):326, 1975.

- Ceriello, A. and Motz, E. Is oxidative stress the pathogenic mechanism underlying insulin resistance, diabetes, and cardiovascular disease? The common soil hypothesis revisited. *Arteriosclerosis, thrombosis, and vascular biology*, 24(5):816–823, 2004.
- Chance, B. and Williams, GR. The respiratory chain and oxidative phosphorylation. *Advances in Enzymology and Related Areas of Molecular Biology*, pages 65–134, 1956.
- Chavez, V., Mohri-Shiomi, A., and Garsin, D.A. Ce-Duox1/BLI-3 generates reactive oxygen species as a protective innate immune mechanism in *Caenorhabditis elegans*. *Infection and immunity*, 77(11):4983, 2009.
- Cho, C.G., Kim, H.J., Chung, S.W., Jung, K.J., Shim, K.H., Yu, B.P., Yodoi, J., and Chung, H.Y. Modulation of glutathione and thioredoxin systems by calorie restriction during the aging process. *Experimental gerontology*, 38(5):539–548, 2003.
- Choi, H.J., Kim, S.J., Mukhopadhyay, P., Cho, S., Woo, J.R., Storz, G., and Ryu, S.E. Structural basis of the redox switch in the OxyR transcription factor. *Cell*, 105(1):103–113, 2001.
- Choi, M.H., Lee, I.K., Kim, G.W., Kim, B.U., Han, Y.H., Yu, D.Y., Park, H.S., Kim, K.Y., Lee, J.S., Choi, C., *et al.* Regulation of PDGF signalling and vascular remodelling by peroxiredoxin II. *Nature*, 435(7040):347–353, 2005.
- Chomczynski, P. and Sacchi, N. Single-step method of RNA isolation by acid guanidinium thiocyanate-phenol-chloroform extraction. *Analytical biochemistry*, 162(1):156–159, 1987.
- Cochemé, H.M. and Murphy, M.P. Complex I is the major site of mitochondrial superoxide production by paraquat. *Journal of Biological Chemistry*, 283(4):1786–1798, 2008.
- Cochemé, H.M., Quin, C., McQuaker, S.J., Cabreiro, F., Logan, A., Prime, T.A., Abakumova, I., Patel, J.V., Fearnley, I.M., James, A.M., *et al.* Measurement of H<sub>2</sub>O<sub>2</sub> within living *Drosophila* during aging using a ratiometric mass spectrometry probe targeted to the mitochondrial matrix. *Cell Metabolism*, 13(3):340–350, 2011.
- Cohen, G. and Hochstein, P. Glutathione Peroxidase: The Primary Agent for the Elimination of Hydrogen Peroxide in Erythrocytes\*. *Biochemistry*, 2(6):1420–1428, 1963.

- Collet, J.F. and Messens, J. Structure, function, and mechanism of thioredoxin proteins. *Antioxidants & redox signaling*, 13(8):1205–1216, 2010.
- Cox, A.G., Winterbourn, C.C., and Hampton, M.B. Measuring the redox state of cellular peroxiredoxins by immunoblotting. *Methods in enzymology*, 474:51–66, 2010.
- D’Auréaux, B. and Toledano, M.B. ROS as signalling molecules: mechanisms that generate specificity in ROS homeostasis. *Nature Reviews Molecular Cell Biology*, 8(10):813–824, 2007.
- Davies, K.J.A. Degradation of oxidized proteins by the 20S proteasome. *Biochimie*, 83(3):301–310, 2001.
- Davis, G.M., Sharma, M., Low, L., and Boag, P.R. Triton X decreases adherence of *C. elegans* to pipette tips in liquid medium. *Worm Breeder’s Gazette*, 18(2):5, 2010.
- De Cuyper, C. and Vanfleteren, J.R. Oxygen consumption during development and aging of the nematode *Caenorhabditis elegans*. *Comparative Biochemistry and Physiology Part A: Physiology*, 73(2):283–289, 1982.
- de Matos, D.G., Furnus, C.C., and Moses, D.F. Glutathione synthesis during in vitro maturation of bovine oocytes: role of cumulus cells. *Biology of reproduction*, 57(6):1420–1425, 1997.
- Dillin, A., Crawford, D.K., and Kenyon, C. Timing requirements for insulin/IGF-1 signaling in *C. elegans*. *Science’s STKE*, 298(5594):830, 2002a.
- Dillin, A., Hsu, A.L., Arantes-Oliveira, N., Lehrer-Graiwer, J., Hsin, H., Fraser, A.G., Kamath, R.S., Ahringer, J., and Kenyon, C. Rates of behavior and aging specified by mitochondrial function during development. *Science*, 298(5602):2398–2401, 2002b.
- Doonan, R., McElwee, J.J., Matthijssens, F., Walker, G.A., Houthoofd, K., Back, P., Matscheski, A., Vanfleteren, J.R., and Gems, D. Against the oxidative damage theory of aging: superoxide dismutases protect against oxidative stress but have little or no effect on life span in *Caenorhabditis elegans*. *Genes & development*, 22(23):3236, 2008.
- Dröge, W. Free radicals in the physiological control of cell function. *Physiological reviews*, 82(1):47–95, 2002.



- Dupuy, C., Virion, A., Ohayon, R., Kaniewski, J., Deme, D., and Pommier, J. Mechanism of hydrogen peroxide formation catalyzed by NADPH oxidase in thyroid plasma membrane. *Journal of Biological Chemistry*, 266(6):3739, 1991.
- Durieux, J., Wolff, S., and Dillin, A. The cell-non-autonomous nature of electron transport chain-mediated longevity. *Cell*, 144(1):79–91, 2011.
- Durusoy, M., Diril, N., and Nihat Bozcuk, A. Age-related activity of catalase in different genotypes of *Drosophila melanogaster*. *Experimental Gerontology*, 30(1):77–86, 1995.
- Duttaroy, A., Paul, A., Kundu, M., and Belton, A. A Sod2 null mutation confers severely reduced adult life span in *Drosophila*. *Genetics*, 165(4):2295, 2003.
- Edens, W.A., Sharling, L., Cheng, G., Shapira, R., Kinkade, J.M., Lee, T., Edens, H.A., Tang, X., Sullards, C., Flaherty, D.B., *et al.* Tyrosine cross-linking of extracellular matrix is catalyzed by Duox, a multidomain oxidase/oxidoreductase with homology to the phagocyte oxidase subunit gp91phox. *The Journal of cell biology*, 154(4):879–892, 2001.
- Elchuri, S., Oberley, T.D., Qi, W., Eisenstein, R.S., Roberts, L.J., Van Remmen, H., Epstein, C.J., and Huang, T.T. CuZnSOD deficiency leads to persistent and widespread oxidative damage and hepatocarcinogenesis later in life. *Oncogene*, 24(3):367–380, 2004.
- Fang-Yen, C., Wasserman, S., Sengupta, P., and Samuel, A.D.T. Agarose immobilization of *C. elegans*. *Worm Breeder's Gazette*, 18:32, 2009.
- Finkel, T. Signal Transduction by Mitochondrial Oxidants. *Journal of Biological Chemistry*, 2011a.
- Finkel, T. Signal transduction by reactive oxygen species. *The Journal of Cell Biology*, 194(1):7, 2011b.
- Finkel, T. and Holbrook, N.J. Oxidants, oxidative stress and the biology of ageing. *NATURE-LONDON*-, pages 239–247, 2000.
- Fontana, L., Partridge, L., and Longo, V.D. Extending healthy life span – from yeast to humans. *science*, 328(5976):321–326, 2010.

- Fridovich, I. Superoxide radical and superoxide dismutase. *Accounts of Chemical Research*, 5(10):321–326, 1972.
- Fu, Y., Cheng, W.H., Ross, D.A., gen Lei, X., *et al.* Cellular glutathione peroxidase protects mice against lethal oxidative stress induced by various doses of diquat. In *Proceedings of the Society for Experimental Biology and Medicine. Society for Experimental Biology and Medicine (New York, NY)*, volume 222, pages 164–169. Royal Society of Medicine, 1999.
- Gems, D., Sutton, A.J., Sundermeyer, M.L., Albert, P.S., King, K.V., Edgley, M.L., Larsen, P.L., and Riddle, D.L. Two pleiotropic classes of daf-2 mutation affect larval arrest, adult behavior, reproduction and longevity in *Caenorhabditis elegans*. *Genetics*, 150(1):129–155, 1998.
- Ghezzi, P., Bonetto, V., and Fratelli, M. Thiol-disulfide balance: from the concept of oxidative stress to that of redox regulation. *Antioxidants & redox signaling*, 7(7-8):964–972, 2005.
- Giorgio, M., Trinei, M., Migliaccio, E., and Pelicci, P.G. Hydrogen peroxide: a metabolic by-product or a common mediator of ageing signals? *Nature Reviews Molecular Cell Biology*, 8(9):722–728, 2007.
- Godon, C., Lagniel, G., Lee, J., Buhler, J.M., Kieffer, S., Perrot, M., Boucherie, H., Toledano, M.B., and Labarre, J. The H<sub>2</sub>O<sub>2</sub> stimulon in *Saccharomyces cerevisiae*. *Journal of Biological Chemistry*, 273(35):22480–22489, 1998.
- Grant, C.M. Metabolic reconfiguration is a regulated response to oxidative stress. *Journal of Biology*, 7:1, 2008.
- Griswold, C.M., Matthews, A.L., Bewley, K.E., and Mahaffey, J.W. Molecular characterization and rescue of acatalasemic mutants of *Drosophila melanogaster*. *Genetics*, 134(3):781–788, 1993.
- Gumienny, T.L., Lambie, E., Hartweg, E., Horvitz, H.R., and Hengartner, M.O. Genetic control of programmed cell death in the *Caenorhabditis elegans* hermaphrodite germline. *Development*, 126(5):1011–1022, 1999.
- Gutscher, M., Sobotta, M.C., Wabnitz, G.H., Ballikaya, S., Meyer, A.J., Samstag, Y., and Dick, T.P. Proximity-based protein thiol oxidation by H<sub>2</sub>O<sub>2</sub>-scavenging peroxidases. *Journal of Biological Chemistry*, 284(46):31532–31540, 2009.

- Hansen, R.E., Roth, D., and Winther, J.R. Quantifying the global cellular thiol–disulfide status. *Proceedings of the National Academy of Sciences*, 106(2):422–427, 2009.
- Harman, D. Aging: A theory based on free radical and radiation chemistry. *Journal of Gerontology*, 11(3):298–300, 1956.
- Hartwig, K., Heidler, T., Moch, J., Daniel, H., and Wenzel, U. Feeding a ROS-generator to *Caenorhabditis elegans* leads to increased expression of small heat shock protein HSP-16.2 and hormesis. *Genes & nutrition*, 4(1):59–67, 2009.
- Heidler, T., Hartwig, K., Daniel, H., and Wenzel, U. *Caenorhabditiselegans* lifespan extension caused by treatment with an orally active ROS-generator is dependent on DAF-16 and SIR-2.1. *Biogerontology*, 11(2):183–195, 2010.
- Hernández-García, D., Wood, C.D., Castro-Obregón, S., and Covarrubias, L. Reactive oxygen species: A radical role in development? *Free Radical Biology and Medicine*, 49(2):130–143, 2010.
- Herndon, L.A., Schmeissner, P.J., Dudaronek, J.M., Brown, P.A., Listner, K.M., Sakano, Y., Paupard, M.C., Hall, D.H., Driscoll, M., *et al.* Stochastic and genetic factors influence tissue-specific decline in ageing *C. elegans*. *Nature*, 419(6909):808–814, 2002.
- Ho, H., Cheng, M., and Chiu, D.T. Glucose-6-phosphate dehydrogenase – from oxidative stress to cellular functions and degenerative diseases. *Redox Report*, 12(3):109–118, 2007.
- Ho, Y.S., Magnenat, J.L., Bronson, R.T., Cao, J., Gargano, M., Sugawara, M., and Funk, C.D. Mice deficient in cellular glutathione peroxidase develop normally and show no increased sensitivity to hyperoxia. *Journal of Biological Chemistry*, 272(26):16644–16651, 1997.
- Ho, Y.S., Xiong, Y., Ma, W., Spector, A., and Ho, D.S. Mice lacking catalase develop normally but show differential sensitivity to oxidant tissue injury. *Journal of Biological Chemistry*, 279(31):32804–32812, 2004.
- Hodgkin, J. Male phenotypes and mating efficiency in *Caenorhabditis elegans*. *Genetics*, 103(1):43–64, 1983.

- Holmgren, A. Thioredoxin. *Annual review of biochemistry*, 54(1):237–271, 1985.
- Holmgren, A., Johansson, C., Berndt, C., Lonn, ME, Hudemann, C., and Lillig, CH. Thiol redox control via thioredoxin and glutaredoxin systems. *Biochemical Society Transactions*, 33(6):1375–1377, 2005.
- Honda, Y. and Honda, S. The daf-2 gene network for longevity regulates oxidative stress resistance and Mn-superoxide dismutase gene expression in *Caenorhabditis elegans*. *The FASEB journal*, 13(11):1385–1393, 1999.
- Hope, I.A. *C. elegans: A practical approach*, volume 213. Oxford University Press, USA, 1999.
- Hosono, R., Mitsui, Y., Sato, Y., Aizawa, S., and Miwa, J. Life span of the wild and mutant nematode *Caenorhabditis elegans*:: Effects of Sex, Sterilization, and Temperature. *Experimental gerontology*, 17(2):163–172, 1982.
- Houthoofd, K., Braeckman, B.P., Lenaerts, I., Brys, K., De Vreese, A., Van Eygen, S., and Vanfleteren, J.R. Axenic growth up-regulates mass-specific metabolic rate, stress resistance, and extends life span in *Caenorhabditis elegans*. *Experimental gerontology*, 37(12):1371–1378, 2002.
- Houthoofd, K., Fidalgo, M.A., Hoogewijs, D., Braeckman, B.P., Lenaerts, I., Brys, K., Matthijssens, F., De Vreese, A., Van Eygen, S., Muñoz, M.J., *et al.* Metabolism, physiology and stress defense in three aging Ins/IGF-1 mutants of the nematode *Caenorhabditis elegans*. *Aging Cell*, 4(2):87–95, 2005.
- Huang, T.T., Carlson, E.J., Gillespie, A.M., Shi, Y., Epstein, C.J., *et al.* Ubiquitous overexpression of CuZn superoxide dismutase does not extend life span in mice. *Journals of Gerontology-Biological Sciences and Medical Sciences*, 55(1):5, 2000.
- Ingram, D.K., Zhu, M., Mamczarz, J., Zou, S., Lane, M.A., Roth, G.S., and DeCabo, R. Calorie restriction mimetics: an emerging research field. *Aging cell*, 5(2):97–108, 2006.
- Jacob, M.H.V.M., Janner, D.R., Araújo, A.S.R., Jahn, M.P., Kucharski, L.C.R., Moraes, T.B., Ribeiro, M.F.M., Belló-Klein, A., *et al.* Redox imbalance influence in the myocardial Akt activation in aged rats treated with DHEA. *Experimental gerontology*, 45(12):957–963, 2010.

- Jee, C., Vanoaica, L., Lee, J., Park, B.J., and Ahnn, J. Thioredoxin is related to life span regulation and oxidative stress response in *Caenorhabditis elegans*. *Genes to Cells*, 10(12):1203–1210, 2005.
- Joe, P.A., Banerjee, A., and Ludueña, R.F. The roles of Cys124 and Ser239 in the functional properties of human  $\beta$ III tubulin. *Cell motility and the cytoskeleton*, 65(6):476–486, 2008.
- Johnson, T.E. Increased life-span of age-1 mutants in *Caenorhabditis elegans* and lower Gompertz rate of aging. *Science*, 249(4971):908–912, 1990.
- Kakihana, T., Nagata, K., and Sitia, R. Peroxides and Peroxidases in the Endoplasmic Reticulum: Integrating Redox Homeostasis and Oxidative Folding. *Antioxidants & Redox Signaling*, (ja), 2011.
- Karlsson, M., Kurz, T., Brunk, U.T., Nilsson, S.E., Frennesson, C.I., *et al.* What does the commonly used DCF-test for oxidative stress really show? *Biochemical Journal*, 428(2):183–190, 2010.
- Keaney, M. and Gems, D. No increase in lifespan in *Caenorhabditis elegans* upon treatment with the superoxide dismutase mimetic EUK-8. *Free Radical Biology and Medicine*, 34(2):277–282, 2003.
- Kenyon, C. The plasticity of aging: insights from long-lived mutants. *Cell*, 120(4):449–460, 2005.
- Kenyon, C., Chang, J., Gensch, E., Rudner, A., Tabtiang, R., *et al.* A *C. elegans* mutant that lives twice as long as wild type. *Nature*, 366(6454):461–464, 1993.
- Kenyon, C.J. The genetics of ageing. *Nature*, 464(7288):504–512, 2010.
- Keston, A.S. and Brandt, R. The fluorometric analysis of ultramicro quantities of hydrogen peroxide. *Analytical biochemistry*, 11:1, 1965.
- Klass, M.R. Aging in the nematode *Caenorhabditis elegans*: major biological and environmental factors influencing life span. *Mechanisms of ageing and development*, 6:413–429, 1977.
- Klichko, V.I., Radyuk, S.N., and Orr, W.C. Profiling catalase gene expression in *Drosophila melanogaster* during development and aging. *Archives of insect biochemistry and physiology*, 56(1):34–50, 2004.

- Klotz, L.O. and Sies, H. Cellular generation of oxidants: relation to oxidative stress. *Redox signaling and regulation in biology and medicine*, pages 45–61, 2009.
- Knoefler, D., Thamsen, M., Koniczek, M., Niemuth, N.J., Diederich, A., and Jakob, U. Quantitative In Vivo Redox Sensors Uncover Oxidative Stress as an Early Event in Life. *Molecular Cell*, accepted for publication, 2012a.
- Knoefler, D., Tienson, H.L., and Jakob, U. Role of Oxidative Stress in Aging. In U. Jakob and D. Reichmann, editors, *Oxidative Stress and Redox Regulation*. Springer, in preparation, 2012b.
- Krause, K.H. Aging: a revisited theory based on free radicals generated by NOX family NADPH oxidases. *Experimental gerontology*, 42(4):256–262, 2007.
- Kullik, I., Toledano, M.B., Tartaglia, L.A., and Storz, G. Mutational analysis of the redox-sensitive transcriptional regulator OxyR: regions important for oxidation and transcriptional activation. *Journal of bacteriology*, 177(5):1275–1284, 1995.
- Kumsta, C., Thamsen, M., and Jakob, U. Effects of oxidative stress on behavior, physiology, and the redox thiol proteome of *Caenorhabditis elegans*. *Antioxidants & redox signaling*, 14(6):1023–1037, 2011.
- Lambeth, J.D. NOX enzymes and the biology of reactive oxygen. *Nature Reviews Immunology*, 4(3):181–189, 2004.
- Lassègue, B. and Griendling, K.K. Reactive oxygen species in hypertension: an update. *American journal of hypertension*, 17(9):852–860, 2004.
- Lee, K.S., Iijima-Ando, K., Iijima, K., Lee, W.J., Lee, J.H., Yu, K., and Lee, D.S. JNK/FOXO-mediated neuronal expression of fly homologue of peroxiredoxin II reduces oxidative stress and extends life span. *Journal of Biological Chemistry*, 284(43):29454–29461, 2009a.
- Lee, S.J., Hwang, A.B., and Kenyon, C. Inhibition of Respiration Extends *C. elegans* Life Span via Reactive Oxygen Species that Increase HIF-1 Activity. *Current Biology*, 20(23):2131–2136, 2010.

- Lee, S.J. and Kenyon, C. Regulation of the longevity response to temperature by thermosensory neurons in *Caenorhabditis elegans*. *Current biology*, 19(9):715–722, 2009.
- Lee, S.J., Murphy, C.T., and Kenyon, C. Glucose Shortens the Life Span of *C. elegans* by Downregulating DAF-16/FOXO Activity and Aquaporin Gene Expression. *Cell metabolism*, 10(5):379–391, 2009b.
- Lee, S.S., Lee, R.Y.N., Fraser, A.G., Kamath, R.S., Ahringer, J., and Ruvkun, G. A systematic RNAi screen identifies a critical role for mitochondria in *C. elegans* longevity. *Nature genetics*, 33(1):40–48, 2002.
- Leichert, L.I. and Jakob, U. Protein thiol modifications visualized in vivo. *PLoS biology*, 2(11):e333, 2004.
- Lettre, G. and Hengartner, M.O. Developmental apoptosis in *C. elegans*: a complex CEDnario. *Nature Reviews Molecular Cell Biology*, 7(2):97–108, 2006.
- Leyens, G., Knoops, B., and Donnay, I. Expression of peroxiredoxins in bovine oocytes and embryos produced in vitro. *Molecular reproduction and development*, 69(3):243–251, 2004.
- Lin, K., Hsin, H., Libina, N., Kenyon, C., *et al.* Regulation of the *Caenorhabditis elegans* longevity protein DAF-16 by insulin/IGF-1 and germline signaling. *Nature genetics*, 28(2):139–146, 2001.
- Lin, S.J., Kaeberlein, M., Andalis, A.A., Sturtz, L.A., Defossez, P.A., Culotta, V.C., Fink, G.R., Guarente, L., *et al.* Calorie restriction extends *Saccharomyces cerevisiae* lifespan by increasing respiration. *Nature*, 418(6895):344–348, 2002.
- Longo, V.D. and Finch, C.E. Evolutionary medicine: from dwarf model systems to healthy centenarians? *Science*, 299(5611):1342–1346, 2003.
- Lopez-Lluch, G., Hunt, N., Jones, B., Zhu, M., Jamieson, H., Hilmer, S., Cascajo, MV, Allard, J., Ingram, DK, Navas, P., *et al.* Calorie restriction induces mitochondrial biogenesis and bioenergetic efficiency. *Proceedings of the National Academy of Sciences of the United States of America*, 103(6):1768–1773, 2006.

- Mackay, W.J. and Bewley, G.C. The genetics of catalase in *Drosophila melanogaster*: isolation and characterization of acatalasemic mutants. *Genetics*, 122(3):643–652, 1989.
- Maeda, K., Finnie, C., and Svensson, B. Cy5 maleimide labelling for sensitive detection of free thiols in native protein extracts: identification of seed proteins targeted by barley thioredoxin h isoforms. *Biochemical Journal*, 378(Pt 2):497, 2004.
- Makino, N., Mochizuki, Y., Bannai, S., and Sugita, Y. Kinetic studies on the removal of extracellular hydrogen peroxide by cultured fibroblasts. *Journal of Biological Chemistry*, 269(2):1020–1025, 1994.
- Margittai, É. and Bánhegyi, G. Oxidative folding in the endoplasmic reticulum: Towards a multiple oxidant hypothesis? *FEBS letters*, 584(14):2995–2998, 2010.
- Markvicheva, K.N., Bilan, D.S., Mishina, N.M., Gorokhovatsky, A.Y., Vinokurov, L.M., Lukyanov, S., and Belousov, V.V. A genetically encoded sensor for H<sub>2</sub>O<sub>2</sub> with expanded dynamic range. *Bioorganic & Medicinal Chemistry*, 19(3):1079–1084, 2011.
- McCay, C.M., Crowell, M.F., and Maynard, L.A. The effect of retarded growth upon the length of life span and upon the ultimate body size. *J Nutr*, 10(1):63–79, 1935.
- McCord, J.M. and Fridovich, I. Superoxide dismutase. *Journal of Biological Chemistry*, 244(22):6049, 1969.
- McCord, J.M., Keele, B.B., and Fridovich, I. An enzyme-based theory of obligate anaerobiosis: the physiological function of superoxide dismutase. *Proceedings of the National Academy of Sciences*, 68(5):1024, 1971.
- Mello, C.C., Kramer, J.M., Stinchcomb, D., and Ambros, V. Efficient gene transfer in *C. elegans*: extrachromosomal maintenance and integration of transforming sequences. *The EMBO journal*, 10(12):3959, 1991.
- Meyer, A.J. and Dick, T.P. Fluorescent protein-based redox probes. *Antioxidants & redox signaling*, 13(5):621–650, 2010.



- Miranda-Vizuete, A., González, J.C.F., Gahmon, G., Burghoorn, J., Navas, P., and Swoboda, P. Lifespan decrease in a *Caenorhabditis elegans* mutant lacking TRX-1, a thioredoxin expressed in ASJ sensory neurons. *FEBS letters*, 580(2):484–490, 2006.
- Mitsui, A., Hamuro, J., Nakamura, H., Kondo, N., Hirabayashi, Y., Ishizaki-Koizumi, S., Hirakawa, T., Inoue, T., and Yodoi, J. Overexpression of human thioredoxin in transgenic mice controls oxidative stress and life span. *Antioxidants and Redox Signaling*, 4(4):693–696, 2002.
- Mockett, R.J., Orr, W.C., Rahmandar, J.J., Benes, J.J., Radyuk, S.N., Klichko, V.I., and Sohal, R.S. Overexpression of Mn-containing superoxide dismutase in transgenic *Drosophila melanogaster*. *Archives of biochemistry and biophysics*, 371(2):260–269, 1999.
- Mockett, R.J., Sohal, B.H., and Sohal, R.S. Expression of multiple copies of mitochondrially targeted catalase or genomic Mn superoxide dismutase transgenes does not extend the life span of *Drosophila melanogaster*. *Free Radical Biology and Medicine*, 49(12):2028–2031, 2010.
- Mori, I. and Ohshima, Y. Neural regulation of thermotaxis in *Caenorhabditis elegans*. *Nature*, 376(6538):344–348, 1995.
- Murphy, C.T. The search for DAF-16/FOXO transcriptional targets: approaches and discoveries. *Experimental gerontology*, 41(10):910–921, 2006.
- Murphy, C.T., McCarroll, S.A., Bargmann, C.I., Fraser, A., Kamath, R.S., Ahringer, J., Li, H., Kenyon, C., *et al.* Genes that act downstream of DAF-16 to influence the lifespan of *Caenorhabditis elegans*. *Nature*, 424(6946):277–283, 2003.
- Murphy, M.I. Mitochondrial Thiols in Antioxidant Protection and Redox Signalling: distinct roles for glutathionylation and other thiol modifications. *Antioxidants & Redox Signaling*, (ja), 2011.
- Nauseef, W.M. Biological roles for the NOX family NADPH oxidases. *Journal of Biological Chemistry*, 283(25):16961, 2008.
- Nemoto, S. and Finkel, T. Redox regulation of forkhead proteins through a p66shc-dependent signaling pathway. *Science's STKE*, 295(5564):2450, 2002.

- Neumann, C.A., Krause, D.S., Carman, C.V., Das, S., Dubey, D.P., Abraham, J.L., Bronson, R.T., Fujiwara, Y., Orkin, S.H., Van Etten, R.A., *et al.* Essential role for the peroxiredoxin Prdx1 in erythrocyte antioxidant defence and tumour suppression. *Nature*, 424(6948):561–565, 2003.
- Nicholls, P., Fita, I., and Loewen, P.C. Enzymology and structure of catalases. *Advances in Inorganic Chemistry*, 51:51–106, 2000.
- Niki, E. Interaction of ascorbate and  $\alpha$ -tocopherol. *Annals of the New York Academy of Sciences*, 498(1):186–199, 1987.
- Nisoli, E., Tonello, C., Cardile, A., Cozzi, V., Bracale, R., Tedesco, L., Falcone, S., Valerio, A., Cantoni, O., Clementi, E., *et al.* Calorie restriction promotes mitochondrial biogenesis by inducing the expression of eNOS. *Science's STKE*, 310(5746):314, 2005.
- Oláhová, M., Taylor, S.R., Khazaipoul, S., Wang, J., Morgan, B.A., Matsumoto, K., Blackwell, T.K., and Veal, E.A. A redox-sensitive peroxiredoxin that is important for longevity has tissue- and stress-specific roles in stress resistance. *Proceedings of the National Academy of Sciences*, 105(50):19839, 2008.
- Olsen, A., Vantipalli, M.C., and Lithgow, G.J. Using *Caenorhabditis elegans* as a model for aging and age-related diseases. *Annals of the New York Academy of Sciences*, 1067(1):120–128, 2006.
- Orrenius, S. and Moldéus, P. The multiple roles of glutathione in drug metabolism. *Trends in Pharmacological Sciences*, 5:432–435, 1984.
- Parihar, M.S., Kunz, E.A., and Brewer, G.J. Age-related decreases in NAD (P) H and glutathione cause redox declines before ATP loss during glutamate treatment of hippocampal neurons. *Journal of neuroscience research*, 86(10):2339–2352, 2008.
- Parkes, T.L., Elia, A.J., Dickinson, D., Hilliker, A.J., Phillips, J.P., Boulianne, G.L., *et al.* Extension of *Drosophila* lifespan by overexpression of human SOD1 in motorneurons. *Nature genetics*, 19(2):171–174, 1998.
- Pearl, R. *The biology of death*. 1921.

- Pérez, V.I., Bokov, A., Remmen, H.V., Mele, J., Ran, Q., Ikeno, Y., and Richardson, A. Is the oxidative stress theory of aging dead? *Biochimica et Biophysica Acta (BBA)-General Subjects*, 1790(10):1005–1014, 2009a.
- Pérez, V.I., Cortez, L.A., Lew, C.M., Rodriguez, M., Webb, C.R., Van Remmen, H., Chaudhuri, A., Qi, W., Lee, S., Bokov, A., *et al.* Thioredoxin 1 overexpression extends mainly the earlier part of life span in mice. *The Journals of Gerontology Series A: Biological Sciences and Medical Sciences*, 66(12):1286–1299, 2011.
- Pérez, V.I., Van Remmen, H., Bokov, A., Epstein, C.J., Vijg, J., and Richardson, A. The overexpression of major antioxidant enzymes does not extend the lifespan of mice. *Aging cell*, 8(1):73–75, 2009b.
- Perichon, R. and Bourre, JM. Peroxisomal beta-oxidation activity and catalase activity during development and aging in mouse liver. *Biochimie*, 77(4):288, 1995.
- Petriv, I. and Rachubinski, R.A. Lack of peroxisomal catalase causes a progeric phenotype in *Caenorhabditis elegans*. *Journal of Biological Chemistry*, 279(19):19996–20001, 2004.
- Phillips, J.P., Campbell, S.D., Michaud, D., Charbonneau, M., and Hilliker, A.J. Null mutation of copper/zinc superoxide dismutase in *Drosophila* confers hypersensitivity to paraquat and reduced longevity. *Proceedings of the National Academy of Sciences*, 86(8):2761, 1989.
- Radi, R., Turrens, J.F., Chang, L.Y., Bush, K.M., Crapo, J.D., and Freeman, B.A. Detection of catalase in rat heart mitochondria. *Journal of Biological Chemistry*, 266(32):22028–22034, 1991.
- Radyuk, S.N., Klichko, V.I., and Orr, W.C. Profiling Cu, Zn-superoxide dismutase expression in *Drosophila melanogaster* - a critical regulatory role for intron/exon sequence within the coding domain. *Gene*, 328:37–48, 2004.
- Radyuk, S.N., Michalak, K., Klichko, V.I., Benes, J., Rebrin, I., Sohal, R.S., and Orr, W.C. Peroxiredoxin 5 confers protection against oxidative stress and apoptosis and also promotes longevity in *Drosophila*. *The Biochemical journal*, 419(2):437, 2009.
- Ran, Q., Liang, H., Ikeno, Y., Qi, W., Prolla, T.A., Roberts II, L.J., Wolf, N., VanRemmen, H., and Richardson, A. Reduction in glutathione peroxidase 4 increases life span through increased

- sensitivity to apoptosis. *The Journals of Gerontology Series A: Biological Sciences and Medical Sciences*, 62(9):932–942, 2007.
- Rando, T.A., Crowley, R.S., Carlson, E.J., Epstein, C.J., and Mohapatra, P.K. Overexpression of copper/zinc superoxide dismutase: a novel cause of murine muscular dystrophy. *Annals of neurology*, 44(3):381–386, 1998.
- Rasband, W.S. ImageJ. *U. S. National Institutes of Health, Bethesda, Maryland, USA*, 1997-2012. URL <http://imagej.nih.gov/ij/>.
- Rea, S. and Johnson, T.E. A metabolic model for life span determination in *Caenorhabditis elegans*. *Developmental cell*, 5(2):197–203, 2003.
- Rea, S.L., Ventura, N., and Johnson, T.E. Relationship between mitochondrial electron transport chain dysfunction, development, and life extension in *Caenorhabditis elegans*. *PLoS biology*, 5(10):e259, 2007.
- Rea, S.L., Wu, D., Cypser, J.R., Vaupel, J.W., and Johnson, T.E. A stress-sensitive reporter predicts longevity in isogenic populations of *Caenorhabditis elegans*. *Nature genetics*, 37(8):894–898, 2005.
- Rebrin, I. and Sohal, R.S. Pro-oxidant shift in glutathione redox state during aging. *Advanced drug delivery reviews*, 60(13):1545–1552, 2008.
- Reuter, S., Gupta, S.C., Chaturvedi, M.M., and Aggarwal, B.B. Oxidative stress, inflammation, and cancer: How are they linked? *Free Radical Biology and Medicine*, 49(11):1603–1616, 2010.
- Reveillaud, I., Niedzwiecki, A., Bensch, KG, and Fleming, JE. Expression of bovine superoxide dismutase in *Drosophila melanogaster* augments resistance of oxidative stress. *Molecular and cellular biology*, 11(2):632–640, 1991.
- Riddle, D.L., Swanson, M.M., Albert, P.S., *et al.* Interacting genes in nematode dauer larva formation. *Nature*, 290(5808):668–671, 1981.
- Rohrbach, S., Gruenler, S., Teschner, M., and Holtz, J. The thioredoxin system in aging muscle: key role of mitochondrial thioredoxin reductase in the protective effects of caloric restriction? *Amer-*

- ican Journal of Physiology-Regulatory, Integrative and Comparative Physiology*, 291(4):R927–R935, 2006.
- Rubner, M. *Das problem der lebensdauer und seine beziehungen zu ernahrung*. R. Oldenbourg, 1908.
- Salvi, M., Battaglia, V., Brunati, A.M., La Rocca, N., Tibaldi, E., Pietrangeli, P., Marcocci, L., Mondovì, B., Rossi, C.A., and Toninello, A. Catalase takes part in rat liver mitochondria oxidative stress defense. *Journal of Biological Chemistry*, 282(33):24407–24415, 2007.
- Schafer, F.Q., Buettner, G.R., *et al.* Redox environment of the cell as viewed through the redox state of the glutathione disulfide/glutathione couple. *Free Radical Biology and Medicine*, 30(11):1191–1212, 2001.
- Schlotterer, A., Kukudov, G., Bozorgmehr, F., Hutter, H., Du, X., Oikonomou, D., Ibrahim, Y., Pfisterer, F., Rabbani, N., Thornalley, P., *et al.* C. elegans as Model for the Study of High Glucose–Mediated Life Span Reduction. *Diabetes*, 58(11):2450–2456, 2009.
- Schnabel, D., Salas-Vidal, E., Narváez, V., del Rayo Sánchez-Carbente, M., Hernández-García, D., Cuervo, R., and Covarrubias, L. Expression and regulation of antioxidant enzymes in the developing limb support a function of ROS in interdigital cell death. *Developmental biology*, 291(2):291–299, 2006.
- Schriner, S.E., Linford, N.J., Martin, G.M., Treuting, P., Ogburn, C.E., Emond, M., Coskun, P.E., Ladiges, W., Wolf, N., Van Remmen, H., *et al.* Extension of murine life span by overexpression of catalase targeted to mitochondria. *Science*, 308(5730):1909–1911, 2005.
- Schulz, T.J., Zarse, K., Voigt, A., Urban, N., Birringer, M., and Ristow, M. Glucose restriction extends *Caenorhabditis elegans* life span by inducing mitochondrial respiration and increasing oxidative stress. *Cell metabolism*, 6(4):280–293, 2007.
- Semsei, I., Rao, G., and Richardson, A. Expression of superoxide dismutase and catalase in rat brain as a function of age. *Mechanisms of ageing and development*, 58(1):13–19, 1991.

- Sentman, M.L., Granström, M., Jakobson, H., Reaume, A., Basu, S., and Marklund, S.L. Phenotypes of mice lacking extracellular superoxide dismutase and copper-and zinc-containing superoxide dismutase. *Journal of Biological Chemistry*, 281(11):6904–6909, 2006.
- Seong, K.H., Ogashiwa, T., Matsuo, T., Fuyama, Y., and Aigaki, T. Application of the gene search system to screen for longevity genes in *Drosophila*. *Biogerontology*, 2(3):209–217, 2001.
- Seto, NO, Hayashi, S., and Tener, G.M. Overexpression of Cu-Zn superoxide dismutase in *Drosophila* does not affect life-span. *Proceedings of the National Academy of Sciences*, 87(11):4270, 1990.
- Shibata, Y., Branicky, R., Landaverde, I.O., and Hekimi, S. Redox regulation of germline and vulval development in *Caenorhabditis elegans*. *Science's STKE*, 302(5651):1779, 2003.
- Sohal, RS, Arnold, L., Orr, W.C., *et al.* Effect of age on superoxide dismutase, catalase, glutathione reductase, inorganic peroxides, TBA-reactive material, GSH/GSSG, NADPH/NADP+ and NADH/NAD+ in *Drosophila melanogaster*. *Mechanisms of ageing and development*, 56(3):223, 1990.
- Sohal, R.S., Ku, H.H., Agarwal, S., Forster, M.J., and Lal, H. Oxidative damage, mitochondrial oxidant generation and antioxidant defenses during aging and in response to food restriction in the mouse. *Mechanisms of ageing and development*, 74(1-2):121–133, 1994.
- Someya, S., Yu, W., Hallows, W.C., Xu, J., Vann, J.M., Leeuwenburgh, C., Tanokura, M., Denu, J.M., and Prolla, T.A. Sirt3 mediates reduction of oxidative damage and prevention of age-related hearing loss under caloric restriction. *Cell*, 143(5):802–812, 2010.
- Sulston, J.E., Schierenberg, E., White, J.G., Thomson, JN, *et al.* The embryonic cell lineage of the nematode *Caenorhabditis elegans*. *Developmental biology*, 100(1):64, 1983.
- Sun, J., Folk, D., Bradley, T.J., and Tower, J. Induced overexpression of mitochondrial Mn-superoxide dismutase extends the life span of adult *Drosophila melanogaster*. *Genetics*, 161(2):661–672, 2002.

- Sun, J., Molitor, J., and Tower, J. Effects of simultaneous over-expression of Cu/ZnSOD and MnSOD on *Drosophila melanogaster* life span. *Mechanisms of ageing and development*, 125(5):341–349, 2004.
- Sun, J. and Tower, J. FLP recombinase-mediated induction of Cu/Zn-superoxide dismutase transgene expression can extend the life span of adult *Drosophila melanogaster* flies. *Molecular and cellular biology*, 19(1):216–228, 1999.
- Sun, L., Sadighi Akha, A.A., Miller, R.A., and Harper, J.M. Life-span extension in mice by preweaning food restriction and by methionine restriction in middle age. *The Journals of Gerontology Series A: Biological Sciences and Medical Sciences*, 64(7):711, 2009.
- Sundaresan, M., Yu, Z.X., Ferrans, V.J., Irani, K., and Finkel, T. Requirement for generation of H<sub>2</sub>O<sub>2</sub> for platelet-derived growth factor signal transduction. *Science*, 270(5234):296–299, 1995.
- Svensson, M.J. and Larsson, J. Thioredoxin-2 affects lifespan and oxidative stress in *Drosophila*. *Hereditas*, 144(1):25–32, 2007.
- Tatar, M., Bartke, A., and Antebi, A. The endocrine regulation of aging by insulin-like signals. *Science*, 299(5611):1346–1351, 2003.
- Thornalley, P.J. and Vašák, M. Possible role for metallothionein in protection against radiation-induced oxidative stress. Kinetics and mechanism of its reaction with superoxide and hydroxyl radicals. *Biochimica et Biophysica Acta (BBA)-Protein Structure and Molecular Enzymology*, 827(1):36–44, 1985.
- Tomek, W., Torner, H., and Kanitz, W. Comparative analysis of protein synthesis, transcription and cytoplasmic polyadenylation of mRNA during maturation of bovine oocytes in vitro. *Reproduction in Domestic Animals*, 37(2):86–91, 2002.
- Trachootham, D., Lu, W., Ogasawara, M.A., Valle, N.R.D., and Huang, P. Redox regulation of cell survival. *Antioxidants & redox signaling*, 10(8):1343–1374, 2008.
- Tsuda, M., Ootaka, R., Ohkura, C., Kishita, Y., Seong, K.H., Matsuo, T., and Aigaki, T. Loss of Trx-2 enhances oxidative stress-dependent phenotypes in *Drosophila*. *FEBS letters*, 584(15):3398–3401, 2010.

- Turrens, J.F. Superoxide production by the mitochondrial respiratory chain. *Bioscience reports*, 17(1):3–8, 1997.
- Ushio-Fukai, M. and Nakamura, Y. Reactive oxygen species and angiogenesis: NADPH oxidase as target for cancer therapy. *Cancer letters*, 266(1):37–52, 2008.
- Van Raamsdonk, J.M. and Hekimi, S. Deletion of the mitochondrial superoxide dismutase sod-2 extends lifespan in *Caenorhabditis elegans*. *PLoS genetics*, 5(2):e1000361, 2009.
- Van Raamsdonk, J.M. and Hekimi, S. Superoxide dismutase is dispensable for normal animal lifespan. *Proceedings of the National Academy of Sciences*, 109(15):5785–5790, 2012.
- Van Remmen, H., Ikeno, Y., Hamilton, M., Pahlavani, M., Wolf, N., Thorpe, S.R., Alderson, N.L., Baynes, J.W., Epstein, C.J., Huang, T.T., *et al.* Life-long reduction in MnSOD activity results in increased DNA damage and higher incidence of cancer but does not accelerate aging. *Physiological genomics*, 16(1):29–37, 2003.
- Van Remmen, H., Qi, W., Sabia, M., Freeman, G., Estlack, L., Yang, H., Mao Guo, Z., Huang, T.T., Strong, R., Lee, S., *et al.* Multiple deficiencies in antioxidant enzymes in mice result in a compound increase in sensitivity to oxidative stress. *Free Radical Biology and Medicine*, 36(12):1625–1634, 2004.
- Vanfleteren, J.R. Oxidative stress and ageing in *Caenorhabditis elegans*. *Biochemical Journal*, 292(Pt 2):605, 1993.
- Victor, V.M., Rocha, M., Sola, E., Banuls, C., Garcia-Malpartida, K., and Hernandez-Mijares, A. Oxidative stress, endothelial dysfunction and atherosclerosis. *Current pharmaceutical design*, 15(26):2988–3002, 2009.
- Wadsworth, W.G. and Riddle, D.L. Developmental regulation of energy metabolism in *Caenorhabditis elegans*. *Developmental biology*, 132(1):167, 1989.
- Ward, S. and Carrel, J.S. Fertilization and sperm competition in the nematode *Caenorhabditis elegans*. *Developmental Biology*, 73(2):304–321, 1979.



- Weinkove, D., Halstead, J.R., Gems, D., and Divecha, N. Long-term starvation and ageing induce AGE-1/PI 3-kinase-dependent translocation of DAF-16/FOXO to the cytoplasm. *BMC biology*, 4(1):1, 2006.
- Welinder, C. and Ekblad, L. Coomassie staining as loading control in Western blot analysis. *Journal of proteome research*, 10(3):1416–1419, 2011.
- White, J. 4 The Anatomy. *Cold Spring Harbor Monograph Archive*, 17(0):81–122, 1988.
- Winterbourn, C.C. and Hampton, M.B. Thiol chemistry and specificity in redox signaling. *Free Radical Biology and Medicine*, 45(5):549–561, 2008.
- Wood, W.B. 1 Introduction to *C. elegans* Biology. *Cold Spring Harbor Monograph Archive*, 17(0):1–16, 1988.
- Wood, Z.A., Schröder, E., Robin Harris, J., and Poole, L.B. Structure, mechanism and regulation of peroxiredoxins. *Trends in biochemical sciences*, 28(1):32–40, 2003.
- Wu, D., Rea, S.L., Cypser, J.R., and Johnson, T.E. Mortality shifts in *Caenorhabditis elegans*: remembrance of conditions past. *Aging cell*, 8(6):666–675, 2009.
- Yanase, S., Onodera, A., Tedesco, P., Johnson, T.E., and Ishii, N. SOD-1 deletions in *Caenorhabditis elegans* alter the localization of intracellular reactive oxygen species and show molecular compensation. *The Journals of Gerontology Series A: Biological Sciences and Medical Sciences*, 64(5):530, 2009.
- Yanase, S., Yasuda, K., and Ishii, N. Adaptive responses to oxidative damage in three mutants of *Caenorhabditis elegans* (*age-1*, *mev-1* and *daf-16*) that affect life span. *Mechanisms of ageing and development*, 123(12):1579–1587, 2002.
- Yang, W. and Hekimi, S. A mitochondrial superoxide signal triggers increased longevity in *Caenorhabditis elegans*. *PLoS biology*, 8(12):e1000556, 2010.
- Yen, K., Patel, H.B., Lublin, A.L., and Mobbs, C.V. SOD isoforms play no role in lifespan in ad lib or dietary restricted conditions, but mutational inactivation of SOD-1 reduces life extension by cold. *Mechanisms of ageing and development*, 130(3):173–178, 2009.

- Yu, B.P. and Chung, H.Y. Stress resistance by caloric restriction for longevity. *Annals of the New York Academy of Sciences*, 928(1):39–47, 2001.
- Yu, B.P. and Yang, R. Critical evaluation of the free radical theory of aging. *Annals of the New York Academy of Sciences*, 786(1):1–11, 1996.
- Zamzami, N., Marchetti, P., Castedo, M., Decaudin, D., Macho, A., Hirsch, T., Susin, S.A., Petit, P.X., Mignotte, B., and Kroemer, G. Sequential reduction of mitochondrial transmembrane potential and generation of reactive oxygen species in early programmed cell death. *The Journal of experimental medicine*, 182(2):367–377, 1995.
- Zangar, R.C., Davydov, D.R., and Verma, S. Mechanisms that regulate production of reactive oxygen species by cytochrome P450. *Toxicology and Applied pharmacology*, 199(3):316–331, 2004.
- Zarse, K., Schmeisser, S., Groth, M., Priebe, S., Beuster, G., Kuhlow, D., Guthke, R., Platzer, M., Kahn, C.R., and Ristow, M. Impaired Insulin/IGF1 Signaling Extends Life Span by Promoting Mitochondrial L-Proline Catabolism to Induce a Transient ROS Signal. *Cell Metabolism*, 15(4):451–465, 2012.
- Zelko, I.N., Mariani, T.J., and Folz, R.J. Superoxide dismutase multigene family: a comparison of the CuZn-SOD (SOD1), Mn-SOD (SOD2), and EC-SOD (SOD3) gene structures, evolution, and expression. *Free Radical Biology and Medicine*, 33(3):337–349, 2002.
- Zhang, Y., Ikeno, Y., Qi, W., Chaudhuri, A., Li, Y., Bokov, A., Thorpe, S.R., Baynes, J.W., Epstein, C., Richardson, A., *et al.* Mice deficient in both Mn superoxide dismutase and glutathione peroxidase-1 have increased oxidative damage and a greater incidence of pathology but no reduction in longevity. *The Journals of Gerontology Series A: Biological Sciences and Medical Sciences*, 64(12):1212, 2009.
- Zheng, M., Åslund, F., and Storz, G. Activation of the OxyR transcription factor by reversible disulfide bond formation. *Science*, 279(5357):1718–1722, 1998.
- Zhou, M., Diwu, Z., Panchuk-Voloshina, N., Haugland, R.P., *et al.* A stable nonfluorescent derivative of resorufin for the fluorometric determination of trace hydrogen peroxide: applications in

---

detecting the activity of phagocyte NADPH oxidase and other oxidases. *Analytical biochemistry*, 253(2):162–168, 1997.



---

## 8 List of Abbreviations

ADP	Adenosine diphosphate
AGE-1	<i>C. elegans</i> ortholog of the phosphoinositide 3-kinase
AMS	4-acetoamido-4'-maleimidylstilbene-2,2'-disulfonic acid
ATP	Adenosine-5'-triphosphate
BSA	Bovine serum albumin
CAT	Catalase
CCO-1	<i>C. elegans</i> ortholog of the cytochrome c oxidase-1 subunit
CGC	Caenorhabditis Genetics Center
CLK-1	<i>C. elegans</i> ortholog of demethoxyubiquinone hydroxylase
cpYFP	circularly permuted yellow fluorescent protein
Cs137	Caesium-137
CTL	Catalase
CYC-1	Component of complex III cytochrome c reductase
DAB	Denaturing Alkylation Buffer
DAF-16	<i>C. elegans</i> FOXO homologue, transcription factor
DAF-2	<i>C. elegans</i> insulin/IGF receptor ortholog, receptor tyrosine kinase
DIC	Differential Interference Contrast
DNA	Deoxyribonucleic acid
dNTP	Deoxyribonucleoside triphosphate

DOG	2-Deoxy-D-glucose
DUOX	Dual oxidase
ECM	Extracellular matrix
ETC	Electron Transport Chain
FOXO	Forkhead box O, transcription factor
FRTA	Free Radical Theory of Aging
FUdR	5'-fluoro-2'-deoxyuridine
fwd	forward
GFP	Green fluorescent protein
GPX	Glutathione peroxidase
GRX	Glutaredoxin
GSH	Glutathione, reduced
GSR	Glutathione reductase
GSSG	Glutathione, oxidized
H <sub>2</sub> DCF-DA	Dihydrodichlorofluorescein diacetate
H <sub>2</sub> O <sub>2</sub>	Hydrogen peroxide
HIF-1	ortholog of the mammalian hypoxia-induced factor HIF-1
HOCl	Hypochlorous acid
HRP	Horseraddish peroxidase
IgG	Immunglobulin G
IIS	Insulin/IGF-1 signaling

---

ISP-1	Rieske iron sulphur protein, subunit of the mitochondrial complex III
LB	Lysogeny broth
LUT	Look-up-table
MAO	Monoamine oxidase
MPO	Myeloperoxidase
mRNA	messenger RNA
NAC	N-acetylcysteine
NADH	Nicotinamide adenine dinucleotide
NADPH	Nicotinamide adenine dinucleotide phosphate
NEM	N-ethylmaleimide
NGM	Nematode growth media
NO	Nitric oxide
NOX	NADPH oxidase
NUO-6	<i>C. elegans</i> ortholog of the subunit of the mitochondrial NADH dehydrogenase (ubiquinone) complex I
O <sub>2</sub> <sup>-</sup>	Superoxide anion
OH <sup>-</sup>	Hydroxyl radical
PCR	Polymerase Chain Reaction
PDGF	Platelet-derived growth factor
PRDX	Peroxiredoxin
PRX	Peroxiredoxin
PVDF	Polyvinylidene fluoride

rev	reverse
ROS	Reactive Oxygen Species
SD	Standard deviation
SDS	Sodium dodecyl sulfate
SDS-PAGE	SDS-Polyacrylamide gel electrophoresis
SEM	Standard error of the mean
SO <sub>2</sub> H	Sulfinic acid
SOD	Superoxide dismutase
SOH	Sulfenic acid
TCA	Trichloroacetic acid
TRX	Thioredoxin
U	Unit
UPR	Unfolded protein response
VEGF	Vascular endothelial growth factor
<i>C. elegans</i>	<i>Caenorhabditis elegans</i>
<i>D. melanogaster</i>	<i>Drosophila melanogaster</i>
<i>E. coli</i>	<i>Escherichia coli</i>